Synthesis of an α-AApeptide derived from an antibiofilm RNase peptid

Diego Defferrari

UNIVERSITÉ DE RENNES 1

THESE DE DOCTORAT DE

L'UNIVERSITE DE RENNES 1
L'UNIVERSIDADE FEDERAL DO RIO GRANDE DO SUL

ECOLE DOCTORALE N° 596
Sciences de la matière, des molécules et matériaux (ED S3M)
Spécialité : Chimie Organique

Par
Diego DEFFERRARI

Synthesis of an α-AApeptide derived from an antibiofilm RNase peptide

Thèse présentée et soutenue à Porto Alegre, le 18 Novembre 2022
Unité de recherche : UMR CNRS 6226 ISCR - Equipe COrInt

Rapporteurs avant soutenance :

Sandy DESRAT	Chargé de recherche, CNRS, Université Paris Saclay
Massuo KATO	Professeur, Universidade de São Paulo

Composition du Jury :

Président :		
Examinateurs :	Adriano ANDRICOPULO	Professeur, Universidade de São Paulo
	Jacques RENAULT	Maitre de conférences, Université de Rennes 1
Dir. de thèse :	Simone GNOATTO	Professeur d'université, Universidade Federal do Rio Grande do Sul
Co-Dir. de thèse :	François-Hugues POREE	Professeur d'université, Université de Rennes 1

In memory of my beloved mom

Pour toi ma maman adorée

Em memória de minha amada mãe

Acknowledgements
Remerciements
Agradecimentos

Dedico este trabalho aos meus pais, que me ensinaram a amar. Obrigado pelo incondicional incentivo à minha constante curiosidade. Se meus sonhos são possíveis, foram vocês que me ensinaram a sonhar o impossível.

Dedico este trabalho também à minha incrível orientadora, uma cientista brilhante e, além disso, um ser humano maravilhoso, com quem tanto aprendi e sigo aprendendo. Sua intuição cientifica e cerne moral sempre serão minha bússola. Não existem palavras em nenhuma língua para descrever a admiração que sinto, muito obrigado por tudo, principalmente pela amizade.

I also would like to thank my wonderful French supervisor, or as I like to call him: Boss. It was an amazing experience learning with you. Doing chemistry by your side was a great pleasure. Thank you for transforming me into a better chemist and teaching me how to work faster and be more assertive in my chemical choices. This international experience was even better because of you. More than an amazing supervisor, a person whom I can also call a friend.

I would also like to thank François-Hugues for all the effort for my cotutelle agreement and the conversations about history, politics, music, and stuff in general, I had a really nice time chatting with you. Gostaria de agradecer também ao Alexandre Macedo por todo o empenho na coordenação do projeto CAPES-COFECUB, sempre disponível e resolutor. A special thanks to Reynald Gillet for the partnership in this work and, on top of that, for his kindness.

O excelente trabalho da Anelise no planejamento do peptídeo foi fundamental para o desenvolvimento desta tese. Obrigado pela sequência de aminoácidos e pelas raclettes.

Um imenso obrigado aos colegas de laboratório pelas discussões químicas e pelas conversas, vocês sempre fizeram o trabalho ser mais leve. Um agradecimento todo especial a Carol, Thaís, Isa e Cesar. Obrigado à Marcela pelos constantes incentivos, mesmo na pior das CCDs. À Nádia, uma grande colega nos dois lados do Equador. Agradeço e dedico esse trabalho ao meu fiel companheiro de bancada e grande amigo, Guilherme, que constantemente me mostra o prazer de ser cientista. À Fernanda, colega de longa data e amiga que sempre me ajudou e me divertiu, um abraço.

Je tiens à remercier mes collègues français pour tous les bons moments au laboratoire et pour leur accueil. A Nicolas pour les conversations chimiques, les blagues et la gentillesse unique. À Miryam pour les recettes, pour l'aide au labo et pour m'avoir toujours appris le français d'une manière douce et gentille, merci du fond du cœur ! À Claudia also, pour les conversations and les good moments. Tu seras toujours my favorite Florentine ! Merci à vous deux pour les déjeuners. Merci à Jeff pour les rires et les bonnes discussions sur le vin. Bonne retraite ! Un merci spécial à mes chers collègues du labo, Cécile, Corentin et Sébastien pour leur compagnie constante et amusante. Merci Philippe pour les moments agréables et pour toutes les discussions, j'ai beaucoup appris de vous. A very special thanks for the very best PhD team, Ali, Julien and Thanh, for the chemistry discussions and kebab eating. Miss you, guys! Merci aussi a Patricia, sua companhia foi fundamental no meu séjour na França e agora, no Brasil. Merci por toda a ajuda com a cotutela, ela só existe graças a toi.

Este trabalho só foi realizado graças ao apoio constante dos meus amigos, esta tese é também dedicada a vocês. Muito obrigado Ana, Marcelo e Carina pelos bons momentos, pelas comilanças, pelas idas à praia. Muito obrigado mesmo. A very special thanks to Carina for the English assistance, if you are reading this, is because of her. Thank you!

Obrigado aos meus amigos franco-brasileiros pela companhia, os confinamentos foram bem mais toleráveis graças a vocês. À Luciana pelas caminhadas em raio de 1 km de casa, à Diana pelas Evidências cantadas a plenos pulmões e ao Rodrigo pelas cidras e testes biológicos.

Ao meu casal favorito, Fábio e Fernanda, pela amizade e parceria ao longo dos anos. Quando crescer, quero ser humano como vocês.

À minha grande amiga Irene pelo apoio, conversas e explicações físico-químicas. Sou um melhor químico orgânico graças a ti. Teu senso de justiça sempre estará comigo, obrigado por tudo.

Ao grupo da química, distante, mas sempre presente. Um abraço em especial para a Alinne, Val e Guilherme.

To my favorite German couple, Andrea and Nico, thanks for the stay and for the history chats, you are amazing. Danke für den Zwiebelkuchen!

Agradeço imensamente à UFRGS por todo o apoio. Je remercie a L'Université de Rennes 1 pour l'aide. Agradeço em especial ao PPGCF por todo o suporte burocrático, principalmente à Valência.

Agradeço ao governo brasileiro pelas politicas de incentivo a ciência e a internacionalização de seus cientistas, em especial a parceria CAPES-COFECUB. Je tiens également à remercier le gouvernement français de m'avoir accueilli.

Dedico esse trabalho a todos que vieram antes de mim e que lutaram por uma educação pública, plural e de altíssima qualidade.

Dedico esse trabalho também a todas as pessoas que amei e que de alguma forma contribuíram para meu crescimento pessoal e profissional.

Obrigado ao Brasil pelo calor humano e jogo de cintura. Merci la France pour le pain, les fromages et les vins.

To see a World in a Grain of Sand
And a Heaven in a Wild Flower
Hold Infinity in the palm of your hand
And Eternity in an hour

Willian Blake

Contents

List of abbreviations

BB	Building block(s)
Bn	Benzyl
Boc	*tert*-butoxycarbonyl
CFU	Colony-forming unit
DCM	Dichloromethane
DEPBT	Diethoxy phosphoryloxy benzotriazinone
DHOBt	Dihydrohydroxyoxobenzotriazine
DIPEA	*N,N*-diisopropylethylamine
DMAP	4-Dimethylaminopyridine
DMF	*N*,*N*-dimethylformamide
E1	Unimolecular elimination
E1cB	Unimolecular elimination conjugate base
EDCI	1-Ethyl-3-(3-dimethylaminopropyl)carbodiimide
EEDQ	*N*-ethoxycarbonyl-2-ethoxy-1,2-dihydroquinoline
EtOAc	Ethyl acetate
FITC	Fluorescein isothiocyanate
Fmoc	*N*-Fluorenylmethoxycarbonyl
HATU	Hexafluorophosphate azabenzotriazole tetramethyluronium
HOAt	Hydroxyazabenzotriazole
MIC	Minimum inhibitory concentration
NMM	*N*-Methylmorpholine
Rf	Retention factor
rt	Room temperature
SEM	Scanning electron microscopy

S_N1	Unimolecular substitution reaction
S_N2	Bimolecular substitution reaction
S_NAc	Nucleophilic acyl substitution
T3P	Propanephosphonic acid anhydride
TEM	Transmission electron microscopy
TFA	Trifluoracetic acid
THF	Tetrahydrofuran
TIS	Triisopropyl silane
TLC	Thin-layer chromatography
Tol	Toluyl
Trt	Trityl

A. Preface

Bacteria naturally produce compounds with antibiotic activity and secrete them into the environment as a form to compete for their sustenance, being the reason why most of the current antibiotics were originated from microorganisms. These antibiotic-producing bacteria will also have resistance genes to avoid self-toxicity[1]. In this scenario, a pattern appears, where species of antimicrobial-producing bacteria will evolutionary pressure other bacterial species, leading to mutual endurance. Multidrug-resistant bacteria were discovered from archeological samples[2], showing that resistance is as old as antibiotics themselves.

Antibiotic or antimicrobial resistance is the ability of a microorganism to survive and grow in concentrations of a drug that is usually used for its eradication. This resistance, due to anthropogenic activities, is accelerated causing resistant mutants to develop at a higher rate than new drugs are developed[3,4].

Biofilm formation is the main precursor of infection and new strategies to prevent or hinder the establishment of this layer of cells are essential. If antibiotics lose their effectiveness, major medical procedures can become too dangerous to perform[5].

About 700,000 people worldwide die annually last decade from drug-resistant infections and, if no action is taken, it is estimated that such infections will kill 10 million people a year by 2050[6,7]. These infections are one of the main causes of rejection in biomedical devices, such as implants, prostheses, valves, central venous accesses, among others.

Although diseases related to bacterial infections are of increasing concern and they are not selective to ethnic groups or regions, there is still little government interest and investment in research by the pharmaceutical industries[8]. Peptides have been studied as a possible drug to avoid biofilm formation or to eradicate the already formed biofilm.

Peptides are known in the clinic for several decades and they have been used to successfully treat diseases, but their peptide bonds are prone to proteolysis, being one of the main concerns of using these molecules as drugs. In the 1970s the concept that a nonpeptidic molecule can perform the same biological effect as a peptide or a protein was postulated[9], but it took a few decades for the interest in the subject to reach medicinal chemists. Among the various type of peptidomimetics, the concept of AApeptides was introduced in 2010s. These pseudopeptides rely on units consisting of *N*-Acylated-*N*-

Aminoethyl amino acid and 2 subtypes, α and γ, have been described depending on the position of the side chain (either the α-C or γ-C relative to the carboxyl group). They present the same number of functional groups as conventional peptides of the same length and a better resistance to proteolytic degradation due to their tertiary amide functional groups.

This PhD-project deals with the synthesis of a novel α-AApeptide that mimics a modified human RNAse and is part of a larger international project consisting in the identification of antibiofilm compounds.

This work was made in the framework of a bilateral partnership between Brazil and France, as part of the CAPES-COFECUB agreement. This collaboration was settled between the Universidade Federal do Rio Grande do Sul, and the Université de Rennes 1, located, respectively, in Porto Alegre, Rio Grande do Sul, Brazil and in Rennes, Bretagne, France. Two laboratories in each country were involved, one specialized in organic synthesis and another one in biological essays. All the laboratories are described below, along with the respected supervisors of this project:

Brazil

- LaFiS – Laboratory of Phytochemistry and Organic Synthesis
  Dr. Simone Cristina Baggio Gnoatto
- LaBDiM – Laboratory of Biofilms & Microbial Diversity
  Dr. Alexandre José Macedo

France

- COrInt – Organic Chemistry & Interfaces
  Dr. Mickäel Jean and Dr. François-Hugues Porée
- CQSP – Quality Control in Protein Synthesis
  Dr. Reynald Gillet

Biological evaluations were conducted by Dr. Anelise Baptista at Gillet's laboratory and by Rodrigo Campos at Macedo's laboratory.

The organic synthesis was conducted by the author of this thesis.

B. Background

I. Bacterial biofilm and antibiofilm strategies

a) Biofilm

Bacterial biofilm is a slimy tridimensional complex structure composed mainly of polysaccharides, lipids, proteins, and nucleic acids in various structural forms[2], its chemical composition is shown in Table 1.

Table 1: Biofilm chemical composition.[10]

Component	Percentage of matrix
Polysaccharide	1 – 2%
Nucleic acids	1 – 2%
Proteins	1 – 2%
Microbial cells s	2 – 5%
Water	Up to 97%

Due to the high-water content, many times its dry weight, a biofilm may also be considered a hydrogel. Those substances are secreted by the cells as an extracellular matrix in response to a number of different factors, which include nutritional cues, cellular recognition of attachment sites, a defense mechanism against antibiotics and the host body's immune system, and also help in the osmotic equilibria of the cells[11]. A colored image by scanning electron microscopy of *Streptococci gordonii* biofilm grown on a dental restorative is shown in Figure 1.

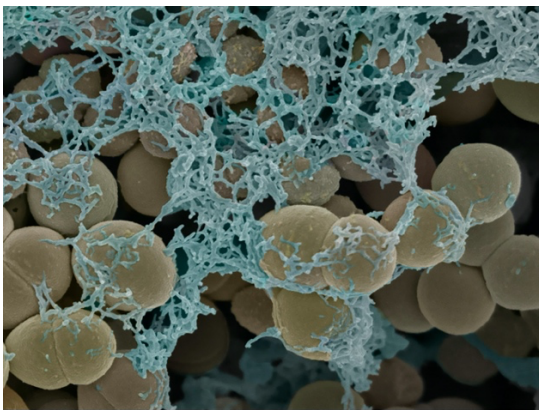

Figure 1: Streptococci gordonii biofilm. Credit: Gemma Cotton.

The first biofilm record dates back 3.25 billion years ago[11], being evidence that this structure is a key component of the life cycle of the bacteria, essential for their survival in diverse environments, sometimes hostile ones.

Microbial cells growing in a biofilm are physiologically distinct from planktonic cells of the same organism, which by contrast, are single cells that float or swim in an aqueous medium. The dense and protected environment of the film allows them to cooperate and interact in various ways

A biofilm begins to form when a free microbial cell attaches to a surface. The formation of a biofilm is shown in Figure 2 and includes 4 main steps consisting of the initial attachment (1), the irreversible attachment (2), the growth step (3), and the maturation step (4) followed by a dispersion process (5).

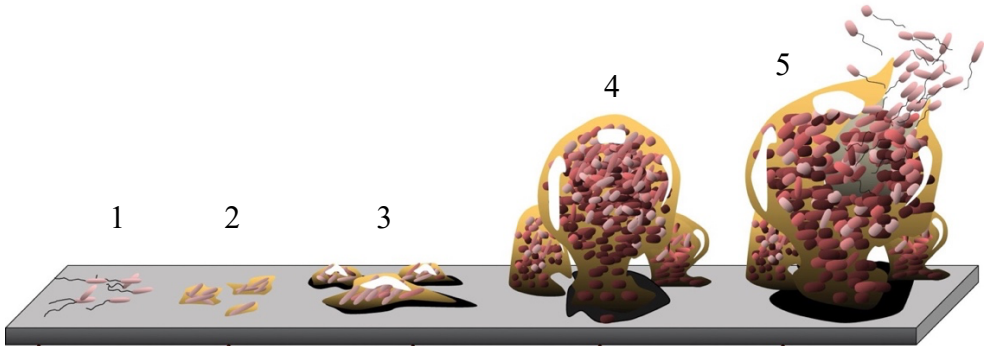

Figure 2: Stages of biofilm development.[12]

In the initial stage, the planktonic phenotype of the bacteria attaches reversibly to a solid living or non-living substratum through van der Waals, steric, and electrostatic interactions. The surface of the substratum is conditioned by the host matrix proteins, fibrinogen, fibronectin, and collagen, forming a conditioning film that facilitates adhesion by the bacteria. A number of the reversibly adsorbed cells remain immobilized and become irreversibly adsorbed as a result of the hydrophobic and hydrophilic interactions between the bacteria and the surface. These bacteria then grow, multiply, and form microcolonies. Once microcolonies are formed and in optimal growth conditions, the biofilm undergoes the maturation stage where a more complex architecture of biofilm is established with water channels allowing the flow of nutrients inside the film. Due to the availability of different physicochemical conditions in terms of oxygen availability, diffusible substrates and metabolic side products, pH, and cell density, cells from different regions of a biofilm can show different gene expression patterns. In the final stage of development, some of the bacteria cells can be dispersed from the biofilm, *via* physical detachment or signaling events followed by the hydrolysis of exopolysaccharide,

and return to the planktonic state to enable the colonization of new sites[13]. A biofilm can be classified as a complex biological system, since bacteria organize themselves into a coordinated functional community and may include a single species or a diverse group of microorganisms, often sharing nutrients among them[14].

Biofilms may form on living and non-living surfaces and can be prevalent in natural, industrial, and hospital settings. Biofilms are omnipresent in organic life, but can generate several hazards in the human body; being responsible for 80% of chronic microbial infections in humans[12,15,16], biofilm infections result in an increase in mortality and morbidity rates and, consequently, lead to an increase in hospitalizations rates and health care costs. Its formation is considered one of the main virulence factors in chronic infections[10,17], causing infections mainly related to medical devices implants like prostheses, heart valves, catheters, and intervertebral discs, being also present in infections nonrelated to surgical processes, such as those of the urinary tract, periodontal tissue, middle-ear infections and less common, but more lethal, such as cystic fibrosis and endocarditis. Some examples of those infections are shown in Figure 3. Bacterial cells within a biofilm are up to 1,000-fold more resistant to multiple antibiotics and disinfectants when compared to their planktonic counterparts, creating enormous challenges in surface sterilization and in preventing or managing biofilm-associated infections.

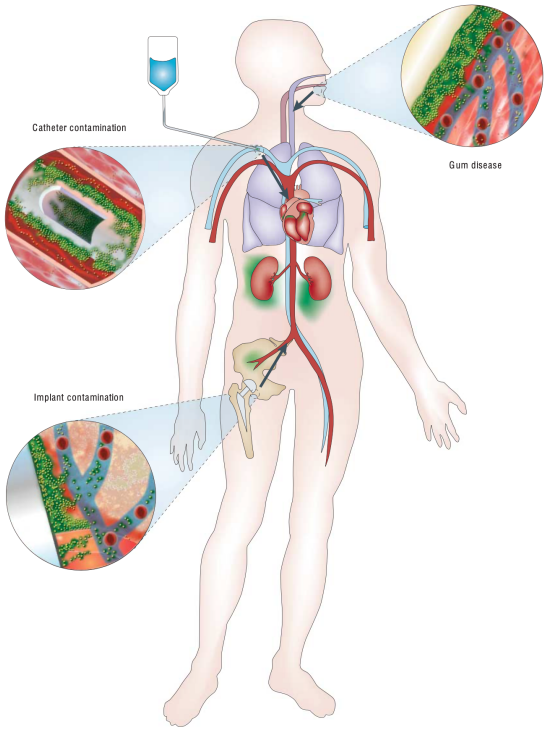

Figure 3: Possible points of entry into the body for infectious biofilm.[11]

Despite the significant health and economic problem of biofilm infections, there are no antibiofilm drugs available to this day. Clinical treatment is often rather aggressive and includes surgical removal of colonized medical devices or tissues, as well as long-term and high-dose of poly-antibiotic therapy. The means of preventing diseases and implant rejections have therefore largely focused on two areas: preventing the adhesion or killing the microorganisms.

b) Antibiofilm

The most used strategy is coating, but they are effective for a short period of time, due to the leaching of the antibiofilm agent of the surface[18]. This approach can be either physical or chemical, focusing on the prevention of microbe growth or microbes' surface attachment.

Physical approaches

- Hydrophobicity

It is way harder for a bacterium to adhere to hydrophobic surfaces[19]. Hydrophobicity implies the long-term maintenance of mechanical properties in contact with fluids, compared to the drastic deterioration in strength that immediately occurs when hydrophilic materials become water-swollen.

Hydrophobic polymers contain materials such as polyethylene, polystyrene, polyvinyl chloride, polytetrafluorethylene, polydimethylsiloxane, some polyesters, some polyurethanes, acrylics, and epoxies. Many such materials have found extensive medical application, in particular, they have been used in situations where a foreign material must be placed in contact with blood and tissues[20]. Artificial kidneys, cardiopulmonary bypass systems, prosthetic heart valves, reconstructed arteries, circulatory assist devices, artificial hearts, catheters, and prosthesis provide examples of such biological fluids-contacting applications.

- Roughness

Rough surfaces are more favorable to biofilm formation and maturation, while smooth surfaces are less susceptible to biofilm adhesion[10]. The roughness of a surface can affect the hydrophobicity of the material, which affects the adhesion ability.

- Surface charge

Modification of the surface charge of polymers is an effective way of biofilm prevention. To avoid the undesirable effects of leaching, antimicrobial agents can be immobilized on surfaces using long, flexible polymeric chains. These chains are anchored to the device surface by covalent bonds, producing non-leaching, contact-killing surfaces.

The charge of polymeric chains can be controlled by using several backbone compounds. Polymers with negative surface charge, like alginic acid, poly-*L*-glutamic acid, dextran sulfate, polyacrylic acid, heparan sulfate, sodium carboxymethyl cellulose, and hyaluronic acid, showed reduced bacterial adherence compared with uncharged surfaces. Dispersion forces between the polymer chains and the bacterial cells prevent bacteria from binding to the surface and initiating biofilm growth. Positively charged polycationic chains generate bactericidal activity[21].

Chemical approaches

Antibiofilm agents should be nontoxic molecules that disperse or inhibit biofilm formation. It is important that such compound has no antibacterial or bacteriostatic properties to avoid evolutionary pressure under the microbes, avoiding the stimulation of tolerance mechanisms. Compounds that are being studied at the moment are going to be discussed below[*]

- **Aryl rhodanines**

Inhibit the adhesion of bacterial cells preventing the initial interaction between the cells and the surface[22]. Opperman *et al.*[23] have studied four compounds, Figure 4, against several stains and in several concentrations, having interesting results for *Staphylococcus and Escherichia,* but those compounds showed no activity for *Pseudomonas*.

[*] The medical uses of silver and silver ions have been known for some time. However, concerns remain over *in vivo* use. Considering the mechanism by which silver interferes with bacterial cell function, silver may have a similar toxic effect on human tissue. For this reason, there has been limited use of silver coatings in vivo. Since silver and silver ions do not fit into the category, they will not be discussed.

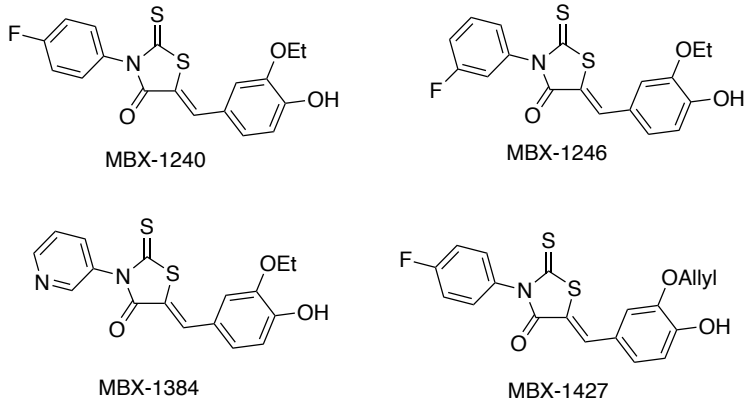

Figure 4: Some active aryl rhodanine.

The mechanism of action involves a physical interaction between the aryl rhodanines and one or more adhesins located on the bacterial cell surface, inhibiting the early stages of biofilm development by preventing bacterial adhesion.

- ***Cis*-2-decenoic acid**

This compound is a fatty acid chemical messenger that can control biofilm formation and induce dispersion of the biofilm, likely by keeping cells in a constant metabolically active and/or dispersive growth state[24]. Davies *et al*.[25] have used this compound in *P. aeruginosa* in concentrations as low as 2.5 nM with good biofilm growth inhibition.

- **Glycosyl hydrolase**

Polysaccharide biosynthetic loci, PslG (Figure 5) is an enzyme involved in the synthesis of a biofilm matrix exopolysaccharide, preventing biofilm formation and disassembles existing biofilms when mature biofilm is treated with it[26]. PslG is an essential protein for the synthesis of Psl, which is predicted to be a protein resembling β-*D*-xylosidases. PslG mainly disrupts the Psl matrix to disperse bacteria from its biofilm[27]. As a glycosyl hydrolase, PslG degrades the polymer of Psl when it is overexpressed or at the wrong location within bacterial cells or in a biofilm.

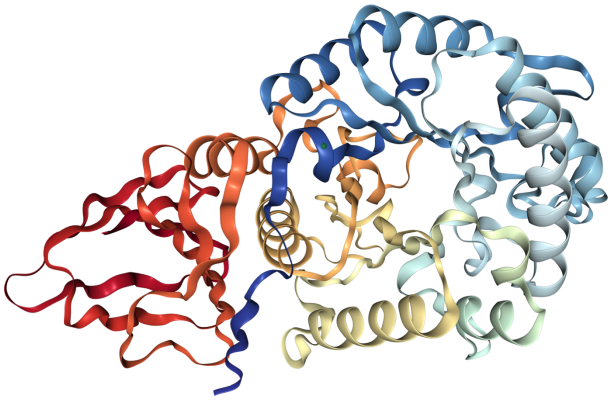

Figure 5: Crystal structure of Ps1G.

(i) Antibiofilm peptides

In 1922, Alexander Fleming identified lysozyme from nasal mucus, which is considered the first human antimicrobial protein. In 1928 Fleming discovered penicillin, beginning the so-called "Golden Age of Antibiotics"[28], new antibiotics were discovered on an almost yearly basis. In the 1940s, along with Howard Florey and Ernst Chain, Fleming brought the therapeutic use of penicillin to fruition, which allowed these scientists to be awarded the Nobel Prize in Medicine in 1945.

Antimicrobial peptides are small molecules (5-100 amino acids) produced by all living organisms that play an essential role in innate immunity[29]. Since the isolation of the first antimicrobial peptide, from the insect *Hyalophora cecropia*, in 1981[30], an increasing number of those compounds have been purified, identified, and studied. In October 2022, The Antimicrobial Peptide Database (https://aps.unmc.edu) contained 3180 antimicrobial peptides from 6 kingdoms: 355 from bacteria, 5 from archaea, 8 from protists, 20 from fungi, 352 from plants, and 2356 from animals. It is considered the largest database of this kind of structures. Several molecules have been studied as potential drug candidates for the treatment of infections and in the past years few of them have gone through pre-clinical and clinical trials, but none of them have already reached the market yet [31].

An antimicrobial peptide can be considered as an antibiofilm compound if the minimum biofilm inhibitory concentration is below the minimum inhibitory concentration[32] (MIC), with a distinct activity compared to the direct antimicrobial property. Eradication of preformed biofilms is much more difficult than the inhibition of its formation, and the minimum biofilm eradication concentration is generally larger than

the MIC. Table 2 summarizes some peptides that have been studied for their antibiofilm activity.

Table 2: Some antibiofilm peptides.

Peptide	Sequence	Source
Protegrin 1[33]	RGGRLCYCRRRFCVCVGR	Leukocytes - Pig
Pleurocidin[34]	GWGSFFKKAAHVGKHVGKAALTHYL	Skin mucous secretions - Winter flounder
LL-37[35]	LLGDFFRKSKEKIGKEFKRIVQRIKDFLRNLVPRTES	Neutrophils, monocytes mast cells, lymphocytes, mesenchymal stem cells - Human
Indolicidin[36]	ILPWKWPWWPWRR	Neutrophils - Cattle
SMAP-29[37]	RGLRRLGRKIAHGVKKYGPTVLRIIRIAG	Leukocytes - Sheep
Human β defensin 3[38]	GIINTLQKYYCRVRGGRCAVLSCLPKEEQIGKCSTRGRKCCRRKK	Skin, tonsils, saliva - Human
HBD-2[39]	GIGDPVTCLKSGAICHPVFCPRRYKQIGTCGLPGTKCCKP	Skin - Human
Aurein 2.5[40]	GLFDIVKKVVGAFGSL	Skin secretions - Frog
Magainin 2[41]	GIGKFLHSAKKFGKAFVGEIMNS	Skin secretions - Frog
Piscidin 3[42]	FIHHIFRGIVHAGRSIGRFLTG	Mast cells - Fish
1037[43]	KRFRIRVRV	Synthetic
Cec4[44]	GWLKKIGKKIERVGQNTRD ATIQAIGVAQQAANVAATLKGK	Synthetic

Since biofilm is a complex structure and differs from one bacterium strain to another and also mixed colonization can occur, the mechanism of action might be difficult to unveil. Different mechanism of action has been reported [45], acting by:

- Blocking initial attachment to a surface by inhibiting motility or interfering with flagellar assembly.
- Inhibiting biofilm development by degrading or preventing the production of important biofilm matrix components.
- Disrupting cell membranes of bacteria within the biofilm or translocating into the cell where they target guanosine tetraphosphate for degradation, disrupting the stringent-stress response required for biofilm formation.
- Promoting the dispersal of biofilm cells, which would make the bacteria susceptible to antibiotics.

Figure 6 shows the mechanisms of action of antibiofilm peptides proposed in the literature.

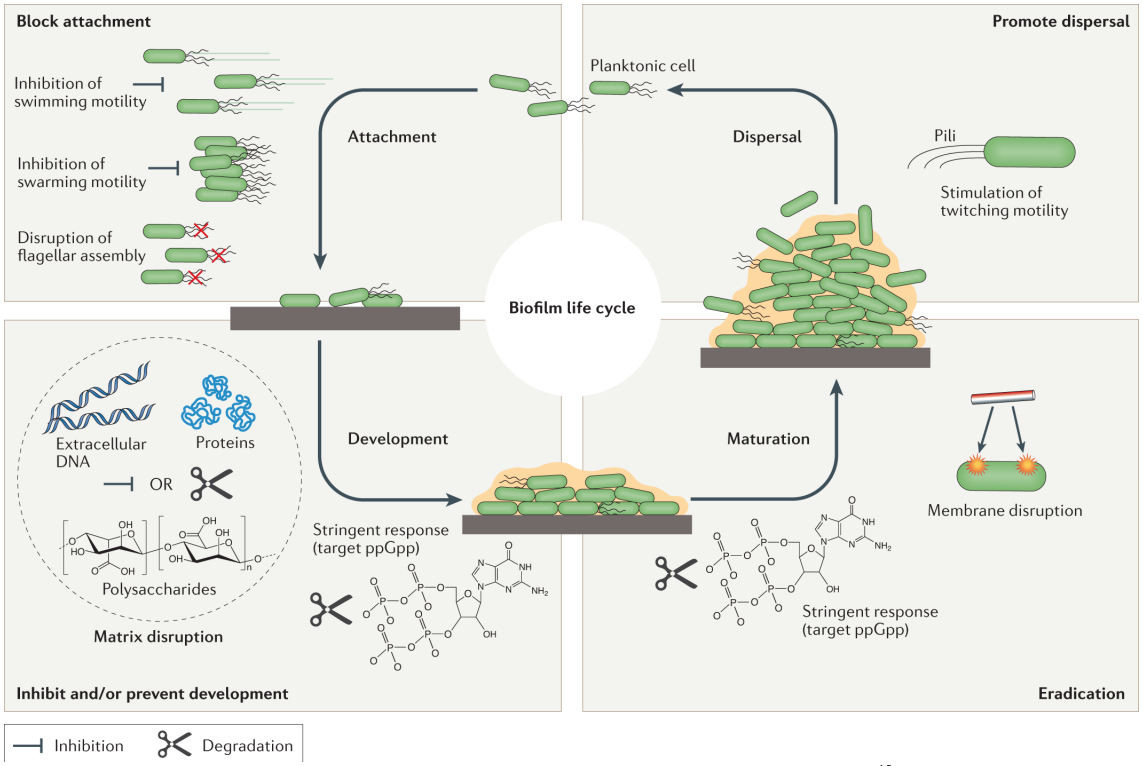

Figure 6: Different mechanisms of action of antibiofilm peptides.[45]

II. Discovery of Ase3 peptide

Previously, a total of 128 sequences of peptides and antimicrobial proteins of human host defense were prospected by Alexandre Macedo's and Reynald Gillet's team, available in the Antimicrobial Peptide Database, with antimicrobial activity reported in the literature. They were aligned using the software Clustal X according to the family of proteins to which they belong, resulting in the selection of 23 conserved sequences that ranged in length from 6 to 11 amino acids and belong to 5 distinct classes: defensins, histatins, catelecidines, RNAses, and chemokines.

All the 23 molecules were synthesized by automated solid-phase peptide synthesis by commercial suppliers. The synthesized peptides are listed in Table 3 below.

Table 3: Conserved sequences of human host antimicrobial proteins and peptides aligned using Clustal X program.

Family	Code	Sequence
Defensines	Def1	CYCRIPACIA
	Def2	ERRYGTCIYQ
	Def3	CYQGRLWAFCC
	Def4	GHCRKK
	Def5	ICRVNEVPE
	Def6	GRYCCLNIKE
Histatines	Hist1	KFHEKHHSHR
	Hist2	DSHAKRHHGY
	Hist3	SNYLYDN
Catelicidines	Cat1	KDFLRNLVPRTES
	Cat2	KRIVQRI
	Cat3	KSKEKIGKEF
RNAses	Ase1	CNSAMSGINNYT
	Ase2	RCKDLNTFLH
	Ase3	FTWAQWFETQH
	Ase4	YVVACDPPQ
	Ase5	VVPVHLDRII
Chemokines	Chem1	QVEVIATLK
	Chem2	ELRCQCLQT
	Chem3	GRKICLNP
	Chem4	MVKKIIEKML
	Chem5	AVIFKTKRG
	Chem6	KEICAPDK

The antibiofilm properties of all the 23 peptide analogues were evaluated in 96-well culture plates according to the crystal violet protocol described by Stepanovic *et al.*[46] and with adaptations by Trentin *et al.*[47]. The commercial antimicrobials rifampicin (8 µg/mL) was used as growth inhibition control for *S. epidermidis* and gentamicin (8 µg/mL) for *P. aeruginosa*. All experiments were performed in technical and biological triplicates.

All classes of analyzed peptides showed some level of biological activity regarding the inhibition of *Staphylococcus epidermidis* biofilm formation at different concentrations tested (Figure 7). The activity of peptides Def2, Chem3, and Ase3 can be highlighted as moderated to good.

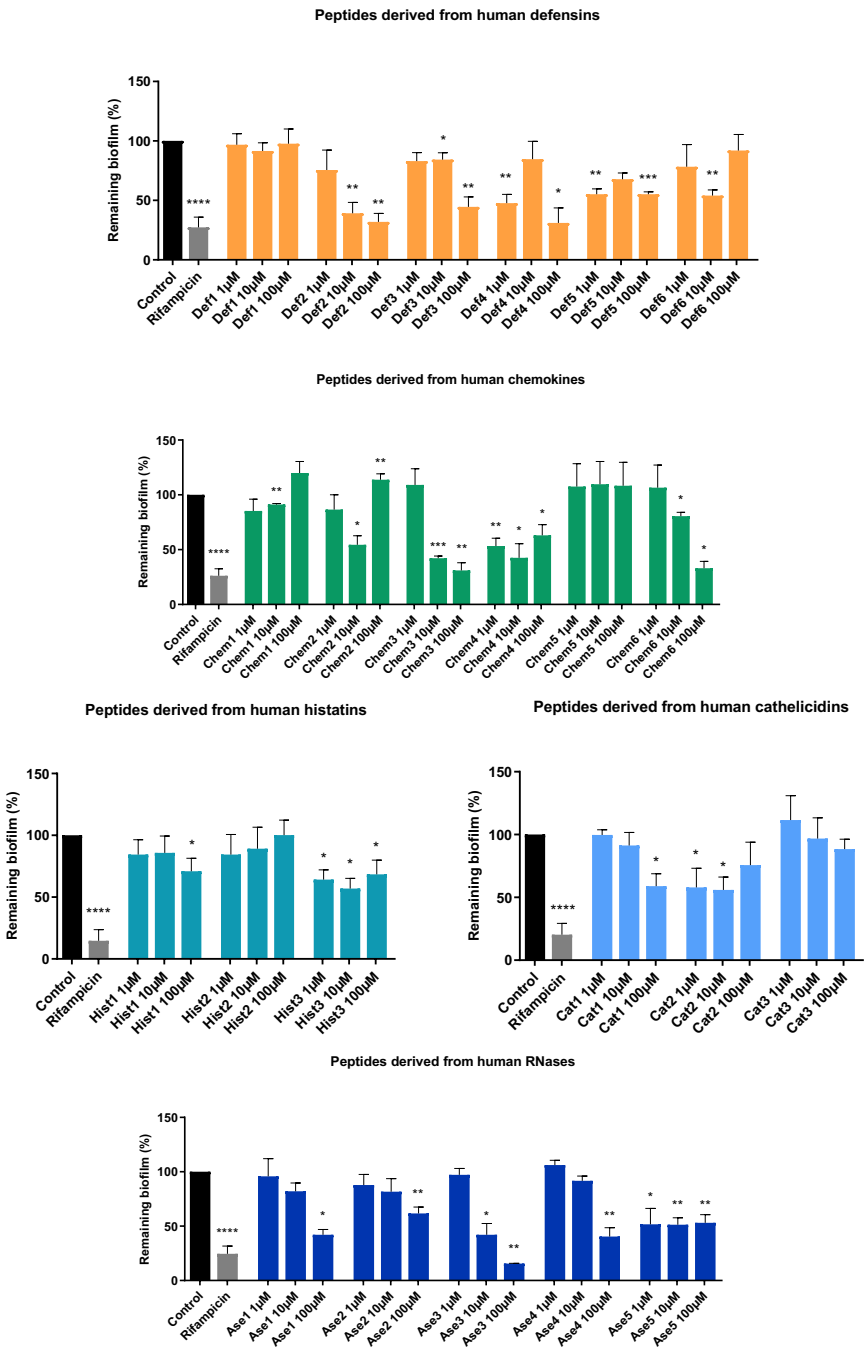

Figure 7: Remaining biofilm from S. epidermidis ATCC 35984 after 24 hours of incubation with peptides synthesized from sequences of defensins, chemokines, histatins, cathelicidins and RNases, and at three test concentrations (1, 10 and 100 µM).

Based on the results, Ase3 was selected for further evaluation. Thus, it also showed activity against *P. aeruginosa* biofilms, inhibiting more than 50% and approximately 30% of *S. epidermidis* and *P. aeruginosa* biofilm formation, respectively, without interfering negatively in the bacterial growth of both evaluated pathogenic species, as shown in Figure 8. Antimicrobial activity was determined by calculating the variation of OD600 readings before and after the period of incubation with the peptide. The untreated control was considered as 100% growth.

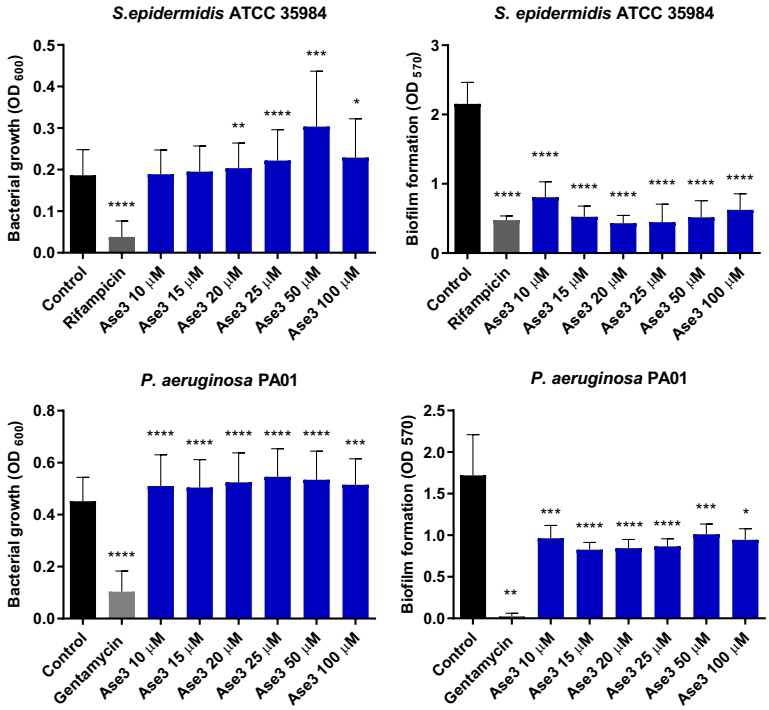

Figure 8: Bacterial growth and remaining biofilm of S. epidermidis ATCC 35984 (top) and P. aeruginosa PA01 (bottom) after 24 hours of incubation with Ase3 at different concentrations.

Considering that the lowest active concentration of the peptide for the two pathogenic bacteria was 15 µM, all further experiments were carried out using this concentration.

A molecular simplification study was conducted to identify the shortest active peptide sequence based on the original sequence. Starting from the C- and N-terminus, reducing one amino acid at a time, three shorter peptides for each extremity were studied. The biological results are shown in Figure 9.

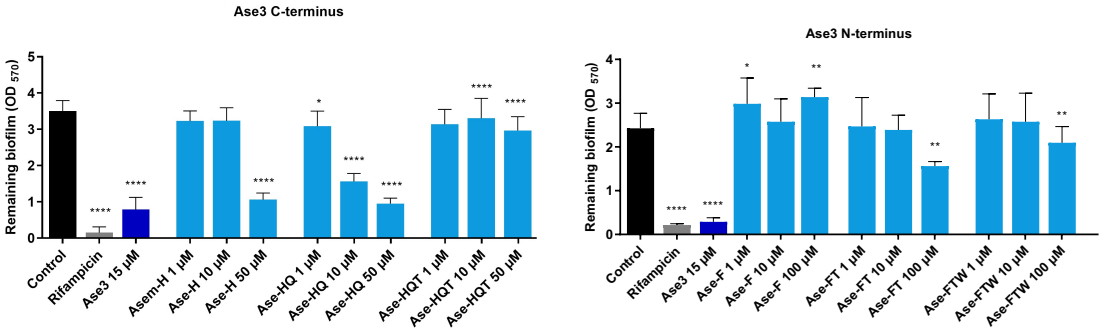

Figure 9: Remaining biofilm of S. epidermidis ATCC 35984 after 24 hours of incubation with Ase3 as control at 15 µM and with peptides without Histidine (-H), Histidine and Glutamine(-HQ), Histidine, Glutamine, and Threonine (-HQT) in the C-terminal portion (top), and with peptides without Phenylalanine (-F), Phenylalanine and Threonine (-FT), Phenylalanine, Threonine and Tryptophan (-FTW) in the N-terminal portion (bottom) at three different concentrations.

The six new shorter peptides were less active as compared to the original Ase3, evidencing the importance of both terminal parts. Since the molecular simplification study has shown that the most active peptide was the unreduced one, all the subsequent tests were performed with the unchanged Ase3.

In order to confirm the non-death-dependent biofilm inhibition, colony-forming unit (CFU) counting experiments were performed as well as growth monitoring by optical density during the 24-hours incubation period of the pathogen with the Ase3 peptide (Figure 10).

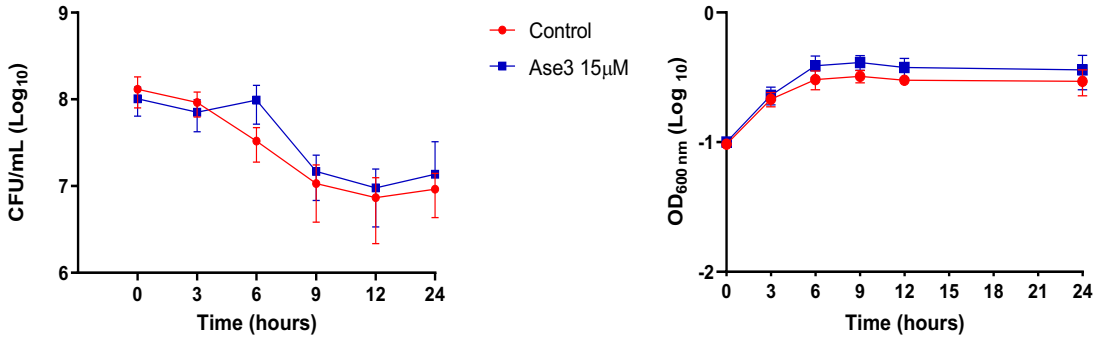

Figure 10: Comparative analysis of cell viability by CFU/mL between untreated control group treated with peptide over 24 hours of assay (left). Comparative analysis of cell growth by optical density between the untreated control group and peptide treated over 24 hours (right).

Cytotoxicity was investigated through multiparameter high-content screening (HCS) and high-content analysis (HCA), using the ImPACcell robotic platform (BIOSIT, Université de Rennes 1). Ase3 was evaluated on 7 different mammalian cell lines: Hct116 (human colon cancer), HuH7 (human liver), CaCO2 (human epithelial colorectal adenocarcinoma), FibroG (fibroblast), H9C2 (myoblastic), C2C12 (myoblastic) and HFobR (human osteoblastic). DMSO was used as a control for the residual cell percentage. The peptide was nontoxic to any of the cell lines analyzed as shown in Figure 11.

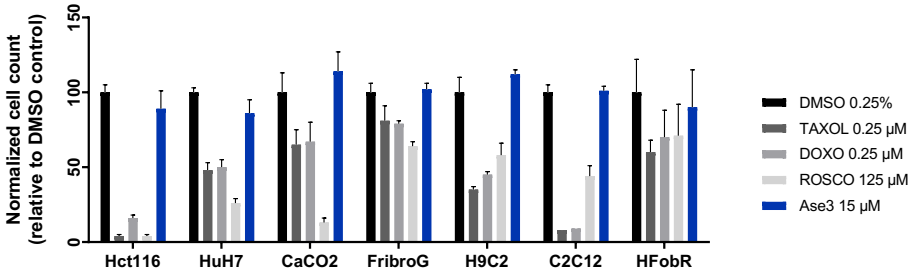

Figure 11: Assessment of Ase3 cytotoxicity in representative human cell lines via an image-based cell content analysis system. Cell counts are presented as residual cell percentages (%) compared to the DMSO control (black). Gray bars represent the cytotoxicity controls (Taxol, Doxorubicin, and Roscovitine), and the blue bars, Ase3 peptide.

The effect of the peptide on the biofilm of *S. epidermidis* ATCC 35984 was evaluated by scanning electron microscopy (SEM) at different incubation times (1, 4, and 24 hours) that correspond to the main stages of biofilm formation: initial adhesion, organization, and maturation. Micrographies are shown in Figure 12. From the initial stages of biofilm formation, a decrease in the adhesion of bacterial cells to the polystyrene plaque in the samples treated with Ase3 is observed compared to untreated controls. In addition, the external appearance of cells exposed to the peptide is very similar to those of untreated control groups, corroborating previous data that the peptide does not induce cell death (which could be suggested if changes were identified in the bacterial cell wall).

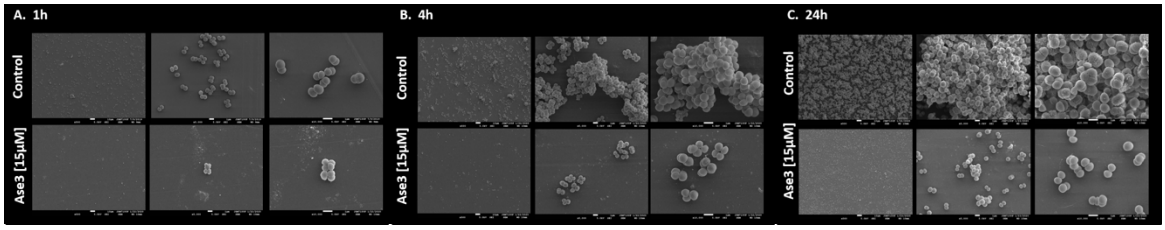

Figure 12: Scanning electron microscopy images of polystyrene slides after 1, 4, and 24 hours of incubation with a culture of S. epidermidis ATCC 35984. First line: control biofilm formed in the absence of peptide. Second line: biofilm formed in the presence of 15µM Ase3 peptide. (A) Biofilms in the early stage of adhesion (1 hour). (B) Structured biofilms (4 hours). (C) Mature biofilms (24 hours).

In addition to the SEM analysis, transmission electron microscopy (TEM) images were also obtained. The images show, as observed in the previous ones, the integrity of the cell walls of the bacteria exposed to the peptide, as observed in the cells of the control groups, Figure 13. It can also be observed that biofilms treated with Ase3 present a small amount of matrix around the cells and this matrix has a fibrillar aspect distinct from what is observed in control biofilms, suggesting that the mechanism of action is linked to the interaction with the matrix and not directly with the bacterial cells.

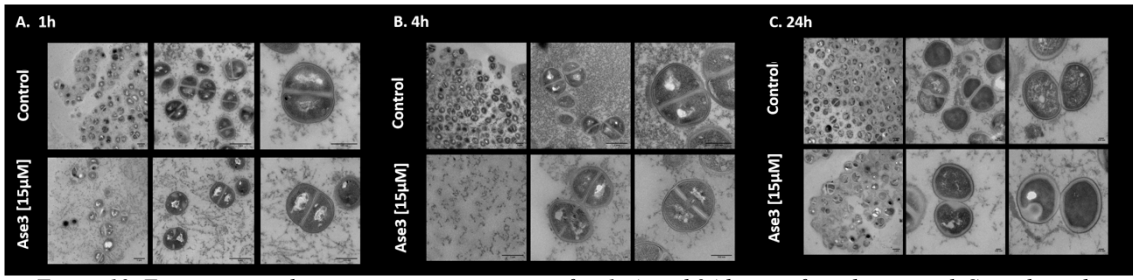

Figure 13. Transmission electron microscopy images after 1, 4, and 24 hours of incubation with S. epidermidis ATCC 35984 culture. First row: control biofilm formed in the absence of peptide. Second row: biofilm formed in the presence of 15µM Ase3 peptide. (A) Biofilms in the early stage of adhesion (1 hour). (B) Structured biofilms (4 hours). (C) Mature biofilms (24 hours).

In order to confirm the interaction of the peptide with the matrix produced by the biofilm of *S. epidermidis* ATCC 35984, preliminary assays were performed with a fluorescent label in order to locate it by confocal microscopy. For this purpose, Ase3 was labeled at the N-terminal part with fluorescein using FITC (fluorescein isothiocyanate). However, the direct functionalization as the use of a linker between the peptide and the fluorescent probe led to inactive compounds (Figure 14)

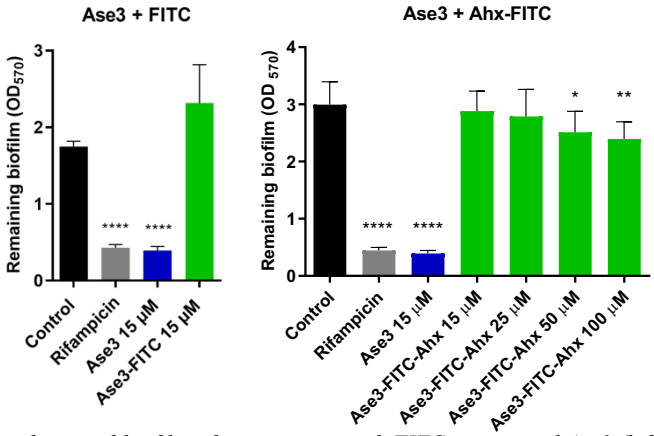

Figure 14: Remaining bacterial biofilm after treatment with FITC-conjugated Ase3 (left) and with FITC spacer-conjugated Ase3 (right).

To bypass these limitations, real-time molecular self-assembly assay was used as an investigation strategy to evaluate the interaction of the peptide with the biofilm matrix, as shown in Figure 15. This *in vitro* assay is based on the polymerization kinetic analysis of the components that mimic those found in *S. epidermidis biofilms* in the presence and in the absence of Ase3 peptide. The results evidenced a change in the polymerization profile in the presence of the peptide, leading to the hypothesis that the compound is able to disarray the matrix assembling.

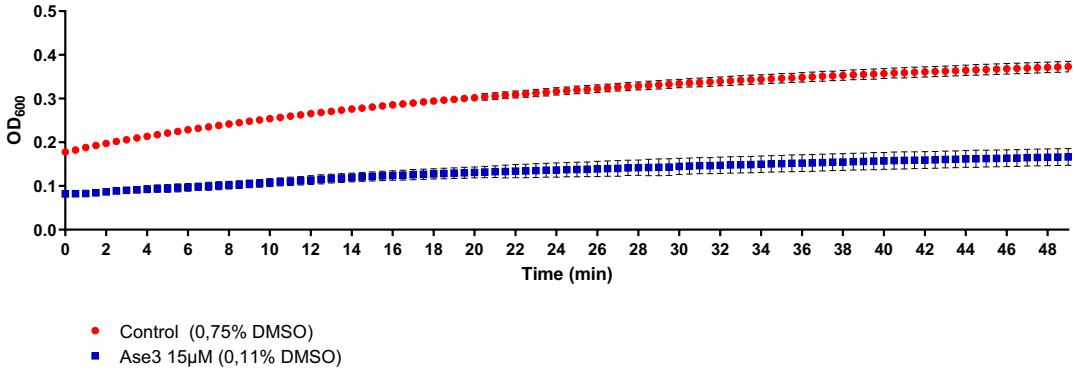

Figure 15: Polymerization kinetics of artificial matrix components in vitro in the presence and absence of Ase3 peptide.

A comprehensive analysis of the obtained data shows that the discovered short amino acid sequence has shown high biological activity *in vitro* against two pathogens of clinical importance worldwide, *S. epidermidis* and *P. aeruginosa*, that were not toxic to any of the 7 human strains evaluated and the activity of the peptide is not dependent regarding bacterial cell death. This discovery aligns with current proposals for anti-virulence molecules that minimize the risk of developing bacterial resistance. Scanning and transmission microscopy, CFU/mL, and artificial matrix *in vitro* analysis strongly suggest that the mechanism of action is based on the interaction of the peptide with the matrix components of the biofilm, even though the fluorescent labeling attempts were unfruitful due to the loss of activity by the N-terminus blockage.

Because of their peculiar characteristics, antibiofilm peptides were considered valid candidates to tackle biofilms, but issues such as poor absorption, biodistribution, metabolism, and excretion properties may explain their failure as antibiofilm agents. An emerging strategy relies on the development of peptidomimetics to overcome the main problems regarding natural peptides. Peptidomimetics are molecules whose pharmacophores mimic a natural peptide or protein in a tridimensional space and which maintain the ability to interact with biological targets, exhibiting pharmacological effects. Those compounds were designed not only to mimic natural peptides but also to overcome their drawbacks.

III. Peptidomimetics

1. Concept

The peptidomimetics concept was a huge breakthrough in several areas of science, more deeply in structural biology, where protein-protein interactions are fundamental for the understanding of cellular processes. Like natural peptides, peptidomimetics have a primary and a secondary structure, sometimes they can have tertiary and quaternary too[48]. Those suprastructures are fundamental for the interactions with proteins, receptors, and enzymes.

In the 1970s, Hughes and Kosterlitz[9] identified that endogenous pentapeptides enkephalins were able to inhibit acetylcholine release from nerves. The same pharmacological effect was observed with morphine. Those findings led to the discovery of molecules that can mimic the structure of peptides. Figure 16 shows the similarity of the active portion of morphine and [Met^5]enkephalin that binds to the receptor[49]. These

discoveries were an important foundation for the entire peptidomimetics development concept. In the early 1980s, Farmer and Ariëns[50] introduced the concept that non-peptidic molecules can play the same role as peptides by binding in the exact same site, developing the term peptidomimetic.

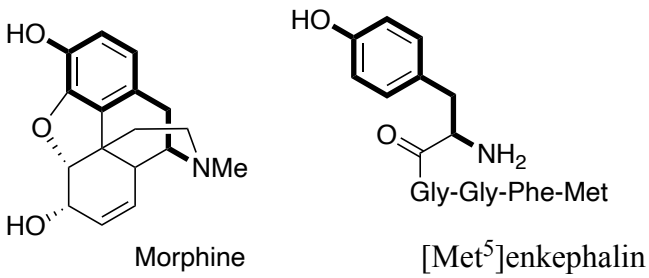

Figure 16: Structural similarities of the pharmacophoric feature in bold of morphine and [Met[5]]enkephalin.

2. Classification and illustrative examples

At the end of the 1990s, Ripka and Rich[51] started to classify the different types of peptidomimetics, placing them into three categories, depending on their structural and functional characteristics:

- Type I – Structural mimetic: Those molecules keep the surrounding topology of the amide bond and normally the backbone structure too. Several bioisosteres can be used.
- Type II – Functional mimetic: These types of compounds may show different structures, quite far from the original peptide, but the biological response must be the same, even when the bidding site is not the same.
- Type III – Functional-structural mimetic: Novel backbone templates, nonrelated to the original peptide, but containing the needed pharmacophores to generate interaction in the same receptor as the original peptide.

In the beginning of the 21[st] century, Adessi and Soto[52] proposed a new classification, from conservative to drastic, based on the importance of the chemical modification, keeping the same pharmacological effect:

- Modified peptides: Peptides with small modifications. The peptide backbone is conserved.

- Pseudopeptides: Partially modified peptides. In those molecules, the amide bond can be changed and/or modified by some chemical groups. Introducing or withdrawing some side-chains is also possible.
- Peptidomimetics: Molecules that no longer contain peptide bonds, but they can present amide bonds.

` Due to inconsistent literature classification of peptides and peptidomimetics, from very narrow, focusing only at the amide bond, to broader, non-peptidic molecules that keep only the same biological mechanism, in the middle of the 2010s, Grossmann and his team[48] introduced a new classification, broader than the previous ones. The authors have suggested a new classification with four classes of peptidomimetics, A to D, in which A keeps the most similarities with the parent peptide and D the least:

- Class A – Modified peptides: Minor variation in the amino acid backbone or in its side chain.
- Class B – Modified peptides/foldamers: All the modified peptides from class A and foldamers.
- Class C – Structural mimetics: Non-peptidic scaffold with substituents that mimic the topology of the natural peptide.
- Class D – Mechanistic mimetic: Non-peptidic molecule that presents the same mode of action of its natural peptide without a direct link to its topology.

Peptidomimetic chemistry is a delicate balance between a way to modify the peptide bond into more resistant chemical entities and trying to keep the molecular topology. Those modifications can be done in several ways:

a) Local modifications

The peptide bond is weak towards proteolysis and this is one of the major drawbacks in peptide drug design. Several attempts have been made to try to avoid molecular degradation[53,54]. The nitrogen can be substituted with isosteric atoms or groups, such as oxygen, keto-methylene, or *N*-hydroxyl; the alpha carbon can be replaced with nitrogen atoms or boron atoms, the carbonyl group has been replaced with thiocarbonyl,

methylene, phosphinic and boronic groups (Figure 17A). A silanediol substitution has been studied too, with interesting *in vitro* results[55,56].

Retro-inverso peptides have been also proposed[57], which consist in an amino acid moiety in which the relative positions of the original amino and carboxylic groups have been reversed, although this kind of peptides no longer had so many reports in the literature. Some modification of the amino acid structure backbone is shown in Figure 17B.

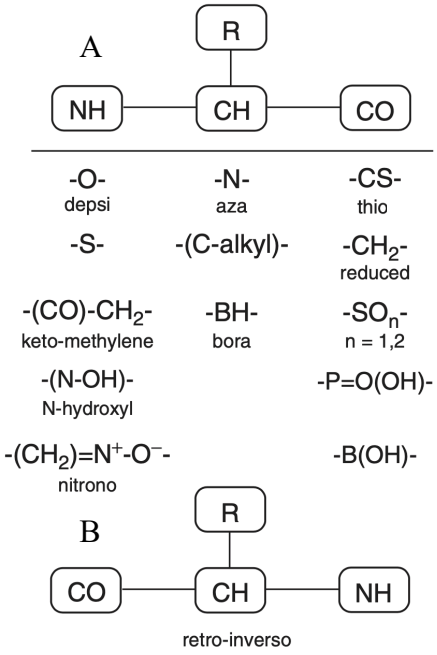

Figure 17: Some modifications of the amino acid, where A shows the possible modifications and B, the inversion of the backbone structure of the peptide.[58]

b) Cyclic peptidomimetics

Cyclized peptides are classical peptidomimetics. The main idea relies on the rigidification of the molecule, which help keep the active conformation due to its rigidity, it is harder to fit into the catalytic pockets of the proteases, increasing its biological half-life, and being more specific to the target. Also, as a cyclic molecule, the absence of the N- and C-terminus extremities decrease its recognition by proteases[59], increasing stability.

There are basically four types of cyclic peptidomimetics[60]: head-to-tail, head-to-side chain, side chain-to-tail, and side chain-to-side chain. The most popular approach is

the head-to-tail generation of a cyclic peptide *via* amide bond formation according to standard peptide chemistry. Another popular approach is the side chain-to-side chain cyclization, this can occur willingly as a prior design or can occur naturally, if it is a cysteine-containing peptide, due to the formation of disulfide bonds.

The cyclization strategy was reported as an alternative strategy to proteolysis-targeting chimeras (PROTACs)[61]. Huang et al.[62,63] have described a cyclic γ-AApeptide (Figure 18) with high affinity to E6AP HECT domain from a screening of 56 different molecules. This enzyme is associated with the human papillomavirus and regulating pathways implicated in neurodevelopmental disorders. This peptidomimetic can stimulate the ubiquitination of E6AP, leading to its degradation.

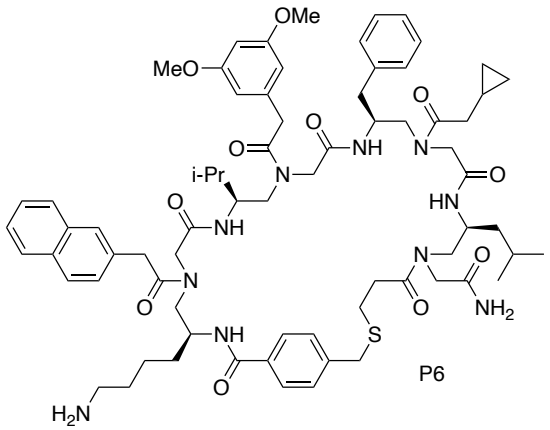

Figure 18: Cyclic γ-AA peptide with high affinity to E6AP HECT domain.

Wtorek et al.[64] reported two new isomeric cyclic opioid β-AApeptides. The natural peptide has shown a high affinity for the mu and kappa opioid receptors, but the mimetic only has an affinity for the mu one, Figure 19.

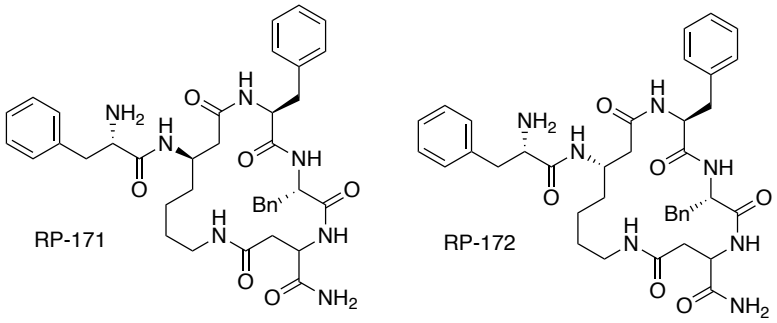

Figure 19: β-AA cyclic peptides.

The synthetic team has used Arndt–Eistert homologation reactions to be able to build the non-commercial β-amino acids, as shown in Scheme 1.

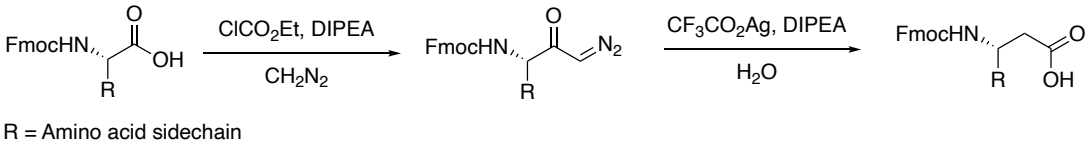

Scheme 1: β-amino acids synthesis by Arndt–Eistert homologation.

c) Backbone modification

The highest degree of modification is the backbone modification, this alteration can be so drastic that can even exclude the amide character of the peptidomimetic. The chemical synthesis of those compounds is more related to classical organic chemistry than peptide chemistry itself. Those molecules have a rigid structure, normally cyclic, and attached to that, structures that mimic the amino acid residues, as an example, in Figure 20, the thyrotropin-releasing hormone (TRH) mimetic contains a cyclohexane scaffold that replaces the peptide backbone while keeping the pharmacophoric groups[65]. A few more examples of peptidomimetics will be presented in the next paragraphs.

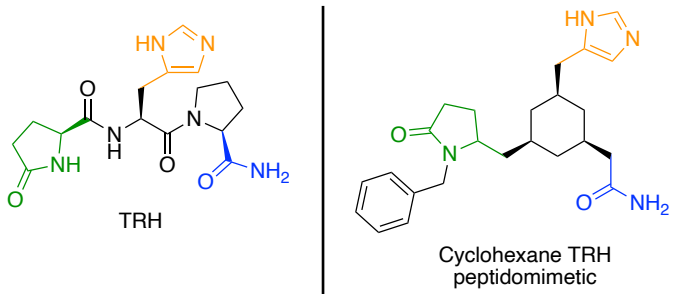

Figure 20: TRH peptide and its peptidomimetic.

Highly active antiretroviral therapy (HAART) is the most effective protocol for HIV/AIDS patients, and protease inhibitors play a very important role in managing this serological status. HIV-1 aspartyl protease, which contains an aspartic acid in the active site that is crucial to the catalytic mechanism, cleaves a polyprotein precursor encoded by the HIV-1 virus genome to produce mature active proteins. The HIV-1 protease enzyme activity can be inhibited by blocking the active site of the protease. In 1995, saquinavir was the first FDA-approved HIV protease inhibitor as a transition-state peptidomimetic, aligning at the enzyme active site (Figure 21). Since then, nine other protease inhibitors

were approved and are on the market today. All those drugs mimic the initiation cleavage site of the HIV-1 polyprotein, but they act as an enzymatic inhibitor, barring the formation of the mature virus[66].

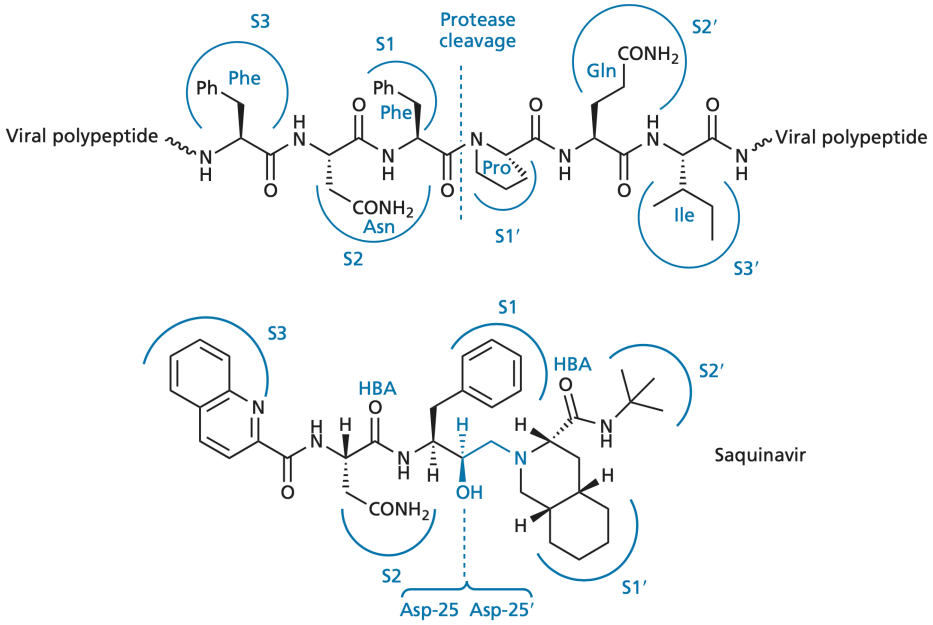

Figure 21: The pentapeptide sequence (Leu– Asn–Phe–Pro–Ile) that was identified as the active site and served as the basis for inhibitor design (top). Saquinavir and its interactions in the active site of the HIV-1 aspartyl protease (bottom).[67]

The brand-new antiviral nirmatrelvir is also considered a peptidomimetic. Associated with ritonavir in Paxlovid®, this combination is the only approved drug for SARS-CoV-2 infection[68], that causes the severe acute respiratory syndrome. Nirmatrelvir acts as a protease 3C-like inhibitor leading to the shedding inhibition of the viral polyprotein[69].

C. AApeptidomimetic of Ase3

In the attempt to improve the biological properties of Ase3 peptide, a novel peptidomimetic was proposed. AApeptides are a conservative approach for the transformation of an α-peptide into a peptidomimetic with a higher success rate since these molecules keep a huge similarity with their parent compounds.

I. AApeptides

AApeptides are derived from the term *N*-acylated-*N*-amino ethyl amino acids and are used as peptidomimetic molecules since those molecules can imitate to some extent the tridimensional structure of the natural peptides and normally have more biological stability toward proteolysis due to its non-natural carbon backbone[70].

AApeptides consist of units mimicking 2 adjacent residues from the natural peptide. These pseudopeptides present two different side chains, one from a regular natural amino acid side chain and the other one from a carboxylic acid residue connected to the tertiary nitrogen as an amide. An amino acid sidechain mimetic comprehends the deaminated natural amino acid. Considering the retain natural amino acid residue, two types of AApeptides, α and γ, have been described (Figure 22).

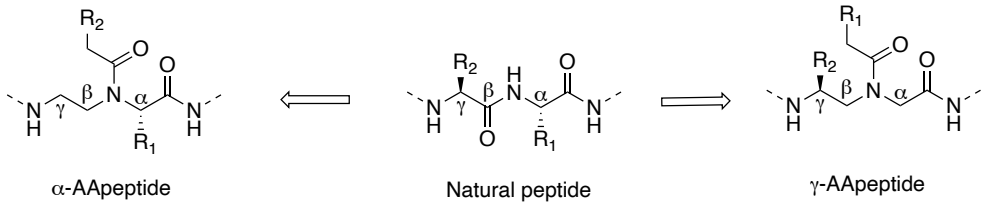

Figure 22: General structures of α- and γ-AApeptide derived from an α-dipeptide.

An AApeptide present fewer chiral centers than the natural peptide, but keeps the same number of functional groups. Due to spatial effects, some of the amides may be bulkier, changing the overall hydrogen bonding number, affecting the biological target interaction[71,72]. AApeptides have more freedom degree than natural peptides due to their methylene and ethylene bridge in the α and γ-AApeptides, respectively. This phenomenon can lead to a higher conformation possibility, resulting in different biological effects compared to the natural peptide sequence.

The synthesis of α and γ-AApeptides differs only in the preparation of the building blocks, although the synthetic pathway is closely related. For both AApeptides, steps of amino acid modification, chain elongation, acylation, and ester deprotection are crucial for the building blocks preparation. Building blocks assembling can be done in liquid or solid phase, using classical peptide chemistry procedures[73]. As a last step, a global deprotection is needed, since protecting groups are usually required to control the expected connections and to avoid side reactions.

1. γ-AApeptides

a) General considerations

Jianfeng Cai[72] and his team developed γ-AApeptides for the treatment of Alzheimer's disease. Aggregation of amyloid β (Aβ) plays a key role in this pathogenesis. Aβ is a proteolytic product of amyloid precursor protein produced by β- and γ-secretases. The imprecise cleavage of γ-secretase at the C-terminus of Aβ sequence results in two major Aβ isoforms: Aβ42 (42 residues long) and Aβ40 (40 residues long)[74]. The best compound is illustrated in Figure 23 and has been described as a potent inhibitor of Aβ40 aggregation, also presenting disassembling properties toward preformed Aβ fibrils.

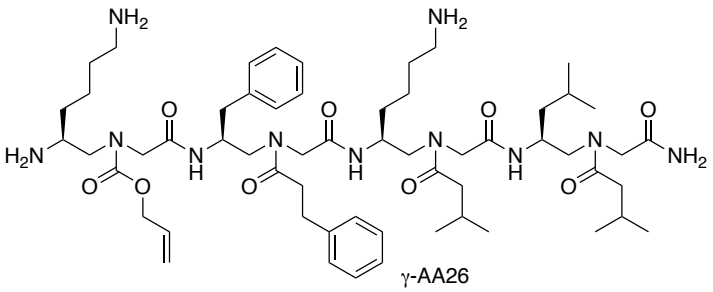

Figure 23: Compound γ-AA26.

b) Building block synthesis

γ-AApeptide building blocks synthesis can be made by conjugation of a Fmoc-amino aldehyde and a glycine ester through a reductive amination reaction. The corresponding secondary amine is then acylated with a carboxyl compound which leads to the expected building block after ester deprotection (Scheme 2)[72]. The required amino aldehyde can be prepared by the reduction of a phenyl thioester or the Weinreb amide[75].

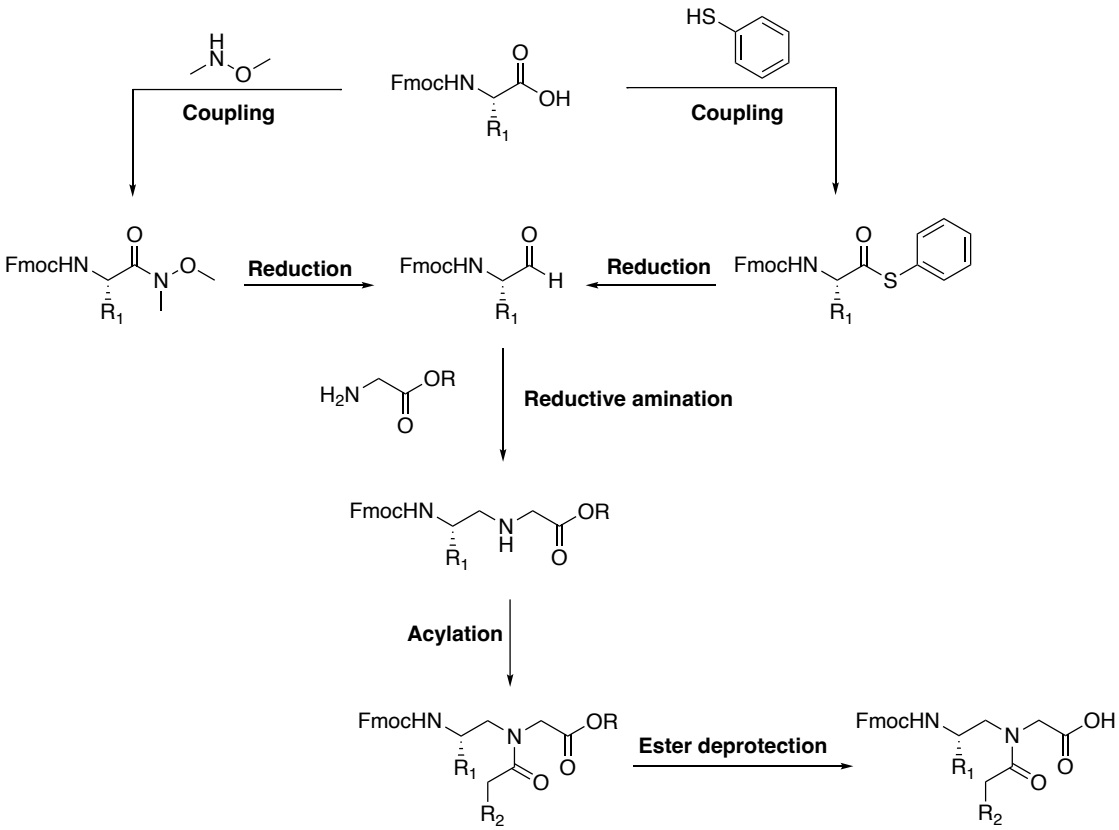

Scheme 2: γ-AApeptides building blocks synthesis.

γ-AA26 synthesis was done using solid phase synthesis and consisted of immobilization of *N*-Alloc protected building blocks on resin prior to acylation and coupling to the other building blocks (Scheme 3). The remotion of the acid labile protecting groups and the cleavage from the solid support is done in the same step, providing the expected peptidomimetic.

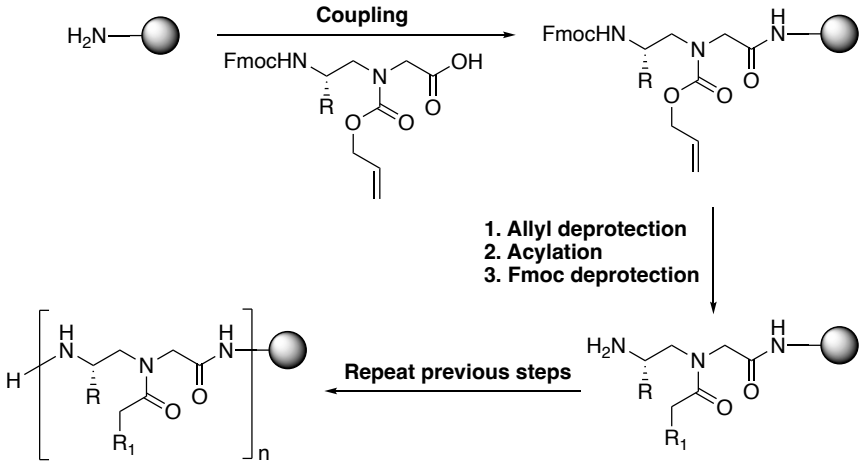

Scheme 3: γ-AApeptide solid phase synthesis.

Hybrids α/γ-AApeptides containing both α-peptides units and γ-AApeptide units exhibit excellent biological activity. Sang et al.[76] described a series of hybrids with broad-spectrum antimicrobial activity. With a mechanism of action based on membrane damage, antimicrobial agents presented a synergic effect when combined with those molecules.

The addition of a hydrophobic tail increases the lipophilicity of the sequences and thereby enhancing their interaction with bacterial membranes. Lipidation was achieved by attaching one or two C16 lipid tails to the α- or at both the α- and ε-NH_2 groups in the lysine residue. Using this approach, this research team was able to produce molecules (*Figure 24*) with high MIC and selectivity indexes toward hemolysis.

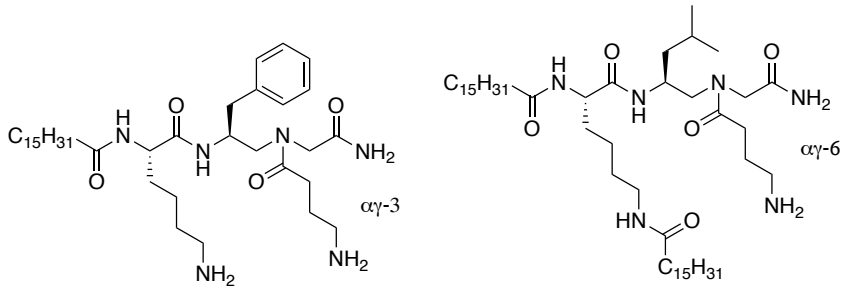

Figure 24: Antimicrobial α/γ-AA hybrid peptides.

2. α-AApeptides

a) General considerations

Jianfeng Cai and his team[77] developed α-AApeptides (Figure 25) designed on the basis of the amphipathic structural motif of host-defense peptides that were active against *Bacillus subtilis*, *Staphylococcus epidermidis*, and *Escherichia coli*. The peptidomimetic was found superior antibiotic in comparison with the natural peptide, not showing any hemolysis at concentrations as high as 250 μg/mL. This early study suggested that α-AApeptides may emerge into a new class of antimicrobial peptidomimetics.

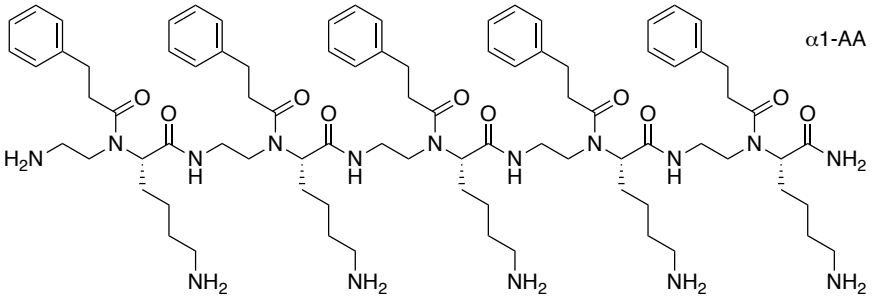

Figure 25: A proposed antimicrobial α-AApeptide.

Mickäel Jean and his team[78,79] have synthesized an α-AApeptide aiming a new lupus treatment. Systemic lupus erythematosus is a chronic autoimmune disease, resulting in autoantibodies production, immune complex formation, and organ and tissue damage. CD95L is a transmembrane glycoprotein that, when cleaved by metalloproteases, releases a soluble form of this glycoprotein. This soluble ligand aggravates inflammation by inducing non-apoptotic signaling pathways in lupus disease. Soluble CD95L activates a calcium response through direct interaction between CD95 and PLCγ1, a cell growth factor.

Using liquid phase peptide synthesis techniques, Jean's team produced a novel α-AApeptidomimetic, Figure 26, able to inhibit CD95-mediated PLCγ1 recruitment calcium signaling.

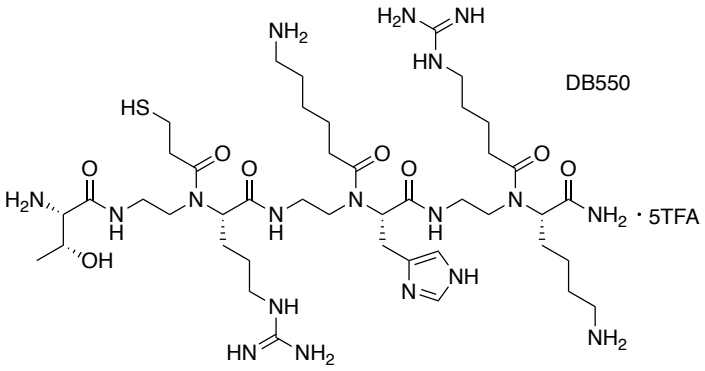

Figure 26: A proposed anti-lupus α-AApeptide.

b) Building block synthesis

Starting from an *N*-Fmoc-protected natural residue, the building block synthesis of an α-AApeptide consists of a *C*-term esterification followed by the deprotection of the α primary amine. Then a chain extension is performed through a reductive amination using Fmoc-glycinaldehyde and a reducing agent to provide a secondary amine which is subsequently acylated with a carboxyl compound. Finally, the carboxylic acid functional

group is deprotected leading to the expected α-AApeptide building block[79,80]. Notice that Fmoc-glycinaldehyde is prepared in 2 steps including a Malaprade–Lemieux–Johnson oxidation of Fmoc-allylamine, Scheme 4.

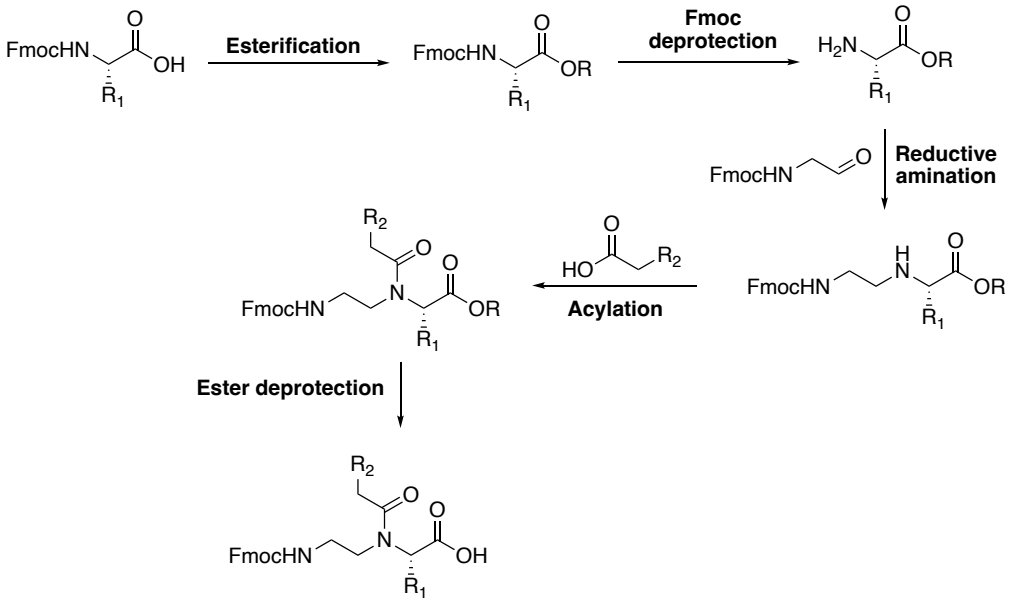

Scheme 4: General synthesis of building blocks.

The key steps of this synthesis will be discussed in the next topics.

(i) C-term functionalization

Esters are a classical way to protect carboxylic acids. Alkyl esters are sensitive to basic conditions and *tert*-butyl esters are acid-sensitive. Allyl and Benzyl esters can be used since they can be easily introduced and removed with high yields and they are orthogonal to several others protecting groups.

A mild protocol with allyl bromide (AllylBr) or benzyl bromide (BnBr)[81] and *N,N*-diisopropylethylamine (DIPEA, DIEA or Hünig's base) is advised, since amino acid molecules as sensitive to harsher conditions. DIPEA is the most used organic base in peptide chemistry. Esterification reactions proceed as a classical S_N2 reaction, where the carboxylate attacks the electrophilic carbon of the bromide (Scheme 5), forming the desired ester.

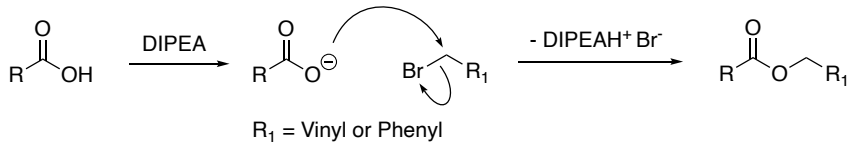

Scheme 5: Esterification mechanism.

Both esters are widely used in AApeptide chemistry, the choice relies on the type of deprotection conditions that will be used, since benzyl deprotection by hydrogenolysis might deprotect some other protecting groups or hydrogenate some sidechains. The purification of the allyl protecting group tends to be more difficult than benzyl.

(ii) Fmoc deprotection

Alkyl amines are common deprotecting agents, being piperidine one of the quickest ones[82]. The deprotection follows an E1cB (unimolecular elimination conjugate base) mechanism (Scheme 6). It is a two-step process, firstly piperidine abstracts a hydrogen to generate a cyclopentadienyl-type anion, then the negative charge moves to the neighboring carbon, expelling the charged carbamate and dibenzofulvene. After protonation, the carbamic acid will decompose into carbon dioxide and will release the free amine. In Fmoc deprotection with piperidine, dibenzofulvene double bond will suffer a nucleophilic addition to form a fluorenyl-piperidine adduct.

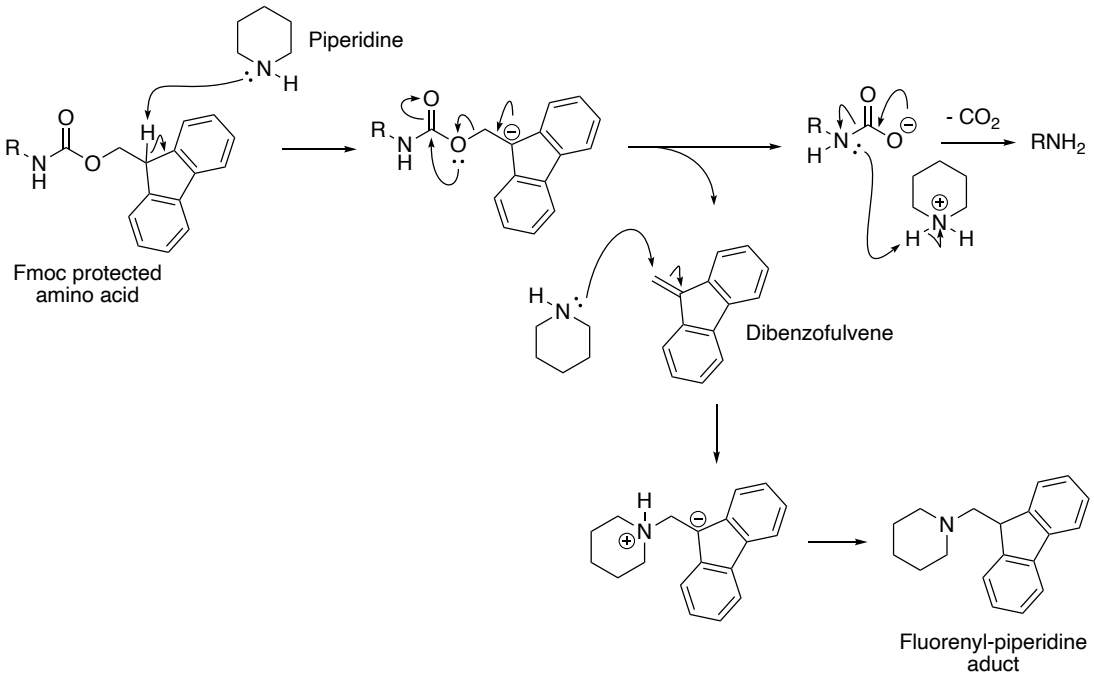

Scheme 6: Fmoc deprotection mechanism.

1,8-Diazabicyclo[5.4.0]undec-7-ene (DBU) is also used for Fmoc deprotection, but in this case, only dibenzofulvene is formed. DIPEA can also deprotect the Fmoc group at a lower rate than piperidine. For this reason, longer reaction times using this base and Fmoc-containing protecting substrates must be done with the awareness of this side reaction.

(iii) Reductive amination

A reductive alkylation is a key step for the preparation of the ethylene bridge and it is essential in AApeptides chemistry. The source of ethyl amine portion comes from glycinaldehyde and must have its amine function protected to avoid competition reactions with the free amine of the amino acid.

Fmoc-glycinaldehyde can be synthesized in two steps using a one-pot protocol on a multigram scale, where allylamine reacts with 9-fluorenylmethyl chloroformate (Fmoc chloride), using sodium bicarbonate as a base, to quantitatively protect the amine[83] (Scheme 7). Fmoc protecting group is one of the most used base-labile protecting groups for amines, as a sterically hindered carbamate, it reduces the reactivity of the nitrogen by electronic and steric effects. It has excellent acid stability and can support oxidative media and hydrogenation conditions, but in some circumstances, it can be cleaved by severer hydrogenation ones, like Pearlman's catalyst or Pt/C, high hydrogen pressure, or longer reaction times[84].

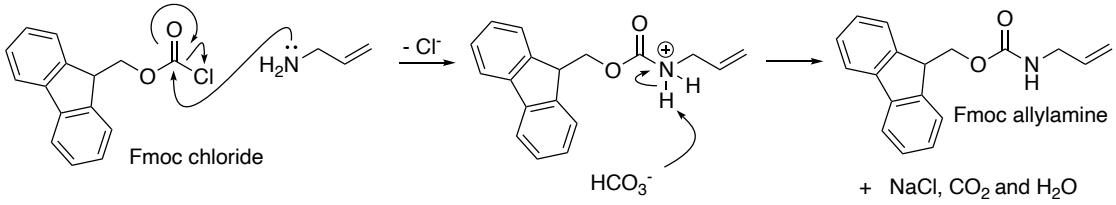

Scheme 7: Allylamine Fmoc-protection reaction mechanism.

The second step is a Malaprade-Lemieux-Johnson oxidation, where the alkene is dihydroxylated by the osmium catalyst, follow by an oxidative cleavage using sodium periodate[85].

Lemieux-Johnson oxidation mechanism includes a cyclic intermediate which comes from a *syn* addition of osmium tetroxide to the double bond. Hydrolysis of this species leads to the 1,2-diol and to osmic acid which is recycled by sodium periodate. The latter oxidant allows also the Malaprade reaction through nucleophilic additions of

the hydroxyl groups to the iodine leading to a cyclic iodate ester which, after a few proton transfer steps, is cleaved into Fmoc-glycinaldehyde and formaldehyde as a byproduct (Scheme 8).

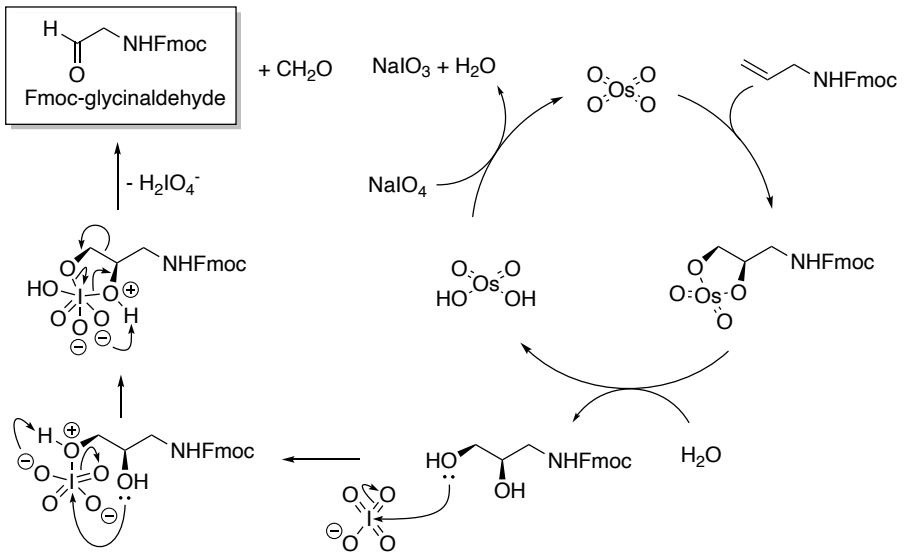

Scheme 8: Malaprade-Lemieux-Johnson oxidation mechanism.

Imines can be easily prepared, where the primary amine will perform a nucleophilic attack on the aldehyde, forming a hemiaminal adduct. By alkylimino-de-oxo-bisubstitution, the adduct will lose a water molecule, by protonation of the hydroxyl group, to form an iminium cation that, with a loss of an acidic hydrogen, will be converted into an imine. A direct reductive amination is also possible where the freshly produced imine can be reduced using a suitable reducing agent[86] (Scheme 9). In this mechanism, the reducing agent can also convert the iminium cation directly into the secondary amine.

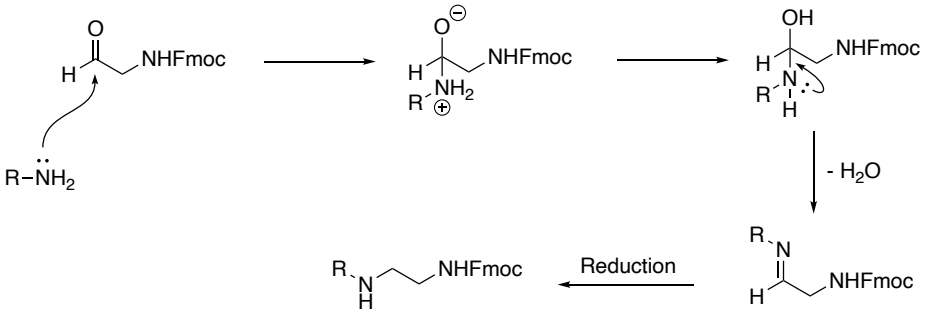

Scheme 9: Direct reductive amination mechanism.

Several reducing agents can be used to perform reductions of the imine like $NaBH_4$, $NaBH_3CN$, $Na(AcO)_3BH$. Even hydrogen gas and a suitable catalyst can be used, being an economical and effective reductive amination method, particularly in largescale

reactions, but the reaction may give a mixture of products and low yields and also can reduce some reducible functional groups[87].

The biggest problem of performing reductive amination of an aldehyde with a primary amine in order to obtain a secondary amine is that the resulting secondary amine, which is more nucleophilic than the primary one, can react with a second equivalent of the aldehyde to form a tertiary amine. To avoid this problem, a milder reducing agent must be used and sodium triacetoxyborohydride (STAB) is a good alternative. The steric and electron-withdrawing effects of the three acetoxy groups stabilize the boron-hydrogen bond and are responsible for its mild reducing properties[88].

STAB decomposes in water and if the solvent is not anhydrous, a larger quantity of the reagent is required. Methanol is not suitable for this reaction either, since increases the aldehyde reduction to alcohol[89]. The most used solvent to perform reductive aminations using STAB is 1,2-dichloroethane (DCE) [90], presenting faster reaction times if compared to other solvents [91].

Shorter reaction times are imperative for these specific subtracts due to the possibility of Fmoc deprotection by the secondary amine formed during the reductive amination.

(iv) Acylation

After the reductive amination step, the secondary amine is ready to be acylated with the carboxylic acid side chain mimetic, this amide bond formation is difficult to form, requiring coupling.

A wide range of coupling agents exists, due in part to their varying effectiveness for particular couplings. Many of these coupling agents were developed to avoid epimerization on amino acids[92], but since the carboxylic acids mimetics side chains do not have a chiral α-carbon, there is no caution regarding this aspect, the choice relies only on the yields and purification.

All mechanisms of coupling agents follow the same three crucial steps: carboxylic acid activation, nucleophilic attack of the amine, and amide bond formation by elimination of the leaving group. Normally the carboxylic acid activation starts with a nucleophilic attack of the carboxylate at the coupling agent and for the formation of the carboxylate, the most used bases are DIPEA and *N*-methylmorpholine (NMM). In some cases, the activated species may react with a second nucleophile that originates from the

reactants or that was added for the purpose to give a more stable active intermediate. To avoid side reactions where the amine can act as a nucleophile and attack the coupling agent before the carboxylate does, a preactivation period is needed, where just the base, the carboxylic acid, and the coupling reagent are mixed together.

(v) Ester deprotection

(a) Allyl

Allyl esters can be deprotected under very mild conditions, being useful for polyfunctional molecules where selective deprotection is needed, with catalytic amounts of Pd or Ru complexes with high efficiency. To perform this deprotection, tetrakis(triphenylphosphine)-palladium(0) ($Pd^0(PPh_3)_4$) is the most used catalyst[93]. The allyl group is removed according to a Tsuji-Trost mechanism (Scheme 10). After the activation of the catalyst, the reaction proceeds through the catalytic cycle with a zerovalent palladium species and the allyl ester. First, the palladium coordinates to the alkene, forming a η^2 π-allyl-Pd^0 complex. The next step occurs an oxidative addition in which the carboxylate is expelled and a η^3 π-allyl-Pd^{II} is created (ionization), followed by a nucleophilic attack of a scavenger that will add to the allyl group regenerating the η^2 π-allyl-Pd^0 complex. At the completion of the reaction, the palladium detaches from the alkene and can restart the catalytic cycle.

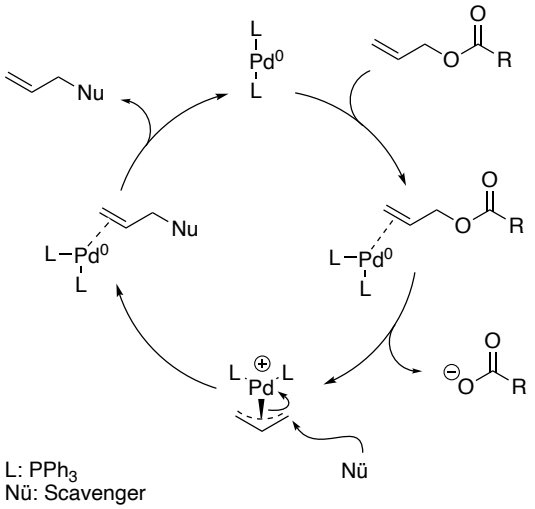

Scheme 10: Allyl ester deprotection catalytic cycle.

As for the π-allyl scavenger the most common ones are dimedone, *para*-toluenesulfinate ($TolSO_2Na$), and a dimethylamino borane complex[94], being efficient

under neutral conditions. In addition to the yield of this transformation, purification concerns must also be considered to decipher which scavenger is the best one.

(b) Benzyl

Heterogeneous hydrogenolysis using palladium, platinum or rhodium on charcoal is a great technique for the deprotection of benzyl esters[95], the catalyst can be filtrated off during the work-up process and the byproduct is toluene, which is easily removed under vacuum. This hydrogenation process proceeds by a Horiuti–Polanyi-like mechanism, where, the carbon-oxygen sigma bond is weakened by the metal and each of those atoms can suffer an addition with the dissociated hydrogen, releasing the carboxylic acid and toluene and regenerating the catalyst.

II. Synthesis of the α-AApeptide of Ase3

Since the sequence of simplification studies on Ase3 was unfruitful, an 11-mer-Ase3 mimic was planned. Based on its sequence, FTWAQWFETQH, the corresponding α-AApeptidomimetic, namely mimAse3, was designed to enhance biological and pharmacodynamical properties (Scheme 11).

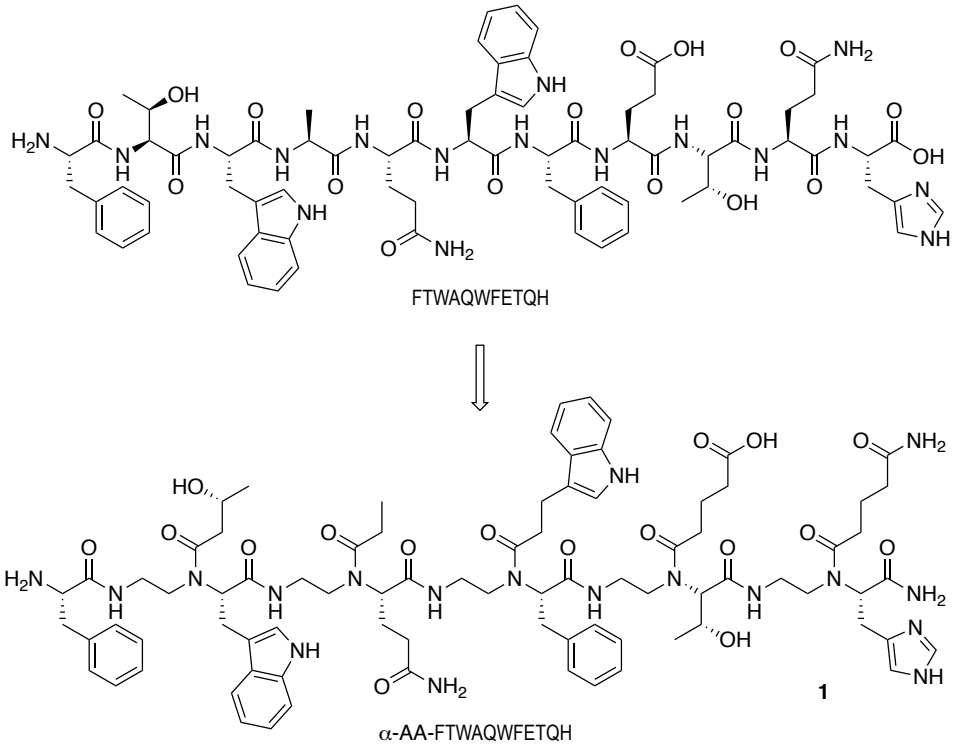

Scheme 11: Transformation of a natural peptide into an α-AApeptide.

1. Retrosynthetic analysis of the targeted mimetic

Considering the synthesis of α-AApeptides as previously mentioned, the retrosynthetic analysis of the targeted α-AA-Ase3 (or mimAse3) highlighted 5 building blocks to prepare (Scheme 12). Of note, the C-terminal building block should be synthesized as a primary amide in order to improve the stability of the peptidomimetic[74].

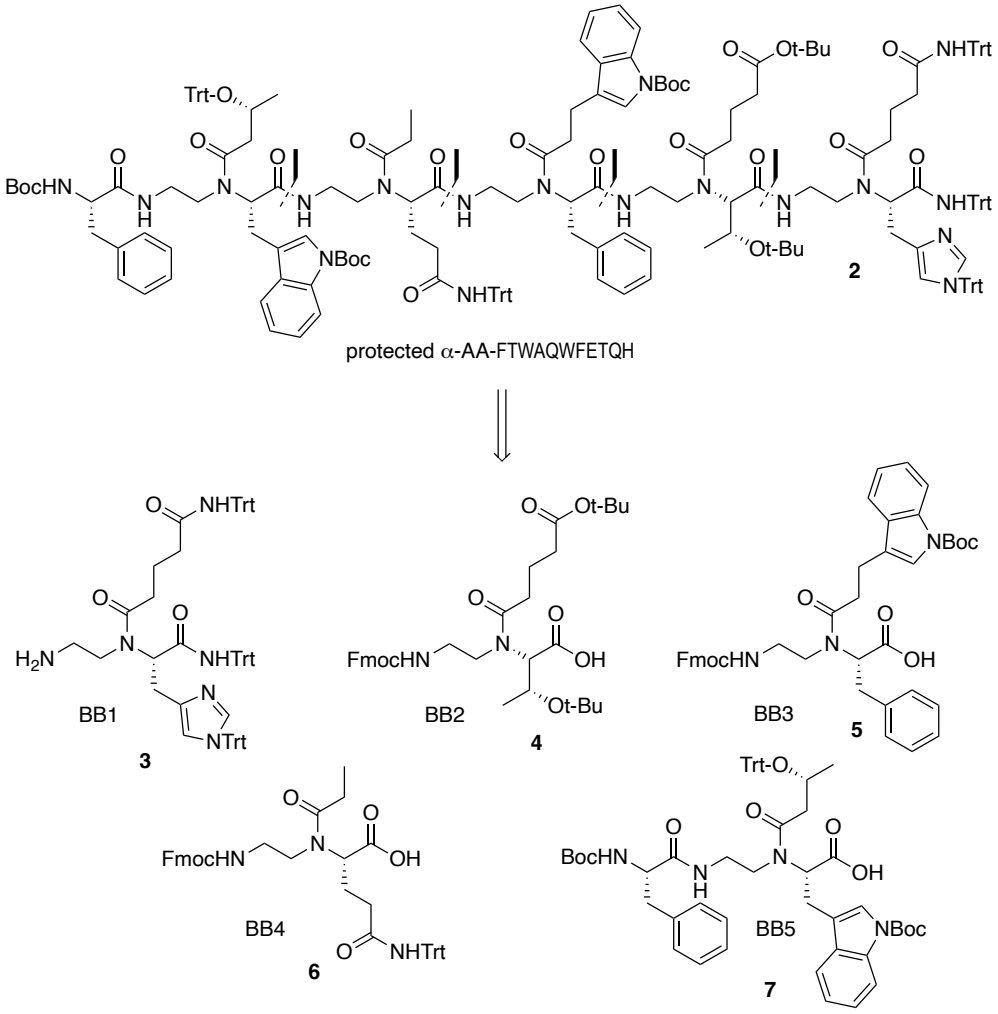

Scheme 12: Retrosynthetic analysis of the prospected compound.

Thus, to reach the goal, orthogonal protecting groups were used to produce the required building blocks and the expected pseudopeptide. The protecting groups for the amino acids sidechain mimetic were chosen in order to match with the respective protecting groups of the natural residues, reducing the number of different deprotection kinetic rates.

Since Ase3 peptide is constituted of an odd number of amino acids, the disconnections can be made using two strategies: to form 5 building blocks containing 2 amino acid residues and one single amino acid or 4 building blocks containing 2 amino

acid residues and one building block containing 3 amino acid residues. In an attempt to maximize the yield, the most convergent one was selected, since fewer building blocks coupling reactions were necessary to build the target molecule. In total, 6 amino acids and 5 amino acids mimetics were used for this synthesis.

The final building block can be synthesized in two different ways: It can have its N-terminal part protected with an acid-labile protecting group, that will be removed along with all the other protecting groups on the global deprotection step or it can be protected with a non-acid-labile protecting group, allowing modifications on the nitrogen, like chain extension or probing labeling. Since the biological results have shown the importance of this position, this final building block was protected with no potential modifications.

Although solid-phase peptide synthesis is a well-established method for α-peptides[96], this technique produces complex mixtures of products yielded during the incomplete coupling and deprotection steps due to the impossibility to perform purifications at intermediate stages[97]. To be able to have more control of the processes and also to be able to work on a multigram scale, this work was performed in solution rather than in solid phase. Liquid-phase peptide synthesis requires the establishment of workup procedures for each intermediate, however, it furnishes high-purity peptides[98].

2. Building blocks synthesis

a) QH building block

The synthesis of the histidine-based building block was performed according to Scheme 13.

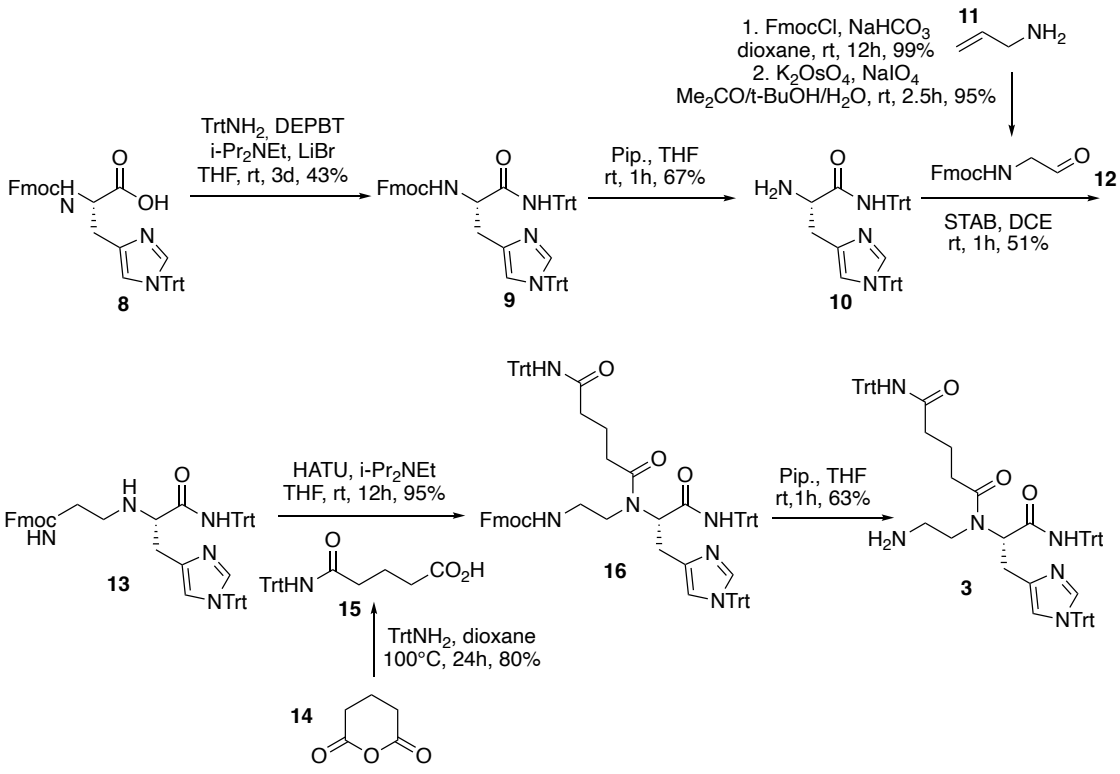

Scheme 13: Synthesis of QH building block.

Since the first building block is presented as a trityl amide, the first and the last step of the synthesis differs if compared to the other building blocks, followed by the same steps of reductive amination and acylation, but, in this case, the Fmoc ethyl amine portion is deprotected.

Trityl group is a wide use protecting group in peptide synthesis because of its chemical stability and due to its steric hindrance may avoid almost all undesirable side reactions. This protecting group is, by far, the most common protecting group suggested for the protection of the thiol group in cysteine, the imidazole ring in histidine, the phenol ring in tyrosine, and in the amide function of asparagine and glutamine[99].

The C-term amide was prepared directly as a protected primary amide through the coupling of Fmoc-His(Trt)-OH **8** with trityl amine. However, the steric hindrance of the latter amine could limit its reactivity (of note, a less hindered amide protecting group (di-(*p*-methoxy)benzyl) was also previously used in the research group, but offered troubles regarding its deprotection). Thus, a mixed anhydride using methyl chloroformate (instead of isobutyl chloroformate as it did not work for this coupling) was the process of choice, despite competition between its nucleophilic attack by trityl amine and the released methanol. Applying these conditions to the protected histidine **8** did not afford the expected amide **9**, only the ester **17**, so other coupling conditions were tested.

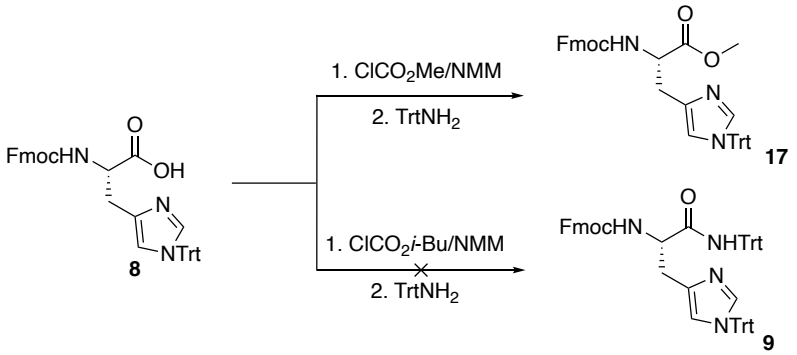

Scheme 14: Attempt to synthesize Fmoc-His(Trt)-NHTrt.

The trityl amide protecting group approach is used to reduce the polarity of the compound, helping in the purification process, but not is overall needed. A primary amide was studied as a viable alternative. Normally, primary amides are stable and are frequently used in peptidomimetics chemistry. The coupling between ammonia and Fmoc-His(Trt)-OH **8** has been successfully done using ammonium chloride as an ammonia source in the presence of EDCI/DHOBt and DIPEA as a base. Unfortunately, the corresponding Fmoc-deprotected compound **18** was unstable as a spontaneous intermolecular cyclization occurred upon the deprotonation step, leading to the 2,5-diketopiperazine **19** (Scheme 15).

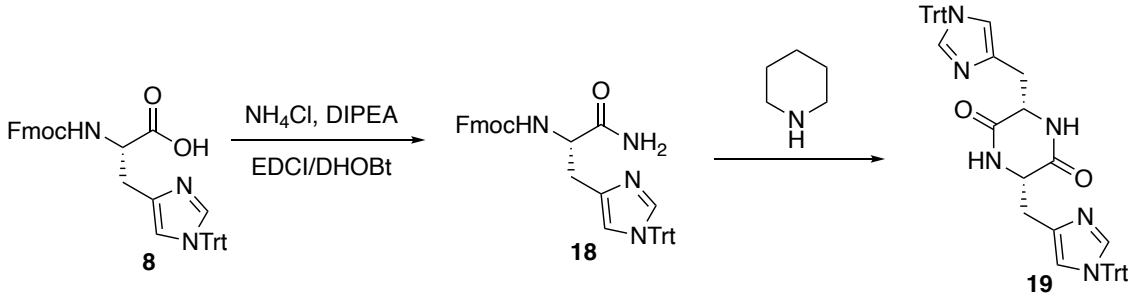

Scheme 15: Formation of the primary amide and cyclization.

The cyclization mechanism occurs with two consecutively S_NAc made by the free primary amine **20** with the loss of an ammonia molecule assisted by the piperidinium cation, forming the obtained compound **19**, as shown in Scheme 16.

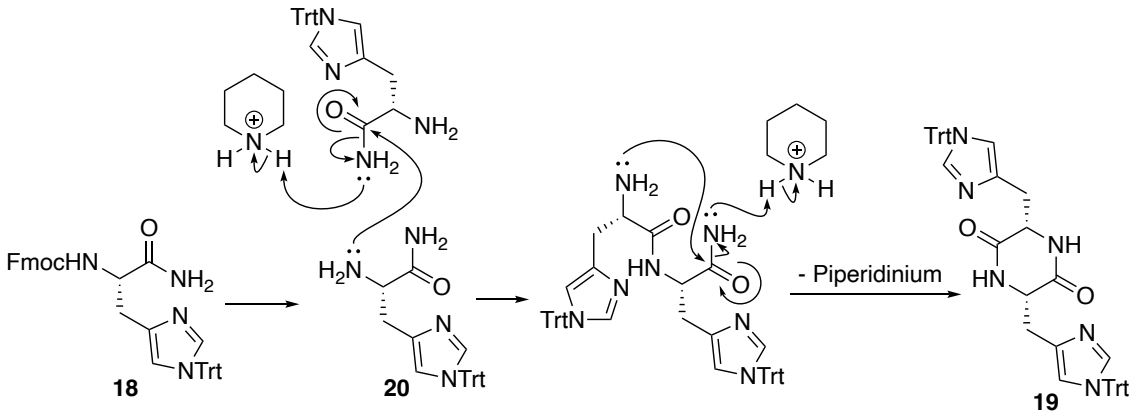

Scheme 16: 2,5-Diketopiperazine formation mechanism.

Based on these results, various conditions have been tested to achieve the coupling between Fmoc-His(Trt)-OH **8** and trityl amine. Among the different coupling agents used, the desired compound was finally obtained by using HATU, EDCI/DHOBt, or DEPBT in THF. The addition of lithium bromide as an additive with DEPBT is known for reducing epimerization reaction[100].

Carboxyl activation by a coupling agent always threatens the chiral center of a carbamate-protected amino acid in basic media[101]. An epimerization reaction can occur by enolization of de α-carbon or by the formation of an oxazolone[102,103]. As shown in Scheme 17, due to the electron-withdrawing effect of the coupling agent, the carboxyl group is more electrophilic and the hydrogen in the α-position is more acidic. A base can form an enolate, that, after protonation, will produce a racemic compound. A base can also form a carboimidate that can attack the activated acyl carbon in order to form a racemic oxazolone, that, after protonation, will lead to a racemic product.

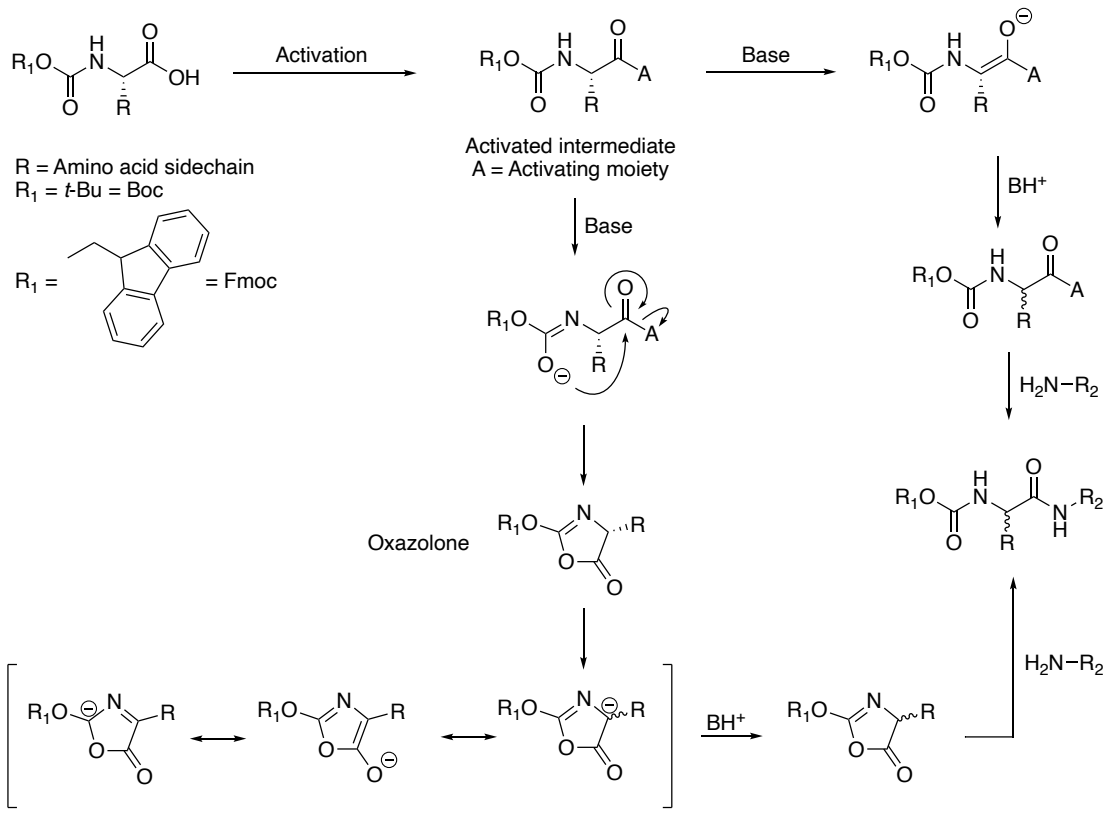

Scheme 17: Epimerization of a α -carbon of a carbamate protected amino acid.

Histidine is the amino acid most prone to racemization, as a result of its imidazole ring[104] and it can form slightly different intermediates, an intimate ionic pair by its basic pyridinic nitrogen of the imidazole ring or a bicyclic zwitterion, formed by an intramolecular nucleophilic attack. Its enolate and oxazolone are shown in Scheme 18.

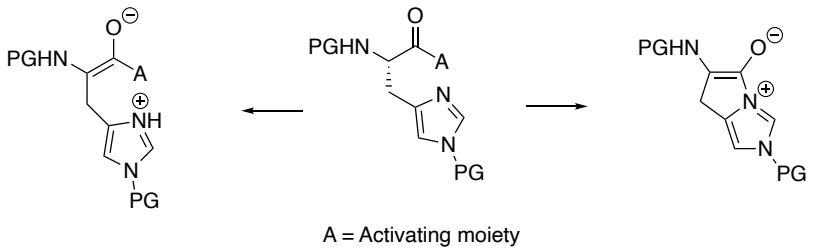

Scheme 18: Oxazolone and enolate of an activated protected histidine.

In order to determine which reaction conditions were the best to avoid epimerization, a racemic trityl amide of **8** was synthesized as a reference for chiral HPLC. The best conditions, presenting 98% of enantiomeric excess, were DEPBT in THF, using DIPEA as a base and LiBr as an additive.

Diethoxy phosphoryloxy benzotriazinone (DEPBT) is a phosphate-based coupling agent that has a dihydrohydroxyoxobenzotriazine (DHOBt) moiety. It is known

for its remarkable resistance to racemization[105] and, because all of its byproducts are water soluble, the purification of the reaction mixture is easier. DEPBT mechanism follows deprotonation of the carboxylic acid by DIPEA, nucleophilic attack of the corresponding carboxylate to the phosphate, with the elimination of DHOBt, the resulting tetrahedral intermediate is decomposed with the release of DHOBt, followed by the addition of the DHOBt anion to the carboxyl group, followed by loss of diethyl phosphate, finishing by a nucleophilic attack of the amine to the activated carboxyl group. This reaction mechanism is shown in Scheme 19.

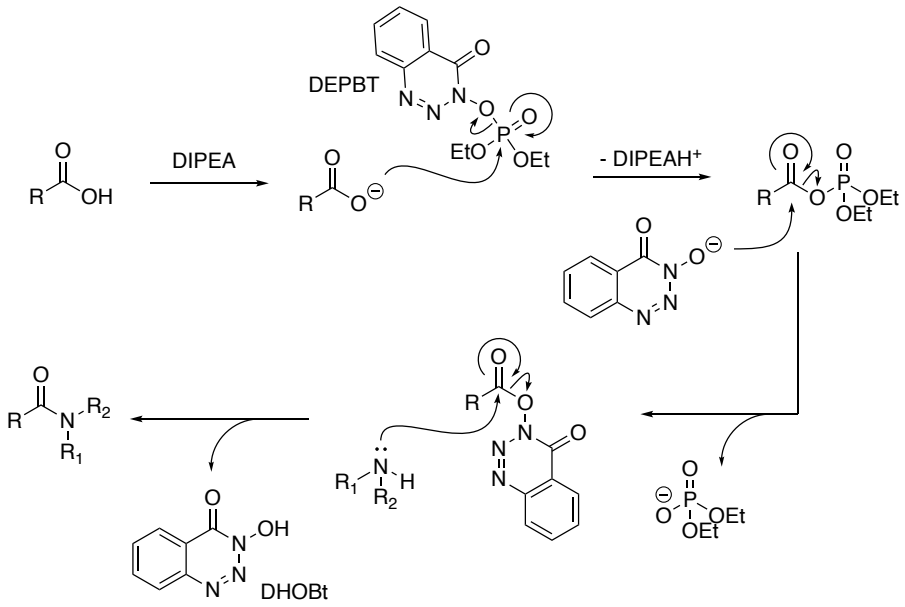

Scheme 19: DEPBT coupling mechanism.

H-His(Trt)-NHTrt **10** was obtained in 67% yield after Fmoc deprotection using piperidine in THF, showing no cyclization side reaction.

HATU/DIPEA was the best coupling condition toward the acylation of **13** with 5-*N*-tritylamidopentanoic acid. Thus, **16** was isolated in 95% yield.

Hexafluorophosphate azabenzotriazole tetramethyluronium (HATU) incorporates hydroxyazabenzotriazole (HOAt) moiety, as a uronium salt of a non-nucleophilic anion. HOAt can form an intramolecular hydrogen bond with the approaching amine, facilitating the formation of the tetrahedral intermediate during the S_NAc, accelerating the chemical reaction[106,107]. This molecule is water soluble, facilitating the purification of the compounds.

The coupling reaction follows the steps: deprotonation of the carboxylic acid by DIPEA, nucleophilic attack of the carboxylate to the uronium reagent, splitting up the

resulting tetrahedral intermediate with the release of the azabenzotriazole, followed by the addition of the released anion to the carboxyl group, followed by loss of a urea derivative, finishing by a nucleophilic attack of the amine to the activated carboxyl group. This reaction mechanism is shown in Scheme 20.

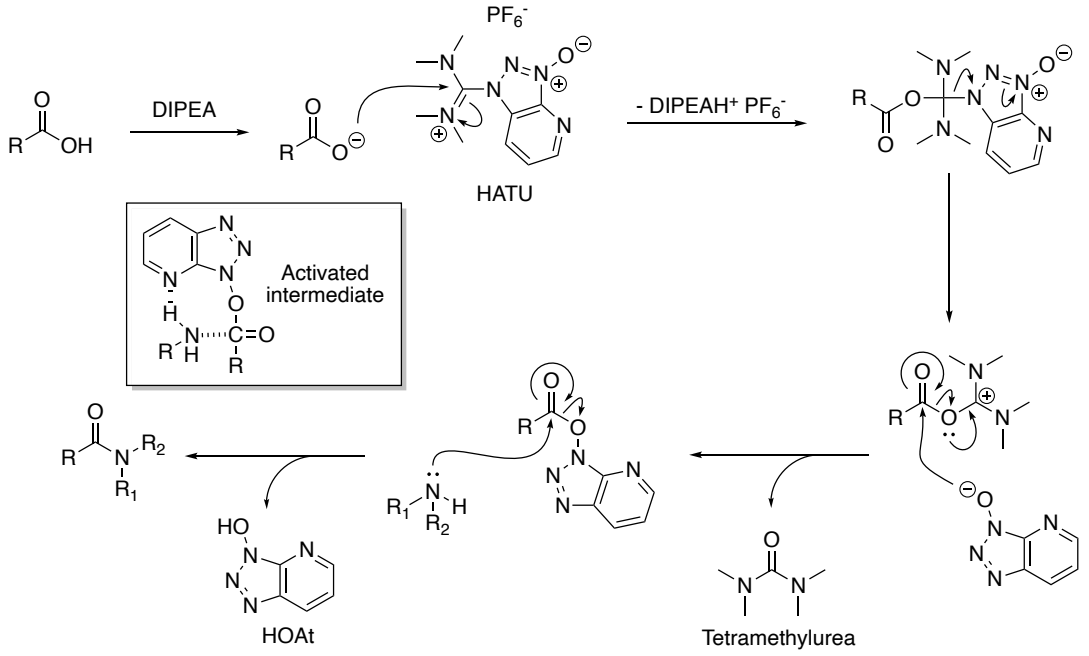

Scheme 20: HATU coupling mechanism.

When the carboxylic acid is not preactivated correctly or the coupling agent is used in excess, the amino group can attack the uronium salt producing an undesired guanidinium ion[108,109]. This is a very common side reaction for uronium reagents. The guanidine formation is shown in Scheme 21.

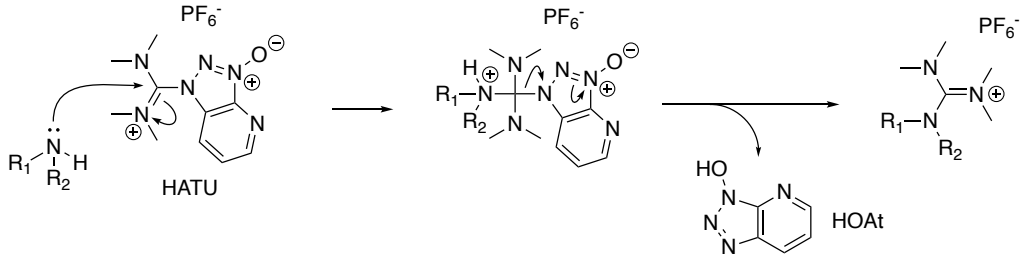

Scheme 21: N-guanidinylation by uronium salt.

All the spectral data obtained for this histidine-based building block and its intermediates were in full accordance with their chemical structures. The obtained overall yield over 5 linear steps was, approximately, 9%.

b) ET building block

The synthesis of the threonine-based building block was performed according to Scheme 22.

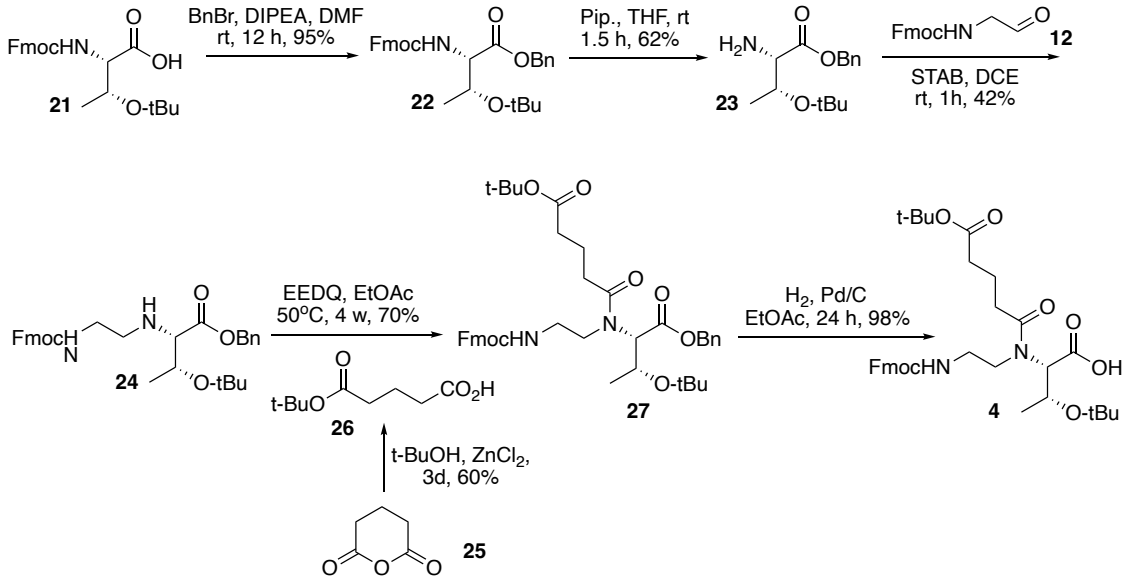

Scheme 22: Synthesis of ET building block.

The coupling between compound **24** and acid **26** presented reactivity issues and only *N*-ethoxycarbonyl-2-ethoxy-1,2-dihydroquinoline (EEDQ) worked, providing the desired compound in 70% yield in a 4 weeks reaction.

EEDQ is one of the only coupling agents that does not need a base for deprotonation of the carboxylic acid[110], the coupling agent itself will deprotonate the acid, releasing ethanol. The carboxylate will perform a nucleophilic attack on the α-carbon of the quinoline and then, the formed carbamate will suffer an intramolecular nucleophilic attack from the sp^2 oxygen of the ester, forming a six-membered ring that collapses, releasing quinoline and forming a mixed anhydride. The amine will attack the mixed anhydride, forming the amide with a release of carbon dioxide, from the decarboxylation, and a second equivalent of ethanol[111] (Scheme 23).

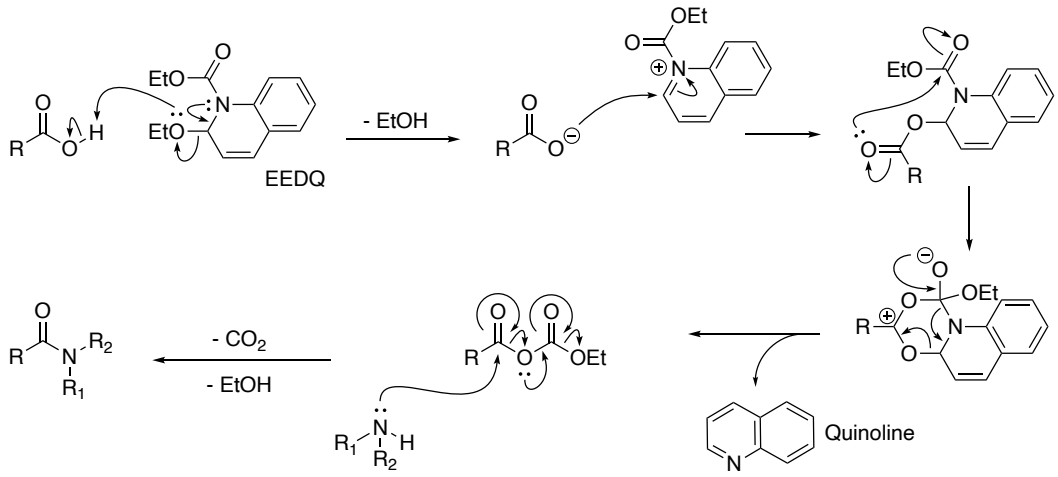

Scheme 23: EEDQ coupling mechanism.

The major drawback of EEDQ is that the first stage of the mechanism, until the formation of the mixed anhydride, is notoriously slow and it is the rate-determining step of this reaction[112]. The reaction was long, but fortunately, it does not need a base to work and, only because of that, the Fmoc group was left untouched.

The first attempt to deprotect the benzyl ester was using ethanol as solvent, but this protocol also deprotected the Fmoc protecting group in just a couple of hours. The fully deprotected compound forms a zwitterion, that is almost impossible to purify, toluene, 9-fluorenylmethane and carbon dioxide (Scheme 24). It is a known problem of Fmoc protecting group and it was detoured by using ethyl acetate as the solvent for the hydrogenation. Almost all of the Fmoc protecting group survived even after 24 hours of hydrogenation and the final acid was obtained in 98% yield.

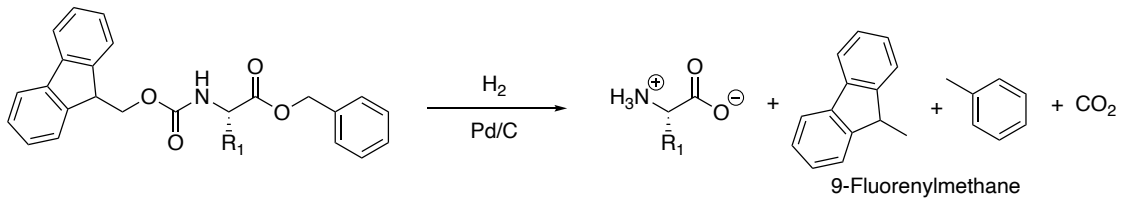

Scheme 24: Hydrogenolysis of Fmoc and Benzyl protecting groups.

All the spectral data obtained for this threonine-based building block and its intermediates were in full accordance with their chemical structures. The obtained overall yield over 5 linear steps was, approximately, 17%.

c) WF building block

The synthesis of the phenylalanine-based building block was performed according to Scheme 25.

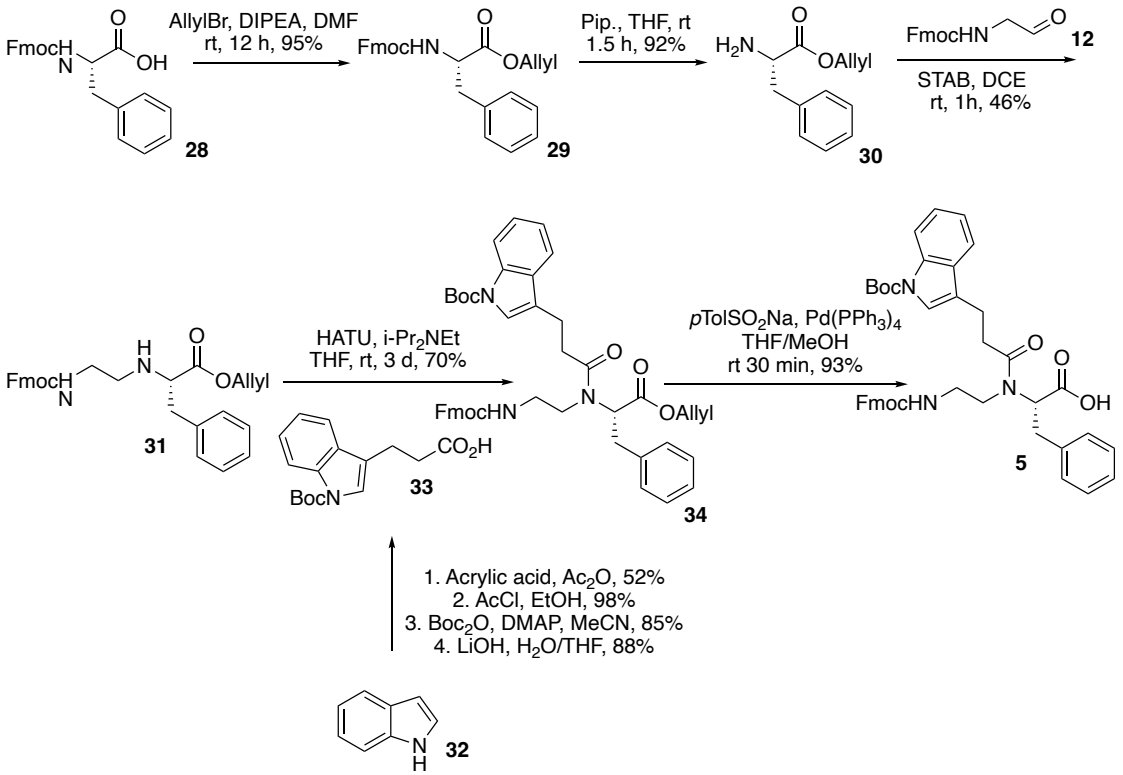

Scheme 25: Synthesis of WF building block.

This building block had its carboxylic acid protected as an allyl ester since the indole moiety on the amino acid mimetic side chain can be reduced to indoline if hydrogenolysis were chosen for a benzyl deprotection.

The direct *N*-Boc protection of indole-3-propionic acid was attempted, but only the bis-Boc compound was formed. The acid was esterified to avoid the nucleophilic attack of the carboxylate into Boc anhydride.

Indole nitrogen atom was successfully Boc protected by using Boc_2O and DMAP as a catalyst. This protecting group is the most widely used for amine function protection. Boc can reduce the nitrogen reactivity due to its electron-withdrawing effect while the *tert*-butyl substituent provides a high steric hindrance. This protecting group can be used to protect the *N*-terminal nitrogen in all amino acids and it is commonly used to protect tryptophane indole ring, the guanidine side chain in arginine, and the primary amine in the lysine side chain.

Boc protecting group can be introduced using di-*tert*-butyl dicarbonate (Boc_2O), with or without the presence of a catalyst. The most used catalyst is 4-dimethylaminopyridine (DMAP) and the protection reaction using this catalyst is shown in Scheme 26.

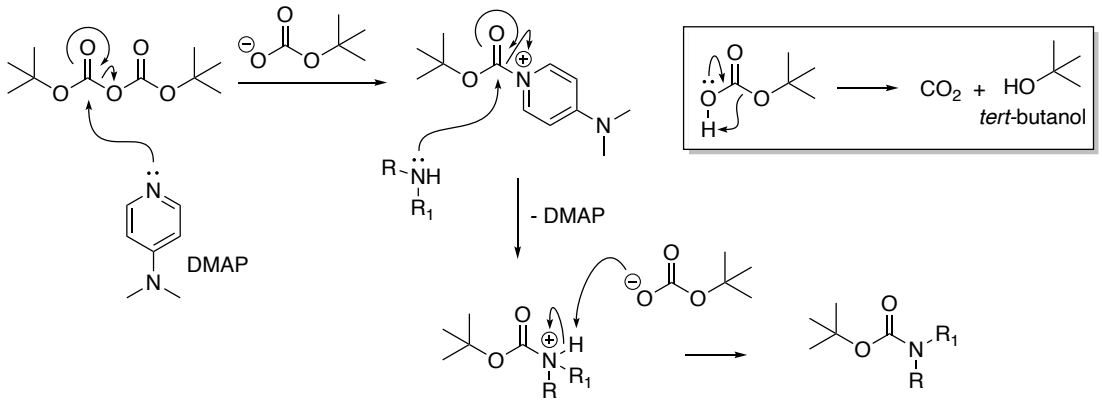

Scheme 26: Boc protection mechanism.

DMAP attacks one of the carboxyl groups of the Boc_2O, forming a highly reactive pyridium carbamate. The amine attacks the carboxyl group, reforming DMAP, and, as the last step, the carbonate takes the acidic hydrogen of the carbamate. *Tert*-butyl hydrogen carbonate decomposes, releasing carbon dioxide and *t*-butanol.

The final step for the formation of acid **33** is the hydrolysis of the ester. Since Boc protecting group is acid-labile, the hydrolysis reaction was performed in a basic medium. To form the carboxylate, the hydroxyl group must attack the electrophilic carbon of the ester, passing throw a tetrahedral intermediate, followed by a loss of an ethoxide anion that will be quickly converted in ethanol by deprotonation of de freshly formed carboxylic acid, forming the desired carboxylic acid during the acid work-up (Scheme 27).

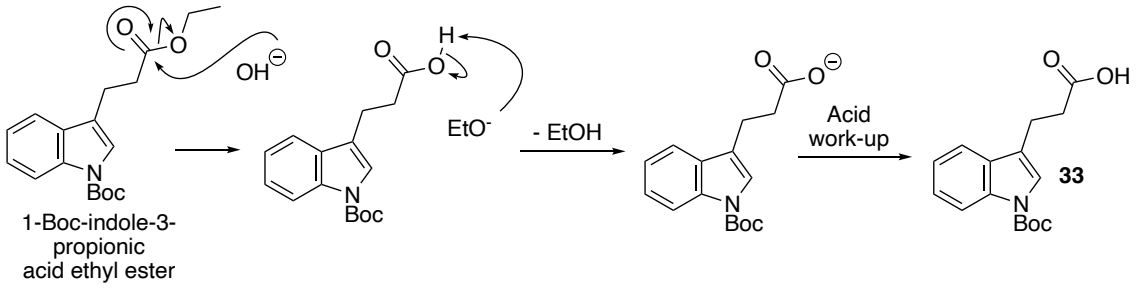

*Scheme 27: Ester hydrolysis as a final step to synthesize acid **33**.*

This deprotection reaction can also deprotect the Boc protecting group in a slower rate than the ester deprotection. For this reason, the reaction time is crucial to minimize the degradation of the compound.

All the spectral data obtained for this phenylalanine-based building block and its intermediates were in full accordance with their chemical structures. The obtained overall yield over 5 linear steps was, approximately, 26%.

d) AQ building block

The synthesis of the glutamine-based building block was performed according to Scheme 28.

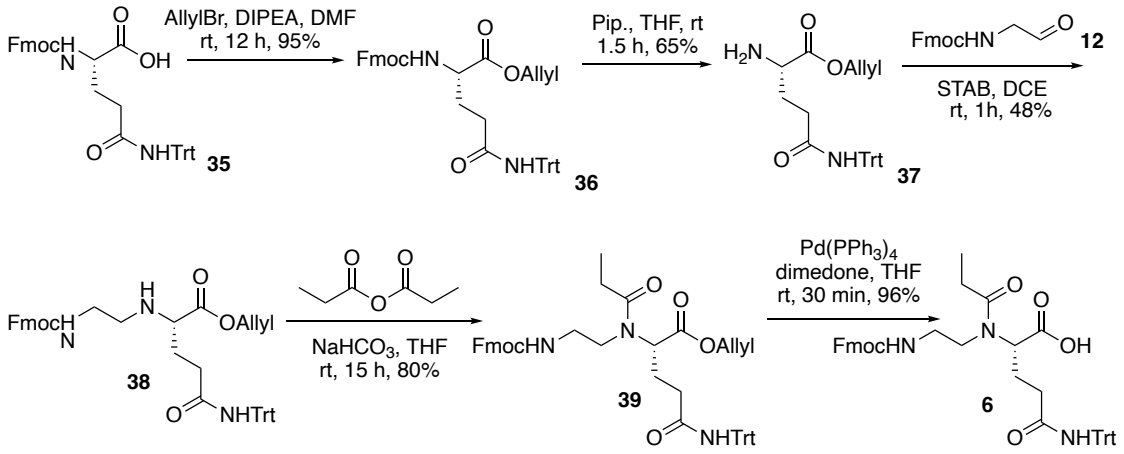

Scheme 28: Synthesis of AQ building block.

This building block contains a trityl, as a glutamine-protecting group, that had already been deprotected under hydrogenolysis by another Jean's PhD student, for this reason, allyl protecting group was used.

Compound **38** was acetylated using propionic anhydride in THF and sodium bicarbonate as a base. Alanine mimetic side chain, along with glycine, proline, valine, and phenylaniline mimetic side chains are commercially available as anhydrides.

All the spectral data obtained for this glutamine-based building block and its intermediates were in full accordance with their chemical structures. The obtained overall yield over 5 linear steps was, approximately, 23%.

e) FTW building block

The synthesis of the tryptophane-based building block is different from the other building blocks, this one is made of two natural amino acids and one amino acid mimetic side chain. Fmoc-glycinaldehyde was not used for the creation of the ethylene bridge, a reductive amination between two amino acids derivatives was used instead. The secondary amine was acylated and the carboxylic acid was deprotected in the same manner as the others building blocks. The synthesis of this tryptophane-based building block was performed according to Scheme 29.

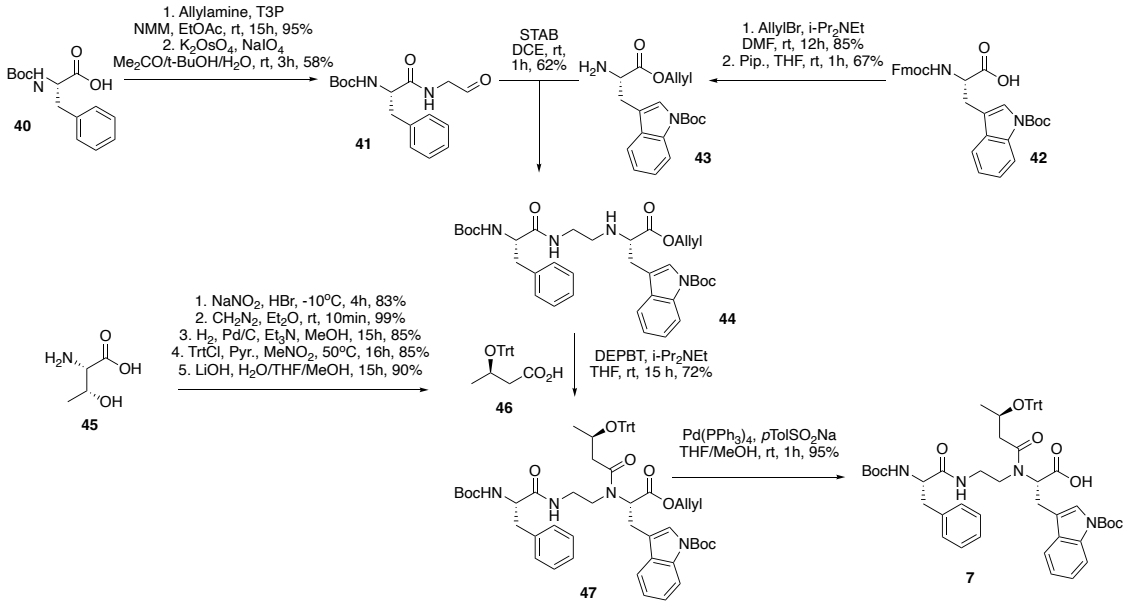

Scheme 29: Synthesis of FTW building block.

To prepare de amino acid derivatives for reductive amination, two steps were needed for each amino acid. Allyl protecting group was chosen over benzyl because of the presence of the indolyl moiety.

Allylamine was coupled with Boc-Phe-OH **40** using T3P as a coupling agent in ethyl acetate (EtOAc) and NMM as a base. All the coupling reagents have worked for this coupling reaction, but T3P was chosen for the easiest purification process. T3P is a cyclic anhydride trimer of propanephosphonic acid. Different from the other coupling agents, T3P most used base is NMM[113]. The reaction mechanism proceeds via an anhydride ring opening by nucleophilic attack by the carboxylate, followed by the formation of a mixed anhydride. The secondary amine will attack the carboxyl group of

the anhydride to yield the amide and, as a byproduct, a water-soluble triphosphonate (Scheme 30)

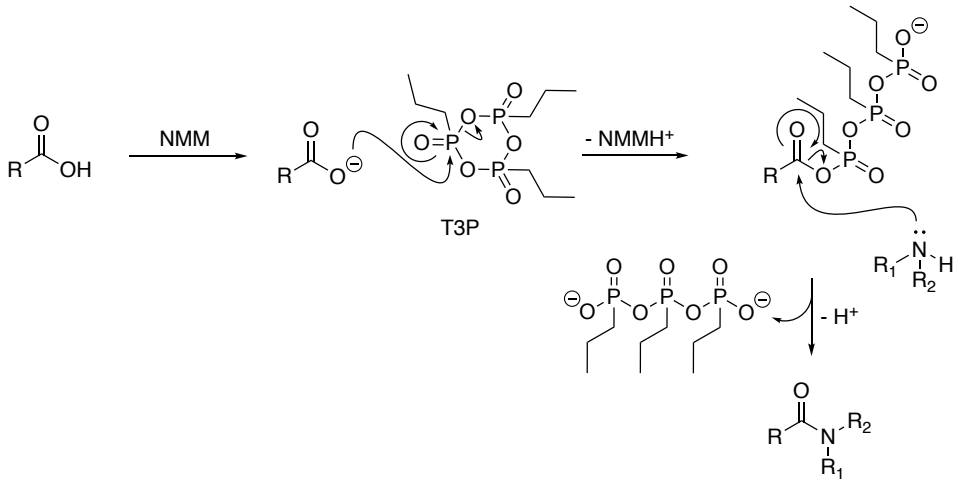

Scheme 30: T3P coupling mechanism.

The allyl amide was oxidized to Boc-Phe-NHCH$_2$CHO **41** using Malaprade-Lemieux-Johnson oxidation with Na_2OsO_4 and $NaIO_4$ in a mixture of acetone, water, and *t*-butanol. The aldehyde was not stable during column chromatography purification, for this reason, the purification was performed as fast as possible to avoid a yield decrease, even though, the purified compound was obtained in 58% yield. This aldehyde was reacted with H-Trp(Boc)-OAllyl **34** to provide the intermediate secondary amine **44** of this building block.

Deaminthreonine **46** was the most complex to achieve of all five amino acid sidechain mimetics. The secondary alcohol on the side chain of the threonine is chiral and, for this reason, the best way to synthesize the optically pure compound is using threonine itself as the backbone for this acid.

L-Threonine **45** was diazotized using $NaNO_2$ and HBr. In an acidic environment, nitrite anion is protonated to generate nitrosonium cation. The amine of the amino acid attacks the *in situ*-formed nitrosonium cation and, after proton transfer steps, water is eliminated and the diazonium salt is formed. Aliphatic diazonium salts containing nucleophilic counterion are unstable and will lead to the elimination of nitrogen gas, forming an unstable secondary carbocation, that will rapidly suffer a nucleophilic attack by the bromine anion (Scheme 31). Even though the bromine atom will be removed later, it is interesting to remark that the stereochemistry of this halogen is *cis* to the hydroxyl group, retaining the original stereochemistry of the amine substituent, even passing throw a carbocation intermediate[114–118]. The hydroxyl group may form a hydrogen bond with

the carboxyl group, forming a six-membered ring intermediate, that, due to the steric hindrance of the axial methyl group, only allows the approach of the bromine ion for the opposite side, adding the bromine in the same side of the hydroxyl group.

Bisulfite solution was used in the work-up to reduce nitrogen oxides that have been formed during the diazotization process. This solution is superior to thiosulphate ones in this case, since, when thiosulphate reduces, elemental sulfur was formed, turning the separatory process more difficult.

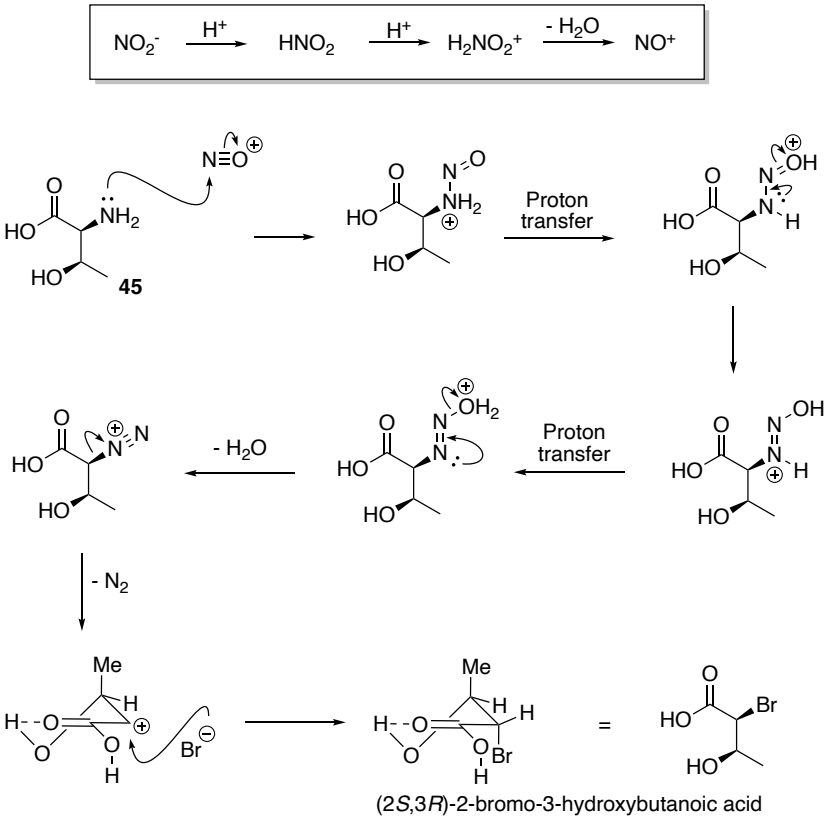

Scheme 31: Diazotization of L-Threonine.

The first attempt to remove the bromine atom was to perform a reduction using zinc and sulfuric acid, using the reported protocol for isoleucine[114], only modifying the substrate. Instead of the debrominated compound, *E*-but-2-enoic acid was formed, as shown in Scheme 32.

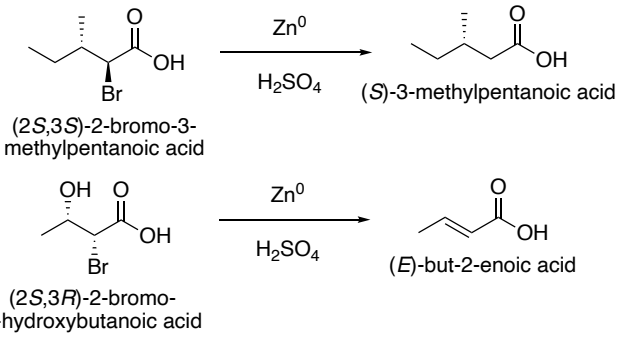

Scheme 32: Attempt to debrominate the deaminated threonine.

In the acidic condition of the reaction, the compound was able to suffer a unimolecular elimination (E_1), forming the undesired unsaturated acid. Another way to debrominate the compound is using hydrogenolysis, but for this synthetic pathway, the carboxyl acid must be esterified. A mild and quick esterification must be used to avoid an elimination reaction.

Methyl (2*S*,3*R*)-2-bromo-3-hydroxybutanoate was synthesized in quantitative yield using diazomethane. Although this reagent is highly toxic and explosive, it is an amazing methodology to perform a fast, efficient, and specific reaction in a neutral environment.

Diazomethane deprotonates the carboxylic acid, forming the alkylating active specie, methane diazonium cation, that is attacked by the carboxylate anion, forming the methyl ester and releasing nitrogen gas (Scheme 33).

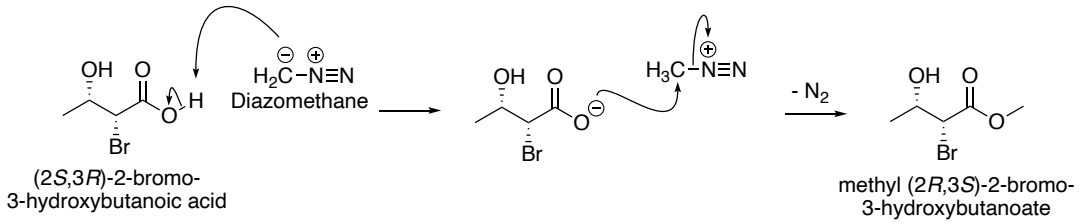

Scheme 33: Diazomethane esterification mechanism.

This reaction was quantitative and there was no need for purification, since the only byproducts are methyl acetate and traces of acetic acid, both easily removed under vacuum.

The ester was then debrominated using hydrogen and palladium on charcoal as the catalyst. The mechanism follows the same steps as the ester deprotection with heterogeneous catalysis, but HBr is formed, for that reason, pyridine was added to neutralize the acid.

The most difficult step of the preparation of this acid was the hydroxyl protection. Since the natural amino acid threonine was acquired as a *t*-butyl protected, the same protecting group was planned to be used. This amino acid mimetic side chain can be protected using silyl ethers, but this protecting group has its one deprotection protocol, and it cannot be deprotected in the global deprotection step, adding one more deprotection and purification step for the, already long, synthetic pathway. For this reason, an acid-labile protecting group was chosen for this hydroxyl group.

Three different methodologies to introduce the *t*-butyl moiety on the hydroxyl group were tested, using two sources of the protecting group, *t*-butyl alcohol, and Boc anhydride under catalysis[119] (Scheme 34). None of the tested conditions work.

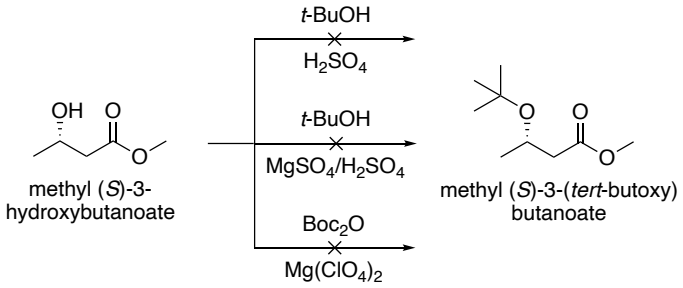

Scheme 34: Attempts to t-butyl protect the hydroxyl group.

The *t*-butyl protecting group was, then, changed for a trityl one with apprehension, since this protecting group is more hindered than the previous one[120]. Trityl group can be introduced using trityl chloride in a S_N1 reaction (Scheme 35).

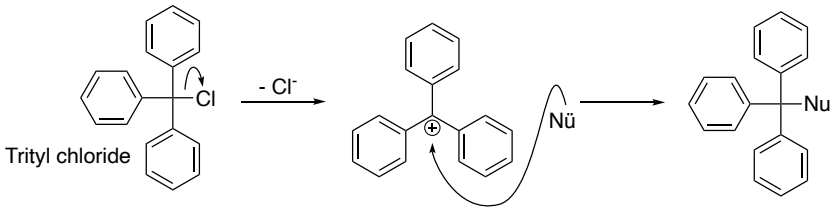

Scheme 35: Trityl protection mechanism.

Initially more classical solvents, THF, dioxane, and DCM, were studied, providing only traces of the product. Unimolecular substitution reactions are favored by polar protic solvents, but they are normally nucleophilic, more than the secondary alcohol of this hydroxybutanoate. *t*-butyl alcohol, one of the only ones classic non-nucleophilic protic solvent, and nitromethane, a non-classic one, were used in this attempt to find a suitable solvent for this reaction. *t*-BuOH did not work, but, fortunately, nitromethane worked, providing an 85% protection yield.

All the spectral data obtained for this tryptophane-based building block and its intermediates were in full accordance with their chemical structures. The obtained overall yield over 3 linear steps was, approximately, 42%.

3. Building blocks coupling

In this step, the amine of the first building block must be deprotected to be coupled with the deprotected carboxylic acid from the second building block, and successively that way, so forth until the last one has been coupled, as shown in Scheme 36. The coupling must always start with the building block containing the C-terminal portion of the peptide, since it is the only one that the carboxyl group is a less reactive amide and, more than that, is protected, otherwise, the nucleophilic primary amine can perform an attack to the electrophilic carbon of the ester.

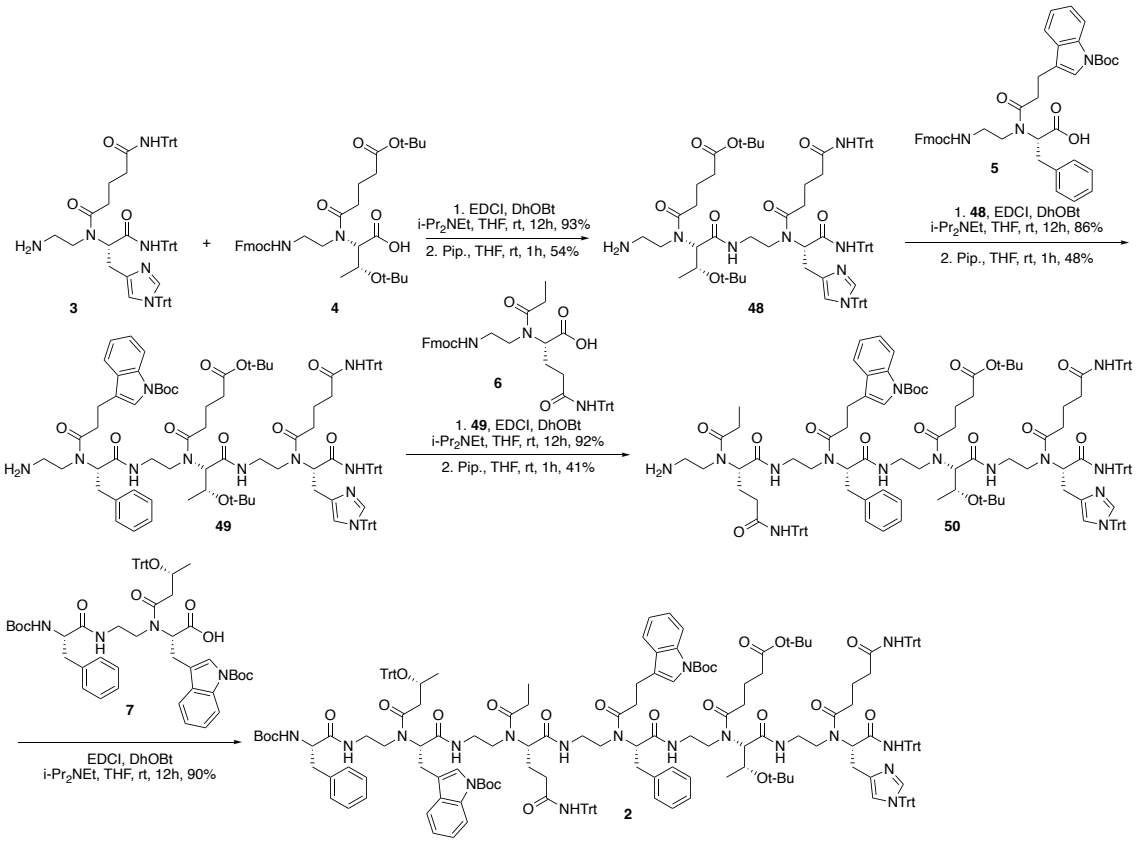

Scheme 36: Building blocks coupling.

Different from the amide bond formation between the secondary amine and the amino acid mimetic, the coupling between building blocks involves a primary amine and a natural amino acid residue that is prone to epimerization. To avoid this problem EDCI was used as a coupling reagent and DHOBt was used as an additive to avoid inversion of

the chiral center of the amino acids. This methodology has already been proved by Jean's research team as being the best one to avoid epimerization for α-AApeptides.

1-ethyl-3-(3-dimethylaminopropyl)carbodiimide (EDCI) is a carbodiimide and this family of reagents is one of the oldest coupling agents used in peptide synthesis[121,122] and does not contain in its structure an additive to avoid epimerization, for this reason, DHOBt was added[123–125]. The mechanism is shown in Scheme 37. After deprotonation, the carboxylate will attack the carbodiimide to produce an *O*-acylisourea. This adduct will react with DHOBt to form the activated species that will react with the amine, forming the desired amide and a water-soluble urea.

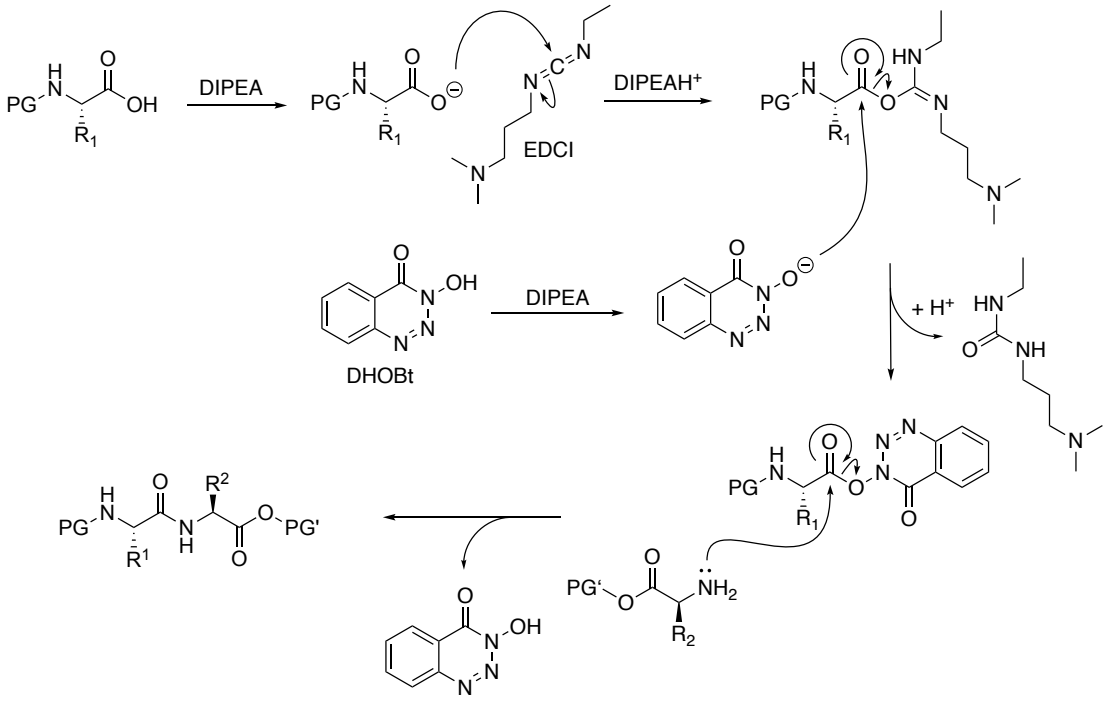

Scheme 37: EDCI/DHOBt coupling mechanism

All the couplings were made in liquid phase, enabling the synthesis in a larger scale than using solid supports. The obtained overall yield over 7 linear steps was, approximately, 7%.

4. Acid-labile global deprotection

This step (Scheme 38) removes all the acid-labile protecting groups and is performed as the last step of the synthesis using TFA in the presence of water and triisopropyl silane as a scavenger (TFA:TIS:H_2O 90:5:5) of electrophilic species released

during the global deprotection. The amount of TFA, the reaction time, and the temperature are important parameters to achieve a complete deprotection without the decomposition of the final compound.

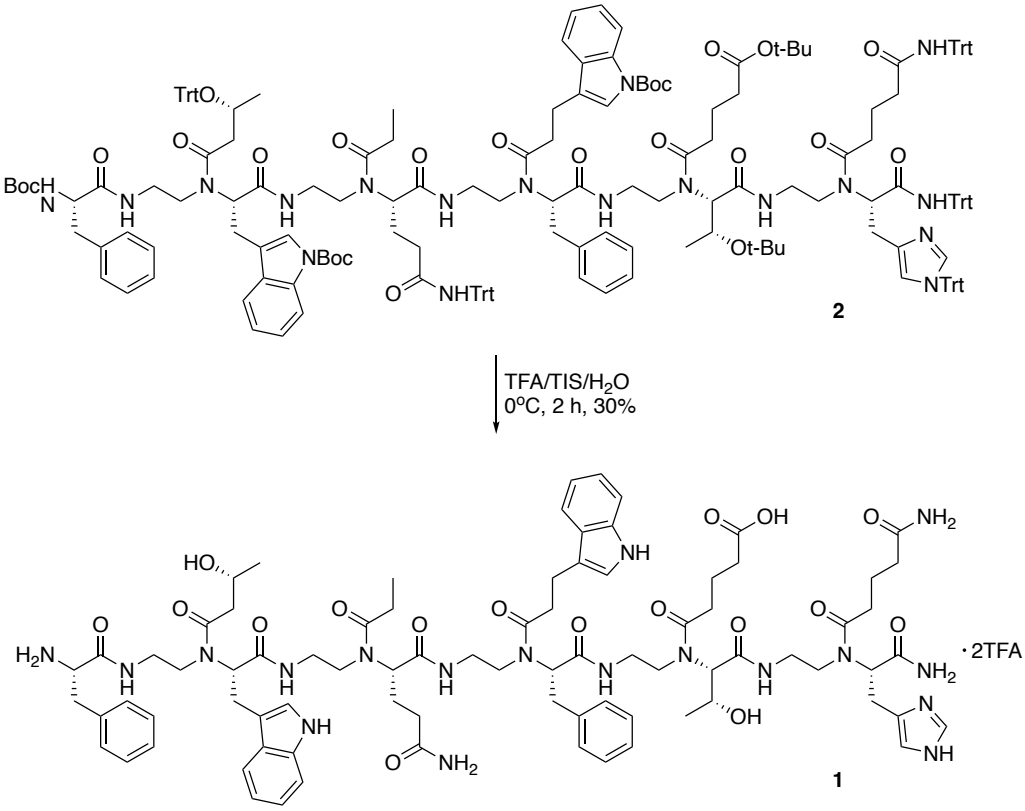

2 **1**

Scheme 38: Global deprotection.

The byproducts of the cleaved protecting groups are trityl and trimethyl carbocations, these electrophilic species can react with the deprotected nucleophilic functional groups, such as indolyl on tryptophan, hydroxyl on threonine, and on threonine mimetic, amine on phenylalanine, imidazolyl on histidine. In order to minimize these side reactions, a scavenger is added to the global deprotection cocktail to trap the reactive carbocations. Anisole, ethanedithiol and trialkyl silanes are commonly used scavengers, being this last ones the most effective ones[126]. Triethylsilane (TES) can reduce de indole moiety and for these reasons, triisopropylsilane (TIS) will be used, since it is a bulkier hydride, not performing this reduction reaction.

The deprotection mechanism of the trityl group occurs in two main steps: protonation and subsequent loss of the protecting group as a trityl carbocation (Scheme 39).

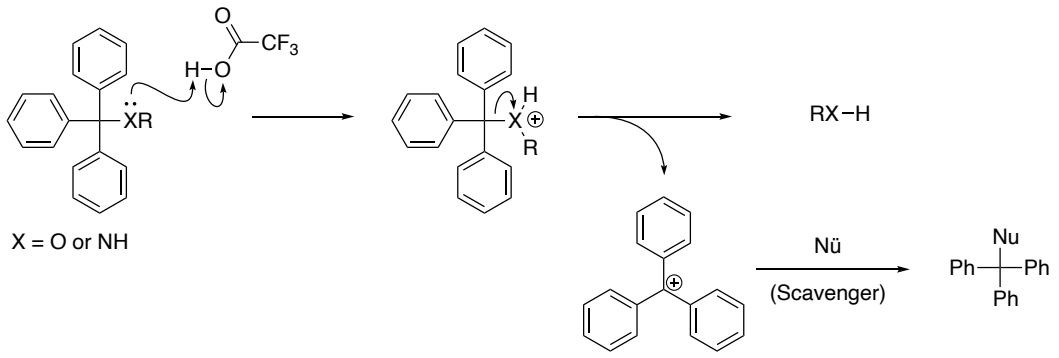

Scheme 39: Trityl deprotection mechanism.

Boc is deprotected by the decarboxylation of the freshly formed carbamic acid releases the free amine that, if it is nucleophilic, will protonate to form a TFA salt (Scheme 40). The trimethyl carbocation is sequestered by TIS or it eliminates a proton, forming isobutylene.

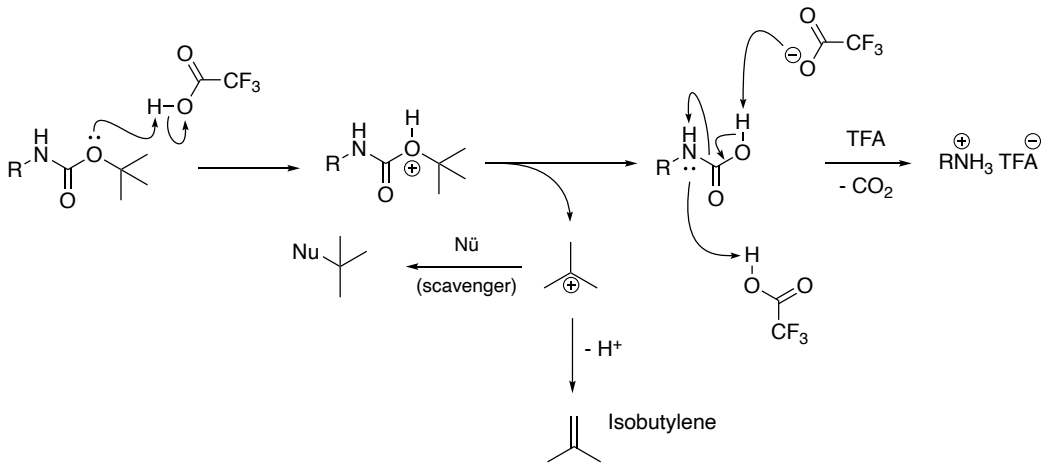

Scheme 40: Boc deprotection mechanism.

Tert-butyl esters and ethers are deprotected in the same manner as Boc, but only releasing the trimethyl carbocation.

The resulting mixture was poured into cold diethyl ether and refrigerated overnight. The product was collected by filtration, and the filter cake was dissolved in water then, water was removed by freeze dryer to get the crude product, which was purified by semipreparative HPLC to afford the desired compound in 30% yield and 95% of purity as a TFA salt.

III. Biological results of mimAse3

The peptidomimetic, mimAse3, was tested in three different concentrations concomitant with Ase3 peptide against two strains that it had already demonstrated activity, *S. epidermidis* and *P. aeruginosa*. Contrary to what was expected, which was an increase in the activity of mimAse3 when compared to Ase3, the peptidomimetic did not inhibited the biofilm formation of all tested strains even at the highest concentrations (Figure 27).

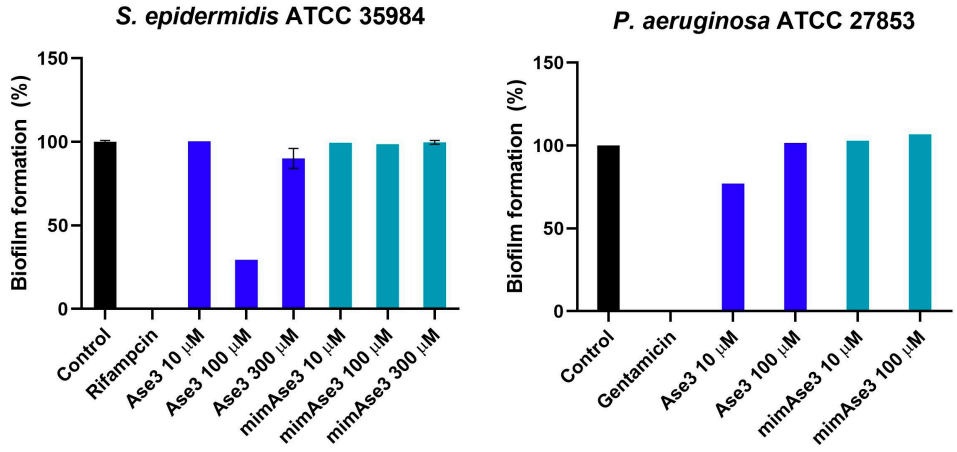

Figure 27: mimAse3 biological results compared to its natural peptide in different concentrations.

The lack of activity may rely on the degradation of the peptidomimetic by bacterial cells or perhaps mimAse3 folding was not what was expected and its active conformation was not achieved. AApeptides can closely relate to their parent peptide, but small changes in the final conformation can lead to a loss of activity. The size of this peptide is important, as shown at the beginning of this work, and for some reason, if the peptide cannot acquire the perfect tridimensional conformation, it will lose its activity. High-field liquid NMR or circular dichroism studies may be carried to be able to verify if the secondary structure of the peptidomimetic keeps the same folding as the natural peptide. *In silico* studies may also help understand its conformation. More studies to try to decipher the precise mechanism of action also can help to understand the results of the biological tests.

D. Conclusions

Starting from 128 known sequences of antibacterial peptides, Macedo's and Gillet's teams were able to propose 23 new peptides using the conserved sequence of the original peptides in five different categories: defensins, histatins, catelecidines, RNAses, and chemokines, containing from 6 to 13 amino acid residues. Within these peptides, Ase3 was the most active compound, an RNAse containing 11 amino acid residues, inhibiting more than 50% and approximately 30% of *S. epidermidis* and *P. aeruginosa* biofilm formation, respectively. A molecular simplification study was carried out in an attempt to reduce the number of amino acids and, in consequence, the synthetic effort to synthesized its mimetic. Not only the size of the peptide was proven important, but the role of the N-terminal portion was also proved essential during the probing assays.

Based on the eleven amino acid residues of Ase3 (FTWAQWFETQH), an original peptidomimetic, named mimAse3, was designed and synthesized. Five building blocks were proposed and the synthetic procedures of peptidomimetics chemistry were optimized to improve the overall yield and simplify the synthetic routes. After 47 synthetic steps, 20 mg of a 95% pure α-AApeptidomimetic was synthesized in a 2.1% global yield.

Unfortunately, mimAse3 did not show the expected biological activity of its natural parent peptide has shown. High-field liquid NMR, circular dichroism, and *in silico* may be helpful to determine the spatial configuration of this psudopeptide.

E. Experimental part

I. Biological

1. General considerations

The untreated growth control was considered to be 100% planktonic cells. Biological assays were carried out at on least three biological and technical replicates. Data were analyzed by the Student t-test in relation to the untreated samples and $p \leq 0.05$ was considered to be significant. Statistical significance was determined using GraphPad Prism 6.0 software.

2. Experimental procedures

- Bacterial strain and culture conditions

Staphylococcus aureus ATCC *25904, Staphylococcus epidermidis* ATCC 35984, and *Pseudomonas aeruginosa* PA01 were used to evaluate antimicrobial and antibiofilm activities of the peptidomimetic. The strains were cultivated on blood agar plates at 37ºC overnight. The inoculum concentration was adjusted in a solution of 0.9% NaCl to an optical density of 0,150 at 600 nm.

- Antibiofilm and antibacterial assays

Biofilm formation was evaluated in standard sterile 96-well microtiter plaques (Corning costar®), according to the adapted protocol from Trentin *et al.* The adherent biofilm layer was stained with 0.4% crystal violet, solubilized in absolute ethanol and the absorbance (570 nm) was measured using a SpectraMax m3 plate reader. Untreated controls correspond to 100% of biofilm formation. Rifampicin (8 µg/mL) was used as growth inhibition control for *S. aureus* and *S. epidermidis* and gentamicin (8 µg/mL) for *P. aeruginosa*. The peptide was tested at three different concentrations (10, 100µM, and 300 µM) together with the original Ase3 peptide. The bacterial growth was assessed by the difference between initial (t = 0) and final (t = 24 h) absorbance at 600 nm.

II. Chemical

1. General considerations

- Reagents and solvents

Commercially available reagents and solvents were purchased from Fluorochem, Sigma-Aldrich, Alfa Aesar, Strem, and Acros, and were used as received. All reactions under inert atmosphere were performed under argon atmosphere.

- TLC and column chromatography

Thin-layer chromatography was performed on TLC silica gel 60 F_{254} aluminum plates. Compounds were visualized by exposure to UV light or by dipping the plates into potassium permanganate, phosphomolybdic acid, anisaldehyde sulfuric acid, or ninhydrin, followed by heating. Flash column chromatography was carried out using silica gel (particle size 40-60 μm). All the purification of the Fmoc deprotection reactions were performed using deactivated silica as a mobile phase. To prepare the silica, the columns were packed using 10% of triethylamine (TEA) in the eluent and, then, all the purification was done using 1% of TEA in the eluent. This additive prevents the formation of ionic pairs between the silica and the amine, facilitating purification. For the purification of the free acids, 1% of acetic acid was used in the column chromatography purifications. These additive yields better elution, improving the resolution of the chromatographic purification.

- NMR spectroscopy

NMR analysis were performed on a Bruker Avance High resolution 300 MHz. Spectra were recorded at room temperature. The compounds were dissolved in deuterated solvents and the solvent used is indicated for each compound. All chemical shifts are reported in parts per million (ppm). Abbreviations used in the description of resonances are s (singlet), d (doublet), t (triplet), q (quartet), sept (septet), doublet of doublets (dd), doublet of triplets (dt), triplet of doublets (dt), bs (broad singlet), and m (multiplet), Coupling constants (J) are quoted to the nearest 0.1Hz.

- High performance liquid chromatography mass spectrometry

HPLC-MS analysis were performed on a Shimadzu Prominence system coupled to an Advion ESI mass spectrometer using Thermoscientific Hypersil Gold aQ column chromatography (5µ, 250×4.6 mm) [method: binary gradient, solvent A = H_2O + 0.1% TFA, solvent B = MeCN + 0.1% TFA, flow = 1 mL/min, 0→0.5 min 100% A, 0.5→20 min 0→32% B/A, 20→30 min 32→100% B/A, 30→40 min 100% B, 40→45 min 100→0% B/A, 45→60 min 100% A]. Semipreparative HPLC was performed on a Shimadzu Prominence system using Hypersil Gold aQ column chromatography (5µ, 250×20 mm) [method: binary gradient, solvent A = H_2O + 0.1% TFA, solvent B = MeCN + 0.1% TFA, λ = 215nm, ow = 10mL/min, 0→5min 100% A, 5→15min 0→30% B/A, 15→20 min 30% B/A, 20→25 min 30→100% B/A, 25→35 min 100% B, 35→40 min 100→0% B/A, 40→50 min 100% A].

- High-resolution mass spectrometry

High-resolution mass (HRMS) spectra were recorded on Bruker Daltonik maXis 4G instrument using electrospray ionization (ESI) techniques.

2. Experimental procedures

Synthesis of Boc-Phe-Thr(Trt)-Trp(boc)-Ala- Gln(Trt)-Trp(Boc)-Phe-Glu(tBu)-Thr(tBu)-Gln(Trt)-His(Trt)-NHTrt α-AA hendecapeptide

Synthesis of H-Gln(Trt)-His (Trt)-NHTrt α-AAdipeptide – QH building block 3

Fmoc-His(Trt)-NHTrt 9

To a solution of Fmoc-His(Trt)-OH **8** (5 g, 8.1 mmol) in THF (100 mL) was added Hunig's base (5.5 mL, 16.2 mmol), DEPBT (7.2 g, 12.15 mmol), trityl amine (8.3 g, 16.2 mmol) and LiBr (0.9 g, 10.0 mmol). The reaction mixture was stirred at room temperature for 5 days, diluted with EtOAc (100 mL), washed with 1:1 1 M HCl/brine (2 × 100 mL), saturated aq. $NaHCO_3$ (100 mL), and brine (50 mL). The organic fraction was dried over

$MgSO_4$, filtered, and concentrated under reduced pressure. Purification by flash column chromatography (20→40% acetone/Pet. Ether, Rf = 0.6) provided the Fmoc-His(Trt)-NHTrt **9** (3.0 g, 43%). ^{1}H NMR (300 MHz, Acetone-d_6) δ 8.52 (bs, 1H), 7.85 (d, *J* = 7.7 Hz, 2H), 7.7 (t, *J* = 5.9 Hz, 2H), 7.42-7.30 (m, 11H), 7.30-7.12 (m, 18H), 7.10-7.02 (m, 6H), 6.97 (d, *J* = 6.7 Hz, 1H), 6.75 (s, 1H), 4.77 (q, *J* = 7.2 Hz, 1H), 4.40-4.12 (m, 3H), 3.62 (m, 1H), 2.95 (d, J = 4.6 Hz, 2H), 1.78 (m, 1H). ^{13}C NMR (75 MHz, Acetone-d_6) δ 171.2, 157.0, 146.0, 145.2, 145.1, 143.5, 142.2, 138.3, 130.7, 130.6, 129.8, 129.0, 129.0, 128.6, 128.5, 128.1, 128.1, 127.6, 126.3, 126.3, 120.9, 120.2, 76.1, 71.1, 68.2, 67.5, 55.7, 48.1.

H-His(Trt)-NHTrt 10

To a solution of Fmoc-His(Trt)-NHTrt **9** (3 g, 3.5 mmol) in THF (60 mL) was added piperidine (9 mL). The reaction mixture was stirred at room temperature for 1 h and concentrated under reduced pressure. Purification by flash column chromatography (2→5% MeOH/DCM, Rf = 0,4) provided H-His(Trt)-NHTrt **10** (1.5 g, 67%). ^{1}H NMR (300 MHz, Acetone-d_6) δ 7.43-7.31 (m, 12H), 7.30-7.05 (m, 19H), 6.51 (s, 1H) 4.13 (dd, *J* = 10.2, 4.0 Hz, 1H), 3.03 (dd, *J* = 14.8, 4.1 Hz, 1H), 2.68 (dd, *J* = 13.5, 9.5 Hz, 1H). ^{13}C NMR (75 MHz, Acetone-d_6) δ 172.1, 146.5, 143.8, 138.6, 130.6, 129.6, 129.0, 128.9, 128.6, 127.7, 120.5, 75.8, 70.3, 65.5.

FmocNHCH$_2$CHO 12

To a solution of allylamine **11** (13,2 mL, 51.0 mmol) in 1,4-dioxane (300 mL) was added $NaHCO_3$ (30.0 g, 357 mmol) and FmocCl (30.0 g, 115,8 mmol). The mixture was stirred at room temperature for 15 h then diluted with EtOAc (600 mL), washed with 1:1 HCl 1 M/brine (2 × 600 mL) and brine (300 mL), dried over $MgSO_4$, filtered, and concentrated under reduced pressure to provide Fmoc-allylamine (32,22 g, 99%) which was used without further purification. ^{1}H NMR (300 MHz, $CDCl_3$) 7.76 (d, *J* = 7.3 Hz, 2H), 7.59 (d, *J* = 7.3 H, 2H), 7.40 (t, *J* = 7.3 Hz, 2H), 7.31 (t, *J* = 7.3 Hz, 2H), 5.88–5.81 (m, 1H), 5.20–5.12 (m, 2H), 4.82 (bs, 1H), 4.43 (d, *J* = 6.8 Hz, 2H), 4.22 (t, *J* = 6.8 Hz, 1H), 3.83 (brs 2H). ^{13}C NMR (75 MHz, $CDCl_3$) 156.1, 143.8, 141.1, 134.3, 127.5, 126.8, 124.8, 119.8, 115.8, 66.4, 47.0, 43.2.

To a solution of Fmoc-allylamine (32,22 g, 115,3 mmol) in 1:1 acetone/tert-butanol (360 mL) was added $NaIO_4$ (49,3 g, 230.0 mmol) and a solution of K_2OsO4 (208 mg, 0.57 mmol) in H_2O (180 mL) under vigorous mechanical stirring. The reaction mixture was stirred at room temperature for 2.5 h then diluted with H_2O (1,35 L), stirred at 0 °C for 0.5 h then filtered. The filter cake was washed with water (1,5 L) then dried to provide Fmoc-glycinaldehyde **12** (27,95 g, 95%) as a grey solid which was used without further purification. ^{1}H NMR (300 MHz, Acetone) δ 9.58 (s, 1H), 7.86 (dq, J = 7.5, 1.1 Hz, 2H), 7.70 (t, J = 5.4 Hz, 2H), 7.47 – 7.26 (m, 4H), 4.41 – 4.17 (m, 4H). ^{13}C NMR (75 MHz, Acetone) δ 199.5, 144.9, 142.0, 127.8, 126.0, 120.7, 67.2, 51.6, 47.9.

FmocNH$(CH_2)_2$-His(Trt)-NHTrt 13

To a mixture of H-His(Trt)NHTrt **10** (1,5 g, 2.3 mmol) and FmocNHCH$_2$CHO **12** (650 mg, 2.3 mmol) was added freshly prepared STAB† suspension (0.14 M in DCE, 30 mL, 3.9 mmol) under inert atmosphere. The mixture was stirred at room temperature for 1 h, diluted with 30 mL of EtOAc, washed with 1:1 saturated aq. $NaHCO_3$/brine (2 times) and brine, dried over $MgSO_4$, filtered, and concentrated under reduced pressure. Purification by flash column chromatography (5→20% (EtOAc/MeOH 4:1)/(DCM/Pet. Ether 1:1), Rf = 0.5) provided FmocNH$(CH_2)_2$-His(Trt)-NHTrt **13** (1.06 g, 51%). ^{1}H NMR (300 MHz, Acetone-d_6) δ 8.97 (s, 1H), 7.83 (d, J = 7.6 Hz, 2H), 7.46-6.99 (m, 35H) 6.77 (s, 1H), 4.41-4.18 (m, 2H), 3.34 (m, 1H), 3.32 (m, 2H), 2.89 (m, 2H), 2.72 (m, 2H). ^{13}C NMR (75 MHz, Acetone-d_6) δ 173.1, 146.4, 146.4, 143.6, 142.2, 139.2, 130.6, 130.6, 129.7, 129.6, 129.6, 129.5, 129.0, 129.0, 128.9, 128.6, 128.6, 128.4, 128.0, 127.6, 126.2, 120.9, 76.1, 70.4, 66.9, 49.2, 48.2.

† General preparation of Na(AcO)$_3$BH (STAB) in DCE: To a suspension of $NaBH_4$ (X mg, 1 equiv) in dry DCE (0.18X mL) under inert atmosphere at 0 °C was added AcOH (4.5X μL, 3 equiv). The suspension was stirred for 15-30 min at 0 °C and then at room temperature for 1 h. The mixture is then stirred for at least a further 1 h before use. It can be stirred for longer, but should be used in 24 h. The resulting suspension is assumed to be 0.14 M for subsequent stoichiometry calculations.

Gln side chain mimetic 15

A solution of glutaric anhydride **14** (4.5 g, 39.4 mmol) and trityl amine (11.2 g, 43.3 mmol) in 50 mL of 1,4-dioxane was refluxed for 24 hours. The reaction mixture was allowed to cool to room temperature and 100 mL of a 1 M NaOH solution was added together with 50 mL of diethyl ether. The aqueous phase was extracted 2 more times with diethyl ether and acidified with concentrated HCl. The solid was filtrated and washed with a small amount of diethyl ether then dried under vacuum, provided the named compound **15** (11.75 g, 80%).^{1}H NMR (300 MHz, Chloroform-*d*) δ 7.37-7.11 (m, 15H), 6.68 (s, 1H), 2.36 (q, *J* = 7.1 Hz, 4H) 1.94 (quin, *J* = 7.0 Hz, 2H). ^{13}C NMR (75 MHz, Acetone-d_6) δ 177.4, 171.4, 144.7, 128.8, 128.1, 127.2, 70.8, 36.2, 33.0, 20.7.

Fmoc-Gln(Trt)-His(Trt)-NHTrt α-AAdipeptide 16

To a mixture of FmocNH$(CH_2)_2$-His(Trt)-NHTrt **13** 16 (1 g, 1.1 mmol), Gln side chain mimetic **15** (620 mg, 1.65 mmol), HATU (63 mg, 1.65 mmol) in THF (10 mL) was added Hunig's base (0.4 mL, 2.2 mmol). The reaction mixture was stirred at room temperature for 12 h, diluted with EtOAc (10 mL), washed with 1:1 1 M HCl/brine (2 × 20 mL), saturated aq. $NaHCO_3$ (20 mL) and brine (20 mL), dried over $MgSO_4$, filtered, and concentrated under reduced pressure. Purification by flash column chromatography (20→50% acetone/Pet. ether) provided the expected compound **16** (1.3 g, 95%). ^{1}H NMR (300 MHz, Acetone-d_6) δ 8.47 (s, 1H), 7.84 (d, *J* = 8.0 Hz, 2H), 7.60 (d, *J* = 7.8 Hz, 2H), 7.43-7.04 (m, 49H), 6.69 (s, 1H), 4.29-4.09 (m, 3H), 3.30-3.06 (m, 4H), 3.03-2.80 (m, 4H), 2.37-2.20 (m, 4H), 1.87-1.68 (m, 3H). ^{13}C NMR (75 MHz, Acetone-d_6) δ 206.3, 205.9, 175.2, 172.4, 170.7, 157.3, 146.4, 146.3, 146.1, 145.8, 145.2, 143.7, 143.6, 143.5, 142.2, 138.7, 130.6, 129.9, 129.7, 129.6, 129.1, 129.1, 129.1, 129.0, 129.0, 128.6, 128.5, 128.5, 128.4, 128.4, 128.0, 127.7, 127.5, 127.4, 126.2, 120.9, 120.8, 120.2, 119.9, 76.0, 70.9, 70.9, 67.1, 55.6, 48.1, 41.0, 36.7, 33.3, 32.1, 30.7, 28.5, 22.4.

H-Gln(Trt)-His(Trt)-NHTrt α-AAdipeptide 3

To a solution of **16** (1.3 g, 1.03 mmol) in THF (20 mL) was added piperidine (3 mL). The reaction mixture was stirred at room temperature for 1 h and preadsorbed on silica gel.

Purification by flash column chromatography (3→10% MeOH/DCM) provided the expected primary amine **3** (675 mg, 63%). ^{1}H NMR (300 MHz, Acetone) δ 7.36 (qd, J = 4.5, 1.8 Hz, 12H), 7.26 – 6.99 (m, 32H), 3.43 – 3.21 (m, 1H), 3.15 (q, J = 5.6, 4.9 Hz, 1H), 3.08 – 2.96 (m, 1H), 2.31 (qd, J = 8.1, 5.8 Hz, 3H), 1.78 (dddd, J = 17.4, 14.9, 6.5, 3.9 Hz, 2H). ^{13}C NMR (75 MHz, Acetone) δ 173.8, 172.3, 169.8, 146.1, 146.0, 145.9, 145.6, 145.1, 143.3, 143.2, 139.1, 138.3, 130.2, 130.1, 129.4, 129.4, 129.3, 128.8, 128.7, 128.7, 128.6, 128.5, 128.2, 128.2, 128.0, 128.0, 127.1, 127.0, 126.9, 119.7, 75.5, 70.4, 70.2, 67.3, 51.3, 44.7, 36.2, 33.0, 30.3, 30.1, 29.8, 29.6, 29.3, 29.1, 28.8, 27.3, 23.2, 21.9.

Synthesis of Fmoc-Glu(tBu)-Thr(tBu)-OH α-AAdipeptide – ET building block 4

Fmoc-Thr(tBu)-OBn 22

To a solution of Fmoc-Thr(tBu)-OH **21** (10 g, 25.16 mmol) in DMF (100 mL) was added benzyl bromide (4.5 mL, 37.74 mmol) and Hunig's base (4.4 mL, 50.32 mmol). The reaction mixture was stirred at room temperature for 12 h, then diluted with EtOAc (200 mL) and washed with 1:1 1 M HCl/brine (2 × 100 mL), saturated aq. $NaHCO_3$ (100 mL) and brine (50 mL). The organic fraction was dried over $MgSO_4$, filtered, and concentrated. Purification by flash column chromatography (5→15% acetone/Pet. Ether, Rf = 0.55) provided Fmoc-Thr(tBu)-OBn **22** (11.66 g, 95%). ^{1}H NMR (300 MHz, Acetone-d_6) δ 7.86 (d, J = 7.8 Hz, 2H), 7.72 (dd, J = 7.7, 2.7 Hz, 2H), 7.49-7.24 (m, 9H), 6.28 (d, J = 9.2 Hz 1H), 5.23 (d, J = 12.2 Hz, 1H), 5.10 (d, J = 12.2 Hz, 1H), 4.45-4.17 (m, 5H), 1.21 (d, , J = 6.1 Hz, 3H), 1.11 (s, 9H). ^{13}C NMR (75 MHz, Acetone-d_6) δ 171.5, 157.4, 145.1, 144.9, 142.1, 136.8, 129.3, 129.1, 129.0, 128.5, 128.0, 127.9, 126.2, 126.1, 125.9, 120.8, 120.4, 74.5, 68.2, 68.0, 67.5, 67.4, 61.4, 60.9, 48.0, 28.7, 21.3, 21.1.

H-Thr(tBu)-OBn 23

To a solution of Fmoc-Thr(tBu)-OBn **22** (10 g, 20.5 mmol) in THF (200 mL) was added piperidine (30 mL). The reaction mixture was stirred at room temperature for 1.5 h and concentrated under reduced pressure. Purification by flash column chromatography (30→50% DCM/Pet. Ether, Rf = 0,3) provided H-Thr(tBu)-OBn **23** (6.4 g, 62%). ^{1}H NMR (300 MHz, Acetone) δ 7.48 – 7.27 (m, 5H), 5.18 (d, J = 12.5 Hz, 1H), 5.06 (d, J =

12.5 Hz, 1H), 4.01 (qd, *J* = 6.2, 3.4 Hz, 1H), 3.29 (d, *J* = 3.4 Hz, 1H), 1.19 (d, *J* = 6.2 Hz, 3H), 1.11 (s, 9H). ^{13}C NMR (75 MHz, Acetone-*d*$_6$) δ 175.4, 137.5, 129.4, 129.2, 128.9, 74.0, 71.6, 66.8, 61.6, 29.0, 20.8.

FmocNH(CH$_2$)$_2$-Thr(tBu)-OBn 24

To a mixture of H-Thr(tBu)-OBn **23** (6 g, 22.6 mmol) and FmocNHCH$_2$CHO **12** (6.39 g, 22.6 mmol) was added freshly prepared STAB suspension (0.14 M in DCE, 300 mL, 39.0 mmol) under inert atmosphere. The mixture was stirred at room temperature for 1 h, diluted with 150 mL of EtOAc, washed with 1:1 saturated aq. NaHCO$_3$/brine (2 times) and brine, dried over MgSO$_4$, filtered, and concentrated under reduced pressure. Purification by flash column chromatography (1→5% acetone/DCM, Rf = 0.5) provided the named compound **24** (5.3 g, 42%). ^{1}H NMR (300 MHz, Acetone-*d*$_6$) δ 7.85 (d, *J* = 7.5 Hz, 2H), 7.69 (d, *J* = 7.4 Hz, 2H), 7.48 – 7.26 (m, 9H), 6.46 (bs, 1H), 5.20 (d, *J* = 12.5 Hz, 1H), 5.10 (d, *J* = 12.5 Hz, 1H), 4.35 – 4.15 (m, 3H), 4.01 (qd, *J* = 6.2, 3.7 Hz, 1H), 3.22 (q, *J* = 5.0 Hz, 4H), 2.85 (dt, *J* = 12.3, 6.3 Hz, 1H), 2.53 (dt, *J* = 12.0, 6.2 Hz, 1H), 1.19 (d, *J* = 6.3 Hz, 3H), 1.10 (s, 9H). ^{13}C NMR (75 MHz, Acetone-*d*$_6$) δ 173.9, 157.1, 145.0, 144.9, 141.9, 137.0, 129.1, 128.8, 128.6, 128.3, 127.7, 125.9, 120.6, 73.9, 69.1, 67.5, 66.7, 66.5, 48.4, 47.9, 41.6, 28.5, 20.3.

Glu side chain mimetic 26

A suspension of glutaric anhydride **25** (5.7 g, 50 mmol) and ZnCl$_2$ (100 mg, 3.3 mmol) in dry tert-butanol (28.4 mL, 300 mmol) was stirred at 60 °C for 3 days. 50 mL of 1 M solution NaOH was added, and stirring continued at ambient temperature for 30 min. The aqueous phase was washed with diethyl ether (2 × 50 mL) and then acidified with concentrated HCl. The acidified aqueous phase was extracted with diethyl ether (3 × 50 mL). The combined organic phases were washed several times with brine, dried over Na$_2$SO$_4$, filtered, and evaporated to give 5-tert-butoxy-5-oxopentanoic acid **26** (5.6 g, 60%). ^{1}H NMR (300 MHz, CDCl3) δ 7.94 – 7.72 (m, 15H), 2.95 (dt, J = 8.4, 7.1 Hz, 4H), 2.53 (p, J = 7.1 Hz, 2H). ^{13}C NMR (75 MHz, CDCl3) δ 177.4, 171.4, 144.7, 128.8, 128.1, 127.2, 70.8, 36.22, 33.0, 20.7.

Fmoc-Thr(tBu)-Glu(tBu)-OBn α-AAdipeptide 27

To a mixture of FmocNH$(CH_2)_2$-Thr(tBu)-OBn **24** (5.3 g, 10 mmol), Glu side chain mimetic **26** (2.8 g, 15 mmol), EEDQ (3.7 g, 15 mmol) in EtOAc (50 mL). The reaction mixture was stirred at 50 °C for 4 weeks, diluted with EtOAc (50 mL), washed with 1:1 1 M HCl/brine (2 × 50 mL), saturated aq. $NaHCO_3$ (50 mL) and brine (50 mL), dried over $MgSO_4$, filtered, and concentrated under reduced pressure. Purification by flash column chromatography (2→10% diethyl ether/DCM, Rf = 0.5) provided the expected compound **27** (4.9 g, 70%).^{1}H NMR (300 MHz, Acetone-d_6) δ 7.86 (d, J = 7.4 Hz, 2H), 7.74 – 7.62 (m, 2H), 7.46 – 7.27 (m, 9H), 6.48 (t, J = 6.1 Hz, 1H), 5.27 – 5.12 (m, 1H), 5.05 (d, J = 12.4 Hz, 1H), 4.54 – 4.28 (m, 3H), 4.25 – 4.07 (m, 1H), 3.81 – 3.61 (m, 1H), 3.60 – 3.42 (m, 1H), 3.32 (ddt, J = 24.9, 13.0, 6.7 Hz, 1H), 2.58 – 2.41 (m, 2H), 2.34 – 2.17 (m, 2H), 1.92 – 1.73 (m, 2H), 1.40 (s, 9H), 1.27 (d, J = 6.0 Hz, 3H), 1.12 (s, 9H). ^{13}C NMR (75 MHz, Acetone-d_6) δ 173.5, 172.8, 170.1, 157.0, 145.0, 144.9, 141.9, 136.9, 129.1, 129.1, 128.9, 128.8, 128.7, 128.3, 128.3, 127.7, 125.9, 125.8, 120.6, 120.6, 80.0, 74.5, 67.3, 66.8, 66.01 65.6, 49.8, 47.8, 40.4, 35.0, 33.1, 32.2, 28.8, 28.1, 22.5, 21.2.

Fmoc-Thr(tBu)-Glu(tBu)-OH α-AAdipeptide 4

To a solution of **27** (4.48 g, 6.4 mmol) in EtOAc (50 mL) was added palladium on charcoal (0.45 g, 0.42 mmol) under a hydrogen atmosphere. The reaction mixture was stirred at room temperature for 24 h then filtered over celite and concentrated under reduced pressure. Purification by flash column chromatography (1→5% MeOH/DCM + 1% AcOH) provided the expected carboxylic acid **4** (3.83 g, 98%). ^{1}H NMR (300 MHz, Acetone-d_6) δ 7.84 (d, J = 7.4 Hz, 2H), 7.68 (d, J = 7.6 Hz, 2H), 7.45 – 7.06 (m, 4H), 4.51 – 4.33 (m, 2H), 4.30 – 4.12 (m, 2H), 3.80 – 3.63 (m, 1H), 3.63 – 3.48 (m, 1H), 3.38 (dq, J = 24.3, 7.7 Hz, 1H), 2.60 – 2.38 (m, 2H), 2.34 – 2.18 (m, 2H), 1.91 – 1.71 (m, 2H), 1.40 (s, 9H), 1.23 (d, J = 6.2 Hz, 3H), 1.15 (s, 9H). ^{13}C NMR (75 MHz, Acetone-d_6) δ 173.9, 172.7, 171.1, 157.0, 144.9, 144.8, 141.8, 141.8, 129.5, 128.7, 128.2, 128.2, 127.6, 125.8, 125.8, 125.7, 120.5, 79.9, 74.4, 67.2, 66.7, 65.7, 49.7, 47.8, 40.3, 34.9, 33.0, 32.2, 28.8, 28.0, 22.2, 20.8.

Synthesis of Fmoc-Phe-Trp(Boc)-OH α-AAdipeptide – FW building block 5

Fmoc-Phe-OAllyl 29

To a solution of Fmoc-Phe-OH **28** (10 g, 25.8 mmol) in DMF (100 mL) was added Allyl bromide (3.4 mL, 38.6 mmol) and Hunig's base (4.5 mL, 51.6 mmol). The reaction mixture was stirred at room temperature for 12 h, then diluted with EtOAc (200 mL) and washed with 1:1 1 M HCl/brine (2 × 100 mL), saturated aq. $NaHCO_3$ (100 mL) and brine (50 mL). The organic fraction was dried over $MgSO_4$, filtered, and concentrated. Purification by flash column chromatography (10→20% acetone/Pet. Ether, Rf = 0.45) provided Fmoc-Phe-OAllyl **29** (10.5 g, 95%). ^{1}H NMR (300 MHz, Acetone-d_6) δ 7.85 (d, J = 7.6 Hz, 2H), 7.65 (d, J = 7.5 Hz, 2H), 7.41 (t, J = 7.5, 3H), 7.36 – 7.16 (m, 6H), 6.85 (d, J = 8.5 Hz, 1H), 5.91 (ddt, J = 17.2, 10.8, 5.5 Hz, 1H), 5.39 – 5.14 (m, 2H), 4.66 – 4.47 (m, 3H), 4.28 (d, J = 8.0 Hz, 2H), 4.19 (q, J = 7.7 Hz, 1H), 3.21 (dd, J = 13.8, 5.3 Hz, 1H), 3.04 (dd, J = 13.8, 9.2 Hz, 1H). ^{13}C NMR (75 MHz, Acetone-d_6) δ 172.2, 156.7, 144.9, 142.0, 138.1, 133.1, 130.1, 129.2, 128.5, 127.9, 127.5, 126.0, 120.7, 118.3, 67.1, 66.0, 56.5, 47.8, 38.2.

H-Phe-OAllyl 30

To a solution of Fmoc-Phe-OAllyl **29** (10.4 g, 24.3 mmol) in THF (200 mL) was added piperidine (30 mL). The reaction mixture was stirred at room temperature for 1.5 h and concentrated under reduced pressure. Purification by flash column chromatography (5→20% (4:1 EtOAc/MeOH)/(1:1 DCM/Pet. Ether) + 1% Et_3N, Rf = 0.4) provided H-Phe-OAllyl **30** (4.6 g, 92%). ^{1}H NMR (300 MHz, Acetone) δ 7.36 – 7.12 (m, 5H), 5.99 – 5.80 (m, 1H), 5.37 – 5.20 (m, 1H), 5.20 – 5.12 (m, 1H), 4.55 (dt, J = 5.6, 1.5 Hz, 2H), 3.68 (dd, J = 7.3, 5.9 Hz, 1H), 3.07 – 2.78 (m, 2H). ^{13}C NMR (75 MHz, Acetone) δ 171.9, 139.4, 133.6, 130.5, 129.0, 127.2, 117.8, 65.5, 57.0, 40.1.

FmocNH$(CH_2)_2$-Phe-OAllyl 31

To a mixture of H-Phe-OAllyl **30** (4.52 g, 22 mmol) and FmocNHCH_2CHO **12** (6.2 g, 22 mmol) was added freshly prepared STAB suspension (0.14 M in DCE, 300 mL, 39.0 mmol) under inert atmosphere. The mixture was stirred at room temperature for 1 h,

diluted with 150 mL of EtOAc, washed with 1:1 saturated aq. $NaHCO_3$/brine (2 times) and brine, dried over $MgSO_4$, filtered, and concentrated under reduced pressure. Purification by flash column chromatography (10→25% EtOAc/DCM, Rf = 0.4) provided the named compound **31** (4.76 g, 46%). ^{1}H NMR (300 MHz, Acetone) δ 7.87 (d, *J* = 7.6 Hz, 2H), 7.69 (d, *J* = 7.6 Hz, 2H), 7.47 – 7.30 (m, 4H), 7.28 – 7.11 (m, 5H), 6.26 (bs, 1H), 5.97 – 5.75 (m, 1H), 5.32 – 5.19 (m, 1H), 5.16 (dq, *J* = 10.5, 1.5 Hz, 1H), 4.54 (d, *J* = 5.7 Hz, 2H), 4.42 – 4.28 (m, 2H), 4.28 – 4.17 (m, 1H), 3.55 (t, *J* = 6.9 Hz, 1H), 3.19 (q, *J* = 6.1 Hz, 2H), 2.92 (d, *J* = 6.9 Hz, 2H), 2.82 – 2.70 (m, 1H), 2.66 – 2.52 (m, 1H). ^{13}C NMR (75 MHz, Acetone) δ 174.4, 157.1, 145.1, 142.0, 138.7, 133.3, 130.1, 128.9, 128.4, 127.8, 127.1, 126.0, 120.7, 118.2, 66.7, 65.4, 63.4, 48.0, 41.6, 40.1.

Trp side chain mimetic 33

To a solution of indole **32** (6 g, 51 mmol) in 25 mL of acetic acid was added acrylic acid (10 mL, 145.7 mmol) and acetic anhydride (10 mL, 105.8 mmol). The reaction mixture was stirred at 95 °C for 15 h then evaporated under reduced pressure. 50 mL of a 2 M NaOH solution was added and stirred for 30 min. The mixture was filtrated and acidified with concentrated HCl. The solid was filtrated and dried under vacuum giving indole-3-propionic acid (5 g, 52%). ^{1}H NMR (300 MHz, Acetone) δ 9.98 (bs, 1H), 7.59 (dd, *J* = 7.8, 0.8 Hz, 1H), 7.37 (dd, *J* = 8.1, 1.0 Hz, 1H), 7.16 (s, 1H), 7.05 (dddd, *J* = 23.1, 8.1, 7.1, 1.2 Hz, 2H), 3.05 (t, *J* = 7.5, 2H), 2.69 (t, *J* = 7.0, 2H). ^{13}C NMR (75 MHz, $CDCl_3$) δ 178.4, 136.4, 127.2, 122.3, 121.6 119.6, 118.8, 114.8, 111.3, 34.6, 20.5.

To a solution of indole-3-propionic (6.62 g, 35 mmol) and acetyl chloride (6 mL, 88 mmol) in ethanol (60 mL) was stirred at room temperature for 15 h. The reaction mixture was diluted with EtOAc (120 mL) and washed with 1:1 1 M HCl/brine (2 × 120 mL) and brine (60 mL), dried over $MgSO_4$, filtered, and concentrated. Purification by flash column chromatography (5-30% acetone/pet. Ether, Rf = 0.3) provided indole-3-propionic acid ethyl ester (7.5 g, 98%). ^{1}H NMR (300 MHz, $CDCl_3$) δ 8.02 (s, 1H), 7.69 – 7.60 (m, 1H), 7.43 – 7.34 (m, 1H), 7.31 – 7.11 (m, 2H), 7.04 – 7.02 (m, 1H), 4.17 (q, J = 7.1 Hz, 2H), 3.15 (dd, J = 8.0, 7.2 Hz, 2H), 2.82 – 2.66 (m, 2H), 1.27 (t, J = 7.1 Hz, 3H). ^{13}C NMR (75 MHz, Acetone) δ 173.2, 137.4, 128.0, 122.7, 121.8, 119.1, 118.9, 114.6, 111.9, 60.3, 35.4, 21.1, 14.3.

To a solution of ethyl indole-3-propionic ethyl ester (3.91 g, 18 mmol), di-tert-butyl dicarbonate (4.7 g, 21.5 mmol) and DMAP (220 mg, 1.8 mmol) in 40 mL acetonitrile was stirred at room temperature for 6 hours. The mixture was preadsorbed on SiO_2 and then purified by flash column chromatography (5-20% diethyl ether/pet. Ether, Rf = 0.5) provided 1-boc-indole-3-propionic acid ethyl ester (4.85 g, 85%). ^{1}H NMR (300 MHz, $CDCl_3$) δ 8.14 (d, J = 7.7 Hz), 7.60 – 7.52 (m, 1H), 7.40 (s, 1H), 7.38 – 7.20 (m, 3H), 4.18 (q, J = 7.1 Hz, 2H), 3.14 – 2.99 (m, 2H), 2.73 (dd, J = 8.5, 6.8 Hz, 2H), 1.68 (s, 9H), 1.28 (t, J = 7.1 Hz, 3H). ^{13}C NMR (75 MHz, Acetone) δ 173.2, 150.1, 136.5, 131.3, 125.3, 123.4, 123.6, 120.7, 119.9, 116.0, 84.2, 60.8, 34.5, 28.4, 20.9, 14.7.

The mixture of 1-boc-indole-3-propionic acid ethyl ester (5.3 g, 16.6 mmol) and lithium hydroxide (910 mg, 38 mmol) in a mixture of THF (60 mL) and H_2O (40 mL) was stirred for 9 hours at room temperature. The reaction mixture was extracted 2 times with Et_2O (50 mL) and acidified with a saturated tartaric acid solution. It was extracted 3 times with diethyl ether (50 mL), dried over $MgSO_4$, filtered, and concentrated. Purification by flash column chromatography (20-40% acetone/pet. ether; 1% CH_3COOH, Rf = 0.5) to provide the desired compound **33** (4.22 g, 88%). ^{1}H NMR (300 MHz, $CDCl_3$) δ 8.15 (d, J = 7.5 Hz, 1H), 7.56 (d, J = 7.4 Hz, 1H), 7.44 (s, 1H), 7.39 – 7.23 (m, 3H), 3.07 (t, J = 7.6 Hz, 2H), 2.81 (t, J = 7.7 Hz, 2H), 1.69 (s, 9H). ^{13}C NMR (75 MHz, $CDCl_3$) δ 179.2, 149.9, 135.6, 130.3, 124.6, 122.7, 122.6, 119.2, 118.8, 115.4, 83.7, 33.8, 28.1, 20.2.

Fmoc-Phe-Trp(Boc)-OAllyl α-AAdipeptide 34

To a mixture of FmocNH$(CH_2)_2$-Phe-OAllyl **31** (4.7 g, 10 mmol), Trp side chain mimetic **33** (4.3 g, 15 mmol), HATU (5.7 g, 15 mmol) in THF (100 mL) was added Hunig's base (3.6 mL, 20 mmol). The reaction mixture was stirred at room temperature for 3 days, diluted with EtOAc (100 mL), washed with 1:1 1 M HCl/brine (2 × 100 mL), saturated aq. $NaHCO_3$ (100 mL) and brine (50 mL), dried over $MgSO_4$, filtered, and concentrated under reduced pressure. Purification by flash column chromatography (1→5% acetone/DCM) provided the expected compound **34** (5.2 g, 70%). ^{1}H NMR (300 MHz, Acetone) δ 8.12 (d, *J* = 8.2 Hz, 1H), 7.83 (d, *J* = 7.5 Hz, 2H), 7.58 (q, *J* = 6.6 Hz, 3H), 7.49 (s, 1H), 7.46 – 7.07 (m, 11H), 6.12 (t, *J* = 6.1 Hz, 1H), 5.93 (ddt, *J* = 17.2, 10.7, 5.4

Hz, 1H), 5.34 (dq, *J* = 17.2, 1.7 Hz, 1H), 5.18 (dq, *J* = 10.5, 1.6 Hz, 1H), 4.62 (dq, *J* = 5.6, 1.5 Hz, 2H), 4.41 – 4.05 (m, 4H), 3.45 – 3.25 (m, 3H), 3.19 – 3.87 (m, 3H), 2.85 – 2.64 (m, 3H), 1.63 (s, *J* = 18.7 Hz, 9H). ^{13}C NMR (75 MHz, Acetone) δ 172.8, 170.9, 157.0, 150.8, 144.8, 141.9, 139.3, 136.2, 133.3, 131.2, 130.0, 129.0, 128.3, 127.7, 127.1, 125.7, 124.8, 123.6, 123.1, 120.9, 120.6, 119.8, 117.9, 115.7, 83.8, 66.8, 65.9, 63.4, 49.7, 47.8, 39.8, 35.1, 32.9, 28.1, 20.6.

Fmoc-Phe-Trp(Boc)-OH α-AAdipeptide 5

To a solution of Fmoc-Phe-Trp(Boc)-OAllyl α-AAdipeptide **34** (5 g, 6.7 mmol) in THF (25 mL) and MeOH (10 mL) was added tetrakis(triphenylphosphine)palladium (200 mg, 170 μmol) followed by sodium *para*-toluenesulfinate (1.8 g, 10 mmol). The mixture was stirred at room temperature for 0.5 h then diluted with EtOAc and washed with 1:1 1 M HCl/brine (2 times) and brine. The organic phase was dried over $MgSO_4$, filtered, and concentrated under reduced pressure. Purification by flash column chromatography (1→5% MeOHDCM + 1% AcOH, Rf = 0.3) provided the expected carboxylic acid **5** (4.37 g, 93%). ^{1}H NMR (300 MHz, Acetone) δ 8.01 (d, *J* = 8.3 Hz, 1H), 7.62 – 7.47 (m, 2H), 7.45 – 7.36 (m, 3H), 7.35 – 7.12 (m, 11H), 6.96 (ddd, *J* = 8.1, 7.2, 1.0 Hz, 1H), 5.96 (d, *J* = 8.4 Hz, 1H), 4.43 (t, *J* = 4.3 Hz, 1H), 4.24 (q, *J* = 8.5 Hz, 3H), 3.89 – 3.74 (m, 3H), 3.53 – 3.39 (m, 3H), 3.31 – 3.21 (m, 2H), 3.03 (dd, *J* = 12.8, 5.1 Hz, 1H) 2.77 (dd, *J* = 13.3, 5.2 Hz, 1H), 1.63 (s, 9H). ^{13}C NMR (75 MHz, Acetone) δ 173.1, 172.6, 157.4, 150.0 145.7, 130.8, 130.7, 129.9, 129.7, 129.5, 128.8, 128.4, 127.6, 125.3, 125.1, 123.0, 120.8, 120.1, 115.3, 87.4, 84.2, 67.7, 59.3, 44.1, 40.9, 28.3, 28.1, 24.1, 18.5.

Synthesis of Fmoc-Ala-Gln(Trt)-OH α-AAdipeptide – AQ building block 6

Fmoc-Gln(Trt)-OAllyl 36

To a solution of Fmoc-Gln(Trt)-OH **35** (10 g, 16.34 mmol) in DMF (100 mL) was added allyl bromide (2.2 mL, 25.6 mmol) and Hunig's base (5.7 mL, 32.8 mmol). The reaction mixture was stirred at room temperature for 15 h, then diluted with EtOAc (80 mL) and washed with 1:1 1 M HCl/brine (2 × 100 mL), saturated aq. $NaHCO_3$ (100 mL) and brine (100 mL). The organic fraction was dried over $MgSO_4$, filtered, and concentrated uncer vacuum. Purification by flash column chromatography (10→20% acetone/Pet. ether)

provided Fmoc-Gln(Trt)-OAllyl **36** (10.1 mg, 95%). ^{1}H NMR (300 MHz, Acetone) δ 7.94 – 7.85 (m, 3H), 7.72 (d, J = 7.4 Hz, 2H), 7.42 (t, J = 7.2 Hz, 2H), 7.34 (d, J = 7.4 Hz, 2H), 7.31 – 7.17 (m, 16H), 6.94 (d, J = 8.3 Hz, 1H), 5.93 (ddd, J = 16.0, 10.6, 5.4 Hz, 1H), 5.34 (ddd, J = 17.3, 3.2, 1.6 Hz, 1H), 5.20 (ddd, J = 10.5, 2.8, 1.3 Hz, 1H), 4.62 (dt, J = 5.5, 1.4 Hz, 3H), 4.40 – 4.18 (m, 4H), 4.25 (s, 1H), 2.66 – 2.45 (m, 3H), 2.22 – 2.13 (m, 1H). ^{13}C NMR (75 MHz, Acetone-d6) δ 171.7, 170.9, 160.2, 145.3, 144.1, 141.1, 132.5, 129.6, 129.5, 128.9, 128.9, 127.6, 127.4, 127.1, 126.5, 125.3, 119.9, 117.2, 66.3, 65.0, 53.8, 47.2, 37.7, 32.7, 32.6, 27.3

H-Gln(Trt)-OAllyl 37

To a solution of Fmoc-Gnl(Trt)-OAllyl **36** (10 g, 13.37 mmol) in THF (100 mL) was added piperidine (15 mL). The reaction mixture was stirred at room temperature for 1.5 h, preadsorbed on silica gel and concentrated under reduced pressure. Purification by flash column chromatography (5→20% (EtOAc/MeOH 4:1)/(DCM/ Pet. ether 1:1 + 1% TEA, Rf = 0.3) provided H-Gln(Trt)-OAllyl **37** (4.24 g, 56%). ^{1}H NMR (300 MHz, Acetone-d6) δ 7.33 – 7.16 (m, 15H), 6.02 – 5.86 (m, 1H), 5.31 (ddq, J = 17.2, 5.1, 1.6 Hz, 1H), 5.19 (dddd, J = 10.5, 4.4, 2.9, 1.4 Hz, 1H), 4.58 (dtd, J = 4.7, 3.1, 1.5 Hz, 2H), 4.10 (ddd, J = 21.4, 11.0, 6.5 Hz, 1H), 3.45 – 3.31 (m, 1H), 2.60 – 2.28 (m, 3H), 2.15 (m, 1H), 2.03 – 1.88 (m, 1H), 1.72 (s, 1H). ^{13}C NMR (75 MHz, Acetone-d6) δ 171.3, 171.2, 169.8, 145.4, 143.2, 142.6, 133.5, 128.9, 127.9, 127.4, 126.4, 117.1, 116.9, 103.2, 69.9, 69.8, 64.6, 64.5, 62.3, 53.7, 33.0, 32.5, 30.2, 26.4.

FmocNH(CH_2)$_2$-Gln(Trt)-OAllyl 38

To a mixture of H-Gln(Trt)-OAllyl **37** (4.2 g, 6.4 mmol) and FmocNHCH$_2$CHO **12** (1.7 g, 6.4 mmol) was added freshly prepared STAB suspension (0.14 M in DCE, 100 mL, 11 mmol) under inert atmosphere. The mixture was stirred at room temperature for 1 h, diluted with EtOAc (100 mL), washed with 1:1 saturated aq. $NaHCO_3$/brine (2 × 100 mL) and brine (50 mL), dried over $MgSO_4$, filtered, and concentrated. Purification by flash column chromatography (20-40% acetone/pet. ether) provided the title secondary amine **38** (3.3 g 48%). ^{1}H NMR (300 MHz, Acetone- d6) δ 7.87 (d, J = 7.6 Hz, 2H), 7.69 (d, J = 7.4 Hz, 2H), 7.42 (t, J = 7.4 Hz, 2H), 7.37 – 7.16 (m, 17H), 6.48 (s, 1H), 5.96 (ddd, J = 22.8, 10.8, 5.6 Hz, 1H), 5.39 – 5.27 (m, 1H), 5.20 (dd, J = 10.5, 1.5 Hz, 1H), 4.62 (dt,

J = 5.6, 1.4 Hz, 2H), 4.30 (d, J = 6.6 Hz, 2H), 4.22 (d, J = 5.9 Hz, 1H), 3.25 (d, J = 5.0 Hz, 1H) 3.19 (d, J = 6.0 Hz, 2H) 2.83 – 2.80 (m, 2H), 2.53 (td, J = 7.2, 2.6 Hz, 2H), 2.10 (s, 2H) 1.88 – 1.80 (m, 1H). ^{13}C NMR (75 MHz, Acetone) δ 172.4, 171.6, 156.5, 145.1, 143.8, 140.5, 132.5, 128.7, 128.0, 127.4, 127.0, 126.8, 125.1, 120.0, 118.2, 70.5, 66.5, 65.8, 59.7, 46.9, 45.9, 39.6, 30.5, 25.0.

Fmoc-Gln(Trt)-Ala-OAllyl α-AAdipeptide 39

To a mixture of FmocNH$(CH_2)_2$-Gln(Trt)-OAllyl **38** (3 g, 4.3 mmol), propionic anhydride (2 mL, 15.7 mmol), in dry THF (100 mL) was added $NaHCO_3$ (800 mg, 9.5 mmol). The reaction mixture was stirred at room temperature for 20 hours, diluted with EtOAc (100 mL), washed with 1:1 1 M HCl/brine (2 × 100 mL), saturated aq. $NaHCO_3$ (100 mL) and brine (50 mL), dried over $MgSO_4$, filtered, and concentrated under reduced pressure. Purification by flash column chromatography (20→40% acetone/PE, Rf = 0,25) provided the expected compound **39** (2.59 g, 80%). ^{1}H NMR (300 MHz, Acetone) δ 7.86 (d, J = 7.5, 2H), 7.66 (d, J = 7.6, 2H), 7.36 – 7.10 (m, 18H), 5.92 (m, 1H), 5.31 (ddq, J = 17.2, 6.0, 1.6 Hz, 1H), 5.18 (ddq, J = 10.4, 5.6, 1.5 Hz, 1H), 4.60 (ddt, J = 18.2, 5.4, 1.5 Hz, 2H), 4.36 (d, J = 6.9 Hz, 1H), 4.33 – 4.14 (m, 2H), 4.05 (dd, J = 9.3, 5.0 Hz, 1H), 3.54 (q, J = 13.1, 10.5 Hz, 1H), 3.36 – 3.17 (m, 2H), 2.52 (q, J = 7.4 Hz, 5H), 2.44 – 2.26 (m, 3H), 2.25 – 2.10 (m, 1H), 1.12 (t, J = 7.4 Hz, 6H), 1.00 (ddd, J = 11.3, 7.4, 4.1 Hz, 3H). ^{13}C NMR (75 MHz, Acetone) δ 175.7, 174.3, 174.1, 172.5, 172.4, 172.1, 171.9, 171.6, 157.2, 146.0, 144.9, 142.0, 133.4, 133.3, 133.0, 129.7, 129.6, 128.4, 127.8, 127.8, 127.3, 126.0, 125.9, 120.7, 118.4, 118.0, 70.8, 70.8, 66.9, 65.7, 59.7, 52.9, 47.9, 40.2, 32.6, 30.6, 30.1, 29.8, 29.0, 27.9, 25.6, 24.4, 10.0, 9.7, 9.4.

Fmoc-Gln(Trt)-Ala-OH α-AAdipeptide 6

To a solution of Fmoc-Gln(Trt)-Ala-OAllyl α-AAdipeptide **39** (2.5 g, 3.3 mmol) in THF (60 mL) and MeOH (25 mL) was added tetrakis(triphenylphosphine)palladium (125 mg, 106 μmol) followed by dimedone (2 g, 14.3 mmol). The mixture was stirred at room temperature for 0.5 h then diluted with 100 mL EtOAc and washed with 1:1 1 M HCl/brine (2 times) and brine. The organic phase was dried over $MgSO_4$, filtered, and concentrated under reduced pressure. Purification by flash column chromatography (30→50% Acetone/PE + 1% AcOH, Rf = 0.15) provided the expected carboxylic acid **6**

(2.28 g, 96%). ^{1}H NMR (300 MHz, Acetone) δ 7.85 (dd, J = 7.6, 1.0 Hz, 2H), 7.74 – 7.62 (m, 2H), 7.41 (td, J = 7.5, 1.4 Hz, 2H), 7.37 – 7.09 (m, 25H), 6.61 (d, J = 13.8 Hz, 1H), 4.37 – 4.16 (m, 3H), 4.09 (dd, J = 8.7, 5.3 Hz, 1H), 3.57 (dd, J = 13.4, 7.7 Hz, 1H), 3.42 – 3.14 (m, 3H), 3.09 (ddd, J = 13.3, 7.8, 5.5 Hz, 1H), 2.68 – 2.34 (m, 4H), 2.31 (d, J = 0.7 Hz, 4H), 2.27 – 2.10 (m, 2H), 1.96 (s, 2H), 1.11 – 0.91 (m, 4H). ^{13}C NMR (75 MHz, Acetone) δ 173.2, 172.6, 146.1, 146.0, 145.0, 142.0, 129.7, 129.0, 128.5, 128.4, 128.3, 127.9, 127.3, 126.1, 126.1, 126.0, 120.8, 120.7, 67.0, 59.7, 48.6, 48.0, 40.3, 33.7, 30.6, 30.3, 30.1, 29.8, 29.5, 29.3, 29.0, 27.0, 26.6, 25.7, 10.0, 9.7.

Synthesis of Boc-Trp(boc)-Thr(Trt)-Phe-OH α-AAtripeptide – FTW building block 7

Boc-Phe-NHAllyl

To a solution of Boc-Phe-OH **40** (5 g, 18.8 mmol) in EtOAc (100 mL) was added allyl amine (3 mL, 11.6 mmol), *N*-Methylmorpholine, (15 mL, 136.4 mmol) and T3P (37.5 mL, 63 mmol). The reaction mixture was stirred at room temperature for 15 h, then diluted with EtOAc (50 mL) and washed with 1:1 1 M HCl/brine (2 × 100 mL), saturated aq. $NaHCO_3$ (100 mL) and brine (50 mL). The organic fraction was dried over $MgSO_4$, filtered, and concentrated under vacuum to provide Boc-Phe-NHAllyl (5.5 g, 95%). ^{1}H NMR (300 MHz, Acetone) δ 7.36 – 7.12 (m, 5H), 5.98 (s, 1H), 5.79 (ddt, *J* = 17.2, 10.5, 5.3 Hz, 1H), 5.19 – 4.96 (m, 2H), 4.34 (q, *J* = 8.2 Hz, 1H), 3.80 (ddt, *J* = 5.6, 3.4, 1.7 Hz, 2H), 3.14 (dd, *J* = 13.8, 5.6 Hz, 1H), 2.91 (dd, *J* = 13.8, 8.5 Hz, 1H), 2.80 – 2.73 (m, 1H), 1.34 (s, 9H). ^{13}C NMR (75 MHz, Acetone) δ 172.0, 156.2, 138.8, 135.8, 130.2, 129.0, 127.2, 115.6, 79.3, 56.8, 42.1, 39.1, 28.5.

Boc-Phe-NHCH$_2$CHO 41

To a solution of Boc-Phe-NHAllyl (1.65 g, 5.4 mmol) in 1:1 acetone/*t*BuOH (10 mL) was added $NaIO_4$ (2.3 g, 10.7 mmol) and a solution of K_2OsO_4 (4.87 mg, 26.7 μmol) in H_2O (5 ml). The mixture was stirred at room temperature for 3 h then diluted with EtOAc, washed with brine, dried over $MgSO_4$, filtered, and concentrated under reduced pressure. Purification by flash column chromatography (20% acetone/DCM, Rf = 0.4) provided Boc-Phe-NHCH$_2$CHO **41** (1.34 g, 58%). ^{1}H NMR (300 MHz, Acetone) δ 9.50 (s, 1H),

7.69 (s, 1H), 7.37 – 7.04 (m, 5H), 6.09 (s, 1H), 4.43 (q, *J* = 8.4 Hz, 1H), 4.00 (d, *J* = 5.4 Hz, 2H), 3.20 (dd, *J* = 13.9, 5.3 Hz, 1H), 2.90 (s, 1H), 2.82 – 2.69 (m, 1H), 1.33 (s, 9H). ^{13}C NMR (75 MHz, Acetone) δ 199.3, 173.1, 156.3, 138.9, 130.3, 129.2, 127.3, 79.5, 56.7, 50.5, 38.9, 28.6. ^{13}C NMR

Fmoc-Trp(Boc)-OAllyl

To a solution of Fmoc-Trp(Boc)-OH **42** (0.8 g, 1.53 mmol) in DMF (5 mL) was added allyl bromide (0.38 mL, 4.40 mmol) and Hunig's base (0.58 mL, 3.34 mmol). The reaction mixture was stirred at room temperature for 15 h, then diluted with EtOAc (25 mL) and washed with 1:1 1 M HCl/brine (2 × 25 mL), saturated aq. $NaHCO_3$ (25 mL) and brine (25 mL). The organic fraction was dried over $MgSO_4$, filtered, and concentrated. Purification by flash column chromatography (2→24% EtOAc/Pet. ether, Rf = 0.5) provided Fmoc-Trp(Boc)-OAllyl (0.78 g, 90%). ^{1}H NMR (300 MHz, Chloroform-*d*) δ 8.17 (d, *J*=8.3Hz,1H), 7.78 (d, *J* = 7.6 Hz, 2H), 7.60 – 7.23 (m, 10H), 5.88 (ddt, *J* = 16.4, 10.4, 5.8 Hz, 1H), 5.52 (d, *J* = 8.2 Hz, 1H), 5.41-5.18 (m, 2H), 4.89-4.76 (m, 1H), 4.62 (d, *J* = 5.8 Hz, 2H), 4.49 – 4.34 (m, 2H), 4.24 (t, *J* = 7.1 Hz, 1H), 3.31 (d, *J* = 5.5 Hz, 2H), 1.68 (s, 9H). δ 171.4, 155.8, 149.6, 143.9, 143.8, 141.3, 135.4, 131.4, 130.6, 127.8, 127.8, 127.1, 127.1, 125.2, 124.7, 124.3, 122.7, 120.0, 119.2, 118.9, 115.4, 114.9, 83.7, 67.3, 66.3, 54.3, 47.2, 28.2, 28.0.

H-Trp(Boc)-OAllyl 43

To a solution of Fmoc-Trp(Boc)-OAllyl (4.5 g, 7.9 mmol) in THF (100 mL) was added piperidine (15 mL). The reaction mixture was stirred at room temperature for 1 h and preadsorbed on silica gel and concentrated under reduced pressure. Purification by flash column chromatography (10→20% acetone/pet. ether + 1% TEA, Rf = 0.3) provided H-Trp(Boc)-OAllyl **43** (2.13 g, 67%). ^{1}H NMR (300 MHz, Chloroform-*d*) δ 8.13 (d, *J* = 7.8 Hz, 1H), 7.55 (d, *J* = 7.7 Hz, 1H), 7.47 (s, 1H), 7.31 (t, *J* = 7.7 Hz, 1H), 7.22 (t, *J* = 7.5 Hz, 1H), 5.97-5.76 (m, 1H), 5.37-5.15 (m, 2H), 4.68-4.53 (m, 2H), 3.92-3.79 (m, 1H), 3.21 (dd, *J* = 14.4, 5.0 Hz, 1H), 2.99 (dd, *J* = 14.4, 7.7 Hz, 1H), 1.65. ^{13}C NMR (75 MHz, Chloroform-*d*) δ 174.7, 149.6, 135.5, 131.8, 130.4, 124.5, 124.2,122.5, 119.0, 118.8, 116.0, 115.3, 83.6, 65.7, 54.5, 43.5, 30.5, 28.2.

Boc-Phe-NH(CH_2)$_2$-Trp(Boc)-OAllyl 44

To a mixture of Boc-Phe-NHCH_2CHO **41** (1.1 g, 3.6 mmol) and H-Trp(Boc)-OAllyl **43** (1.24 g, 1.24 mmol) was added freshly prepared STAB suspension (0.14 M in DCE, 19 mL, 2.1 mmol) at 0 °C under inert atmosphere. The mixture was stirred at room temperature for 1 h, diluted with EtOAc, washed with 1:1 saturated aq. $NaHCO_3$/brine (2 times) and brine, dried over $MgSO_4$, filtered, and concentrated under reduced pressure. Purification by flash column chromatography (20→40% Et_2O/DCM) provided the named compound (1.41 g, 62%) ^{1}H NMR (300 MHz, Acetone) δ 8.11 (d, *J* = 8.2 Hz, 1H), 7.62 (d, *J* = 8.0 Hz, 1H), 7.58 – 7.37 (m, 3H), 7.36 – 7.13 (m, 5H), 5.98 – 5.74 (m, 2H), 5.29 – 5.09 (m, 2H), 4.52 (dt, *J* = 5.7, 1.4 Hz, 2H), 4.34 – 4.23 (m, 1H), 3.66 (t, *J* = 6.7 Hz, 1H), 3.42 – 3.22 (m, 1H), 3.18 – 3.01 (m, 2H), 2.89 (t, *J* = 6.4 Hz, 1H), 2.81 – 2.67 (m, 2H), 2.68 – 2.53 (m, 1H), 1.67 (s, 9H), 1.33 (s, 9H). ^{13}C NMR (75 MHz, Acetone) δ 174.7, 172.1, 139.0, 133.5, 131.7, 130.3, 129.1, 127.3, 125.2, 125.0, 123.4, 120.2, 118.4, 117.6, 116.0, 84.3, 79.3, 65.7, 62.3, 56.9, 48.0, 40.1, 39.2, 30.7, 30.5, 30.2, 29.9, 29.7, 29.6, 29.4, 29.2, 28.6, 28.4.

Thr side chain mimetic

To a suspension of *L*-Threonine **45** (10 g, 84 mmol) in water (25 mL) at -5 °C was added 48% HBr (57 mL). A sodium nitrite (11.6 g, 168 mmol) solution in water (20 mL) was added slowly, maintaining the reaction temperature at 0 °C. The resultant mixture was warmed to room temperature and stirred for 4 h. The dark-red solution was extracted with diethyl ether. The combined red organic extracts were washed with a saturated solution of sodium bisulfite, brine, and concentrated in vacuo to afford (2*S*,3*R*)-2-bromo-3-hydroxybutanoic acid (12.68 g, 83%). ^{1}H NMR (300 MHz, $CDCl_3$) δ 4.30 (d, *J* = 4.4 Hz, 1H), 4.19 (qd, *J* = 6.2, 4.4 Hz, 1H), 1.35 (d, *J* = 6.3 Hz, 3H). ^{13}C NMR (75 MHz, $CDCl_3$) δ 172.4, 67.7, 52.6, 20.1.

To an ethereal solution (20 mL) of (2*S*,3*R*)-2-bromo-3-hydroxybutanoic acid (1 g, 5.5 mmol) a diazomethane solution in diethyl ether was added dropwise until the yellow color persisted. AcOH was added until the solution turned colorless again. The solution was evaporated under reduced pressure to afford methyl (2*S*,3*R*)-2-bromo-3-hydroxybutanoate (1.06 g, 99%). ^{1}H NMR (300 MHz, $CDCl_3$) δ 4.24 (d, *J* = 4.8 Hz, 1H),

4.12 (qd, *J* = 6.2, 4.8 Hz, 1H), 3.81 (s, 3H), 1.30 (d, *J* = 6.3 Hz, 3H). ^{13}C NMR (75 MHz, $CDCl_3$) δ 169.8, 67.5, 53.3, 53.0, 20.1.

Methyl (2*S*,3*R*)-2-bromo-3-hydroxybutanoate (3.4 g, 17.2 mmol) and Et_3N (3 mL g, 22 mmol) are dissolved into MeOH (75 mL). 10% Pd on charcoal (350 mg) is then added and the mixture is stirred under 1 atm H_2 pressure at room temperature. After 20 h, the solution is filtered over celite, diluted with EtOAc (100 mL), and washed with 1 M HCl (2 × 50 mL), saturated aq. $NaHCO_3$ (50 mL) and brine (50 mL). The organic fraction was dried over $MgSO_4$, filtered, and concentrated. Purification by flash column chromatography (5→15% acetone/DCM, Rf = 0.6) provided methyl (*S*)-3-hydroxybutanoate (1,7 g, 85%). ^{1}H NMR (300 MHz, $CDCl_3$) δ 4.20 (dqd, *J* = 8.4, 6.3, 3.7 Hz, 1H), 3.71 (s, 3H), 2.62 – 2.35 (m, 2H), 1.23 (d, *J* = 6.3 Hz, 3H). ^{13}C NMR (75 MHz, $CDCl_3$) δ 173.5, 64.3, 51.9, 42.6, 22.6.

To a solution of methyl (*S*)-3-hydroxybutanoate (3.3 g, 27.8 mmol) in nitromethane (60 mL) was added trityl chloride (8.5 g, 30.5 mmol) and pyridine (5 mL, 62 mmol). The reaction mixture was stirred at 50 °C for 15 h and then evaporated under reduced pressure. The remaining material was diluted with EtOAc (100 mL) and washed with 1 M HCl (2 × 50 mL), saturated aq. $NaHCO_3$ (50 mL) and brine (50 mL). The organic fraction was dried over $MgSO_4$, filtered, and concentrated. Purification by flash column chromatography (5% acetone/pet. ether, Rf = 0.4) provided methyl (*S*)-3-(trityloxy)butanoate (8.5 g, 85%). ^{1}H NMR (300 MHz, $CDCl_3$) δ 7.55 – 7.44 (m, 5H), 7.35 – 7.17 (m, 10H), 3.99 (dqd, *J* = 8.1, 6.1, 4.6 Hz, 1H), 3.54 (s, 3H), 2.23 – 1.92 (m, 2H), 1.04 (d, *J* = 6.0 Hz, 3H). ^{13}C NMR (75 MHz, $CDCl_3$) δ 172.0, 145.0, 129.1, 127.85, 127.2, 87.1, 67.4, 51.4, 42.5, 22.1.

The mixture of methyl (*S*)-3-(trityloxy)butanoate (1.1 g, 3 mmol) and lithium hydroxide (600 mg, 25 mmol) in a mixture of THF (30 mL), MeOH (45 mL) and H_2O (50 mL) was stirred for 12 hours at room temperature. The reaction mixture was extracted 2 times with DCM (50 mL) and acidified with a saturated tartaric acid solution. It was extracted 3 times with EtOAc (50 mL), dried over $MgSO_4$, filtered, and concentrated under vacuum to provide the desired compound **46** (950 mg, 90%). ^{1}H NMR (300 MHz, $CDCl_3$) δ 7.55 – 7.44 (m, 5H), 7.39 – 7.19 (m, 10H), 4.03 (td, *J* = 6.3, 4.8 Hz, 1H), 1.96 – 1.89 (m, 2H),

1.18 (d, *J* = 6.2 Hz, 3H). ^{13}C NMR (75 MHz, $CDCl_3$) δ 175.6, 144.6, 128.9, 128.0, 127.4, 87.7, 67.2, 41.9, 22.0.

Boc-Trp(boc)-Thr(Trt)-Phe-OAllyl α-AAtripeptide 47

To a mixture of Boc-Phe-NH$(CH_2)_2$-Trp(Boc)-OAllyl **44** (1.3 g, 2 mmol), Thr side chain mimetic **46** (1.4 g, 4 mmol), DEPBT (3.5 g, 6 mmol) in THF (50 mL) was added Hunig's base (1.5 mL, 8 mmol). The reaction mixture was stirred at room temperature for 15 h, diluted with EtOAc (100 mL), washed with 1:1 1 M HCl/brine (2 × 100 mL), saturated aq. $NaHCO_3$ (100 mL) and brine (50 mL), dried over $MgSO_4$, filtered, and concentrated under reduced pressure. Purification by flash column chromatography (10→100% Et2O/DCM) provided the expected compound **47** (1.39 g, 72%). ^{1}H NMR (300 MHz, Acetone) δ 8.17 (d, J = 8.3 Hz, 1H), 7.61 – 7.46 (m, 4H), 7.35 – 7.16 (m, 6H), 7.06 (s, 1H), 6.04 – 5.83 (m, 1H), 5.42 – 5.26 (m, 1H), 5.20 (dq, J = 10.5, 1.5 Hz, 1H), 4.72 – 4.56 (m, 1H), 4.37 – 4.10 (m, 1H), 3.45 – 3.16 (m, 1H), 3.15 – 2.79 (m, 3H), 2.51 (dd, J = 14.9, 7.3 Hz, 0H), 2.34 – 2.18 (m, 0H), 1.95 – 1.78 (m, 1H), 1.66 (d, J = 1.7 Hz, 5H), 1.33 (d, J = 2.5 Hz, 5H), 1.17 – 1.06 (m, 2H). ^{13}C NMR (75 MHz, Acetone) δ 173.8, 172.3, 169.8, 146.0, 146.0, 145.9, 145.6, 145.1, 143.3, 143.2, 139.1, 138.3, 130.2, 130.1, 129.4, 129.4, 129.3, 128.8, 128.7, 128.7, 128.6, 128.5, 128.2, 128.2, 128.0, 128.0, 127.1, 127.0, 126.9, 119.7, 75.5, 70.4, 70.2, 67.3, 51.3, 44.7, 36.2, 33.0, 30.3, 30.1, 29.8, 29.6, 29.3, 29.1, 28.8, 27.3, 23.2, 21.9.

Boc-Trp(boc)-Thr(Trt)-Phe-OH α-AAtripeptide 7

To a solution of Boc-Trp(boc)-Thr(Trt)-Phe-OAllyl α-AAtripeptide **47** (1.5 g, 1.55 mmol) in THF (25 mL) and MeOH (10 mL) was added tetrakis(triphenylphosphine)palladium (50 mg, 40 μmol) followed by sodium *para*-toluenesulfinate (5.6 g, 3.1 mmol). The mixture was stirred at room temperature for 0.5 h then diluted with EtOAc and washed with 1:1 1 M HCl/brine (2 times) and brine. The organic phase was dried over $MgSO_4$, filtered, and concentrated under reduced pressure. Purification by flash column chromatography (2→4% MeOH/DCM + 1% AcOH) provided the expected carboxylic acid **7** (1.36 g, 95%). ^{1}H NMR (300 MHz, Acetone) δ 8.16 (d, J = 8.2 Hz, 1H), 7.72 (ddt, J = 11.9, 6.7, 1.6 Hz, 1H), 7.54 (s, 0H), 7.54 – 7.47 (m, 5H), 7.39 – 7.15 (m, 15H), 6.00 (d, J = 8.4 Hz, 1H), 4.22 (d, J = 7.7 Hz, 2H), 3.33 (td,

J = 21.9, 19.1, 9.8 Hz, 1H), 3.04 (dd, J = 13.6, 6.7 Hz, 1H), 2.86 (dd, J = 13.6, 8.1 Hz, 0H), 1.66 (s, 9H), 1.32 (d, J = 6.6 Hz, 9H), 1.16 (d, J = 5.9 Hz, 2H). ^{13}C NMR (75 MHz, Acetone) δ 206.2, 172.3, 171.6, 162.4, 160.5, 150.3, 146.1, 138.7, 136.4, 132.9, 132.9, 132.8, 131.5, 130.3, 129.9, 129.8, 129.7, 129.5, 129.1, 128.7, 128.6, 127.9, 127.6, 127.3, 125.3, 124.9, 123.6, 123.5, 120.9, 120.8, 120.0, 118.3, 116.2, 116.1, 106.0, 87.9, 84.3, 79.5, 68.7, 68.3, 61.3, 57.0, 55.0, 48.7, 41.9, 39.1, 38.7, 30.7, 30.6, 30.4, 30.2, 29.9, 29.7, 29.4, 29.1, 28.6, 28.4, 28.4, 24.9, 23.3.

Synthesis of Fmoc-Thr(tBu)-Glu(tBu)-His(Trt)-Gln(Trt)-NHTrt α-AAtetrapeptide

To a solution of **3** (1 g, 0.96 mmol), **4** (2 g, 1.92 mmol), EDCI (555 mg, 2.9 mmol) and DHOBt (470 mg, 2.9 mmol) in THF (20 mL) was added Hunig's base (0.7 mL, 3.8 mmol). The reaction mixture was stirred at room temperature for 12 h and then diluted with EtOAc. The solution was washed with 1:1 1 M HCl/brine (2 times), saturated aq. $NaHCO_3$ and brine. The organic phase was dried over magnesium sulfate, filtered, and concentrated under vacuum. Purification by flash column chromatography (5→20% (1:4 MeOH/EtOAc)/(1:1 DCM/PE)) provided Fmoc-Thr(tBu)-Glu(tBu)-His(Trt)-Gln(Trt)-NHTrt α-AAtetrapeptide (1.45 g, 93%).

Synthesis of H-Thr(tBu)-Glu(tBu)-His(Trt)-Gln(Trt)-NHTrt α-AAtetrapeptide 48

To a solution of Fmoc-Thr(tBu)-Glu(tBu)-His(Trt)-Gln(Trt)-NHTrt α-AAtetrapeptide (1.4 g, 0.85 mmol) in THF (40 mL) was added piperidine (10 mL). The reaction mixture was stirred at room temperature for 1 h and preadsorbed on silica gel and concentrated under reduced pressure. Purification by flash column chromatography (5→10% MeOH/DCM + 1% TEA) provided H-Thr(tBu)-Glu(tBu)-His(Trt)-Gln(Trt)-NHTrt α-AAtetrapeptide **48** (645 mg, 54%)

Synthesis of Fmoc-Phe-Trp(Boc)-Thr(tBu)-Glu(tBu)-His(Trt)-Gln(Trt)-NHTrt α-AAhexapeptide

To a solution of **48** (620 mg, 0.45 mmol), **5** (630 g, 0.9 mmol), EDCI (260 mg, 1.35 mmol) and DHOBt (260 mg, 1.35 mmol) in THF (15 mL) was added Hunig's base (0.25 mL, 1.2 mmol). The reaction mixture was stirred at room temperature for 3 h and then

diluted with EtOAc. The solution was washed with 1:1 1 M HCl/brine (2 times), saturated aq. $NaHCO_3$ and brine. The organic phase was dried over magnesium sulfate, filtered, and concentrated under vacuum. Purification by flash column chromatography (5→30% (1:4 MeOH/EtOAc)/(1:1 DCM/PE)) provided Fmoc-Phe-Trp(Boc)-Thr(tBu)-Glu(tBu)-His(Trt)-Gln(Trt)-NHTrt α-AAhexapeptide (810 mg, 86%).

Synthesis of H-Phe-Trp(Boc)-Thr(tBu)-Glu(tBu)-His(Trt)-Gln(Trt)-NHTrt α-AAhexapeptide 49

To a solution of Fmoc-Phe-Trp(Boc)-Thr(tBu)-Glu(tBu)-His(Trt)-Gln(Trt)-NHTrt α-AAhexapeptide (800 mg, 0.38 mmol) in THF (20 mL) was added piperidine (5 mL). The reaction mixture was stirred at room temperature for 1 h and preadsorbed on silica gel and concentrated under reduced pressure. Purification by flash column chromatography (2→5% MeOH/DCM + 1% TEA) provided H-Thr(tBu)-Glu(tBu)-His(Trt)-Gln(Trt)-NHTrt α-AAtetrapeptide **49** (340 mg, 48%).

Synthesis of Fmoc-Gln(Trt)-Ala-Phe-Trp(Boc)-Thr(tBu)-Glu(tBu)-His(Trt)-Gln(Trt)-NHTrt α-AAoctapeptide

To a solution of **49** (320 mg, 0.17 mmol), **6** (240 g, 0.34 mmol), EDCI (150 mg, 0.5 mmol) and DHOBt (150 mg, 0.5 mmol) in THF (5 mL) was added Hunig's base (50 μL, 0.22 mmol). The reaction mixture was stirred at room temperature for 2 h and then diluted with EtOAc. The solution was washed with 1:1 1 M HCl/brine (2 times), saturated aq. $NaHCO_3$ and brine. The organic phase was dried over magnesium sulfate, filtered, and concentrated under vacuum. Purification by flash column chromatography (5→15% (1:4 MeOH/EtOAc)/(1:1 DCM/PE)) provided Fmoc-Gln(Trt)-Ala-Phe-Trp(Boc)-Thr(tBu)-Glu(tBu)-His(Trt)-Gln(Trt)-NHTrt α-AAoctapeptide (400 mg, 92%).

Synthesis of H-Gln(Trt)-Ala-Phe-Trp(Boc)-Thr(tBu)-Glu(tBu)-His(Trt)-Gln(Trt)-NHTrt α-AAoctapeptide 50

To a solution of Fmoc-Gln(Trt)-Ala-Phe-Trp(Boc)-Thr(tBu)-Glu(tBu)-His(Trt)-Gln(Trt)-NHTrt α-AAoctapeptide (375 mg, 0.15 mmol) in THF (10 mL) was added piperidine (2 mL). The reaction mixture was stirred at room temperature for 1 h and

preadsorbed on silica gel and concentrated under reduced pressure. Purification by flash column chromatography (1→3% MeOH/DCM + 1% TEA) provided the named compound (120 mg, 41%).

Synthesis of Boc-Trp(boc)-Thr(Trt)-Phe-Gln(Trt)-Ala-Phe-Trp(Boc)-Thr(tBu)-Glu(tBu)-His(Trt)-Gln(Trt)-NHTrt α-AAhendecapeptide 2

To a solution of **50** (120 mg, 0.05 mmol), **7** (95 g, 0.1 mmol), EDCI (45 mg, 0.15 mmol) and DHOBt (45 mg, 0.15 mmol) in THF (2 mL) was added Hunig's base (20 μL, 0.09 mmol). The reaction mixture was stirred at room temperature for 3 h and then diluted with EtOAc. The solution was washed with 1:1 1 M HCl/brine (2 times), saturated aq. $NaHCO_3$ and brine. The organic phase was dried over magnesium sulfate, filtered, and concentrated under vacuum. Purification by flash column chromatography (10→30% (1:4 MeOH/EtOAc)/(1:1 DCM/PE)) provided the named compound **2** (130 mg, 90%).

Synthesis of H-Trp-Thr-Phe-Gln-Ala-Phe-Trp-Thr-Glu-His-Gln-NH_2 α-AAhendecapeptide 1

Boc-Trp(boc)-Thr(Trt)-Phe-Gln(Trt)-Ala-Phe-Trp(Boc)-Thr(tBu)-Glu(tBu)-His(Trt)-Gln(Trt)-NHTrt **2** (115 mg, 35.4 μmol) was dissolved in TFA/TIS/H_2O 90:5:5 (12 mL) at 0 °C. After stirring at room temperature for 2 h, the solution was poured into cold Et_2O (120 mL) and stored at 0 °C for 15 h. The product was collected by filtration and the filter cake was then dissolved in water and freeze-dried. Purification by semipreparative HPLC provided the titled compound **1** (20 mg, 30%) as a white foam after freeze-drying. HRMS ESI $[M+H]^+$ Calc. for $C_{82}H_{110}N_{18}O_{17}$ 1617.82236 ; Found 1617.8236.

F. References

1. Durand, G. A., Raoult, D. & Dubourg, G. Antibiotic discovery: history, methods and perspectives. *Int J Antimicrob Agents* **53**, 371–382 (2019).
2. D'Costa, V. M. *et al.* Antibiotic resistance is ancient. *Nature* **477**, 457–461 (2011).
3. Jensen, S. O. & Lyon, B. R. Genetics of antimicrobial resistance in Staphylococcus aureus. *Future Microbiol* **4**, 565–582 (2009).
4. Mendelson, M. *et al.* The One Health stewardship of colistin as an antibiotic of last resort for human health in South Africa. *Lancet Infect Dis* **18**, e288–e294 (2018).
5. Cassir, N., Rolain, J.-M. & Brouqui, P. A new strategy to fight antimicrobial resistance: the revival of old antibiotics. *Front Microbiol* **5**, (2014).
6. Tacconelli, E. *et al.* Discovery, research, and development of new antibiotics: the WHO priority list of antibiotic-resistant bacteria and tuberculosis. *Lancet Infect Dis* **18**, 318–327 (2018).
7. Willyard, C. The drug-resistant bacteria that pose the greatest health threats. *Nature* **543**, 15–15 (2017).
8. Blaskovich, M. A. T., Butler, M. S. & Cooper, M. A. Polishing the tarnished silver bullet: the quest for new antibiotics. *Essays Biochem* **61**, 103–114 (2017).
9. Hughes, J. *et al.* Identification of two related pentapeptides from the brain with potent opiate agonist activity. *Nature* **258**, 577–579 (1975).
10. Mansour, R. & Elshafei, A. M. Protection of metal surfaces from microbial colonization. *Annu Res Rev Biol* **14**, (2017).
11. Hall-Stoodley, L., Costerton, J. W. & Stoodley, P. Bacterial biofilms: From the natural environment to infectious diseases. *Nature Reviews Microbiology* vol. 2 95–108 (2004).
12. Goudarzi, M., Navidinia, M., Khadembashi, N. & Rasouli, R. Biofilm Matrix Formation in Human: Clinical Significance, Diagnostic Techniques, and Therapeutic Drugs. *Arch Clin Infect Dis* **16**, (2021).
13. Muhammad, M. H. *et al.* Beyond Risk: Bacterial Biofilms and Their Regulating Approaches. *Frontiers in Microbiology* vol. 11 Preprint at (2020).
14. Watnick, P. & Kolter, R. Biofilm, city of microbes. *Journal of Bacteriology* vol. 182 2675–2679 (2000).
15. Jamal, M. *et al.* Bacterial biofilm and associated infections. *Journal of the Chinese Medical Association* vol. 81 7–11 (2018).
16. Chung, P. Y. & Toh, Y. S. Anti-biofilm agents: Recent breakthrough against multi-drug resistant Staphylococcus aureus. *Pathogens and Disease* vol. 70 231–239 (2014).
17. Vestby, L. K., Grønseth, T., Simm, R. & Nesse, L. L. Bacterial biofilm and its role in the pathogenesis of disease. *Antibiotics* vol. 9 Preprint at (2020).
18. Dror, N., Mandel, M., Hazan, Z. & Lavie, G. Advances in Microbial Biofilm Prevention on Indwelling Medical Devices with Emphasis on Usage of Acoustic Energy. *Sensors* **9**, 2538–2554 (2009).
19. Jansen, B. & Kohnen, W. *Prevention of biofilm formation by polymer modification*. *Journal of industrial Microbiology* vol. 15 (1995).
20. Brash, J. L. *42. Hydrophobic Polymers as Materials for Interfacing with Blood**.

21. Schlegel, A. *et al.* Anionic polymers for decreased toxicity and enhanced in vivo delivery of siRNA complexed with cationic liposomes. *Journal of Controlled Release* **152**, 393–401 (2011).
22. Bhatti, R. S., Shah, S., Suresh, Krishan, P. & Sandhu, J. S. Recent Pharmacological Developments on Rhodanines and 2,4-Thiazolidinediones. *Int J Med Chem* **2013**, 1–16 (2013).
23. Opperman, T. J. *et al.* Aryl rhodanines specifically inhibit staphylococcal and enterococcal biofilm formation. *Antimicrob Agents Chemother* **53**, 4357–4367 (2009).
24. Marques, C. N. H., Davies, D. G. & Sauer, K. Control of biofilms with the fatty acid signaling molecule cis-2-Decenoic acid. *Pharmaceuticals* vol. 8 816–835 (2015).
25. Davies, D. G. & Marques, C. N. H. A Fatty Acid Messenger Is Responsible for Inducing Dispersion in Microbial Biofilms. *J Bacteriol* **191**, 1393–1403 (2009).
26. Ma, L., Jackson, K. D., Landry, R. M., Parsek, M. R. & Wozniak, D. J. Analysis of *Pseudomonas aeruginosa* Conditional Psl Variants Reveals Roles for the Psl Polysaccharide in Adhesion and Maintaining Biofilm Structure Postattachment. *J Bacteriol* **188**, 8213–8221 (2006).
27. Yu, S. *et al.* PslG, a self-produced glycosyl hydrolase, triggers biofilm disassembly by disrupting exopolysaccharide matrix. *Cell Res* **25**, 1352–1367 (2015).
28. di Somma, A., Moretta, A., Canè, C., Cirillo, A. & Duilio, A. Antimicrobial and antibiofilm peptides. *Biomolecules* vol. 10 (2020).
29. Harris, F., Dennison, S. R. & Phoenix, D. A. *Anionic Antimicrobial Peptides from Eukaryotic Organisms*. (2009).
30. Steiner, H., Hultmark, D., Engström, Å., Bennich, H. & Boman, H. G. Sequence and specificity of two antibacterial proteins involved in insect immunity. *Nature* **292**, (1981).
31. Malik, E., Dennison, S. R., Harris, F. & Phoenix, D. A. PH dependent antimicrobial peptides and proteins, their mechanisms of action and potential as therapeutic agents. *Pharmaceuticals* vol. 9 (2016).
32. di Somma, A., Moretta, A., Canè, C., Cirillo, A. & Duilio, A. Antimicrobial and Antibiofilm Peptides. *Biomolecules* **10**, 652 (2020).
33. de la Fuente-Núñez, C., Cardoso, M. H., de Souza Cândido, E., Franco, O. L. & Hancock, R. E. W. Synthetic antibiofilm peptides. *Biochimica et Biophysica Acta (BBA) - Biomembranes* **1858**, 1061–1069 (2016).
34. Blower, R. J., Barksdale, S. M. & van Hoek, M. L. Snake Cathelicidin NA-CATH and Smaller Helical Antimicrobial Peptides Are Effective against Burkholderia thailandensis. *PLoS Negl Trop Dis* **9**, e0003862 (2015).
35. Sutton, J. M. & Pritts, T. A. Human beta-defensin 3: a novel inhibitor of Staphylococcus-Produced biofilm production. Commentary on "Human β-defensin 3 inhibits antibiotic-resistant Staphylococcus biofilm formation". *Journal of Surgical Research* **186**, 99–100 (2014).
36. Arslan, S. Y., Leung, K. P. & Wu, C. D. The effect of lactoferrin on oral bacterial attachment. *Oral Microbiol Immunol* **24**, 411–416 (2009).
37. Overhage, J. *et al.* Human Host Defense Peptide LL-37 Prevents Bacterial Biofilm Formation. *Infect Immun* **76**, 4176–4182 (2008).
38. Okuda, K. *et al.* Effects of Bacteriocins on Methicillin-Resistant Staphylococcus aureus Biofilm. *Antimicrob Agents Chemother* **57**, 5572–5579 (2013).

39. Parducho, K. R. *et al.* The Antimicrobial Peptide Human Beta-Defensin 2 Inhibits Biofilm Production of Pseudomonas aeruginosa Without Compromising Metabolic Activity. *Front Immunol* **11**, (2020).
40. Dennison, S. R., Harris, F., Morton, L. H. G. & Phoenix, D. A. Antimicrobial activity of aurein 2.5 against yeasts. *FEMS Microbiol Lett* **346**, 140–145 (2013).
41. Kim, M. *et al.* Antibacterial and Antibiofilm Activity and Mode of Action of Magainin 2 against Drug-Resistant Acinetobacter baumannii. *Int J Mol Sci* **19**, 3041 (2018).
42. Libardo, M. D. J. *et al.* Nuclease activity gives an edge to host-defense peptide piscidin 3 over piscidin 1, rendering it more effective against persisters and biofilms. *FEBS J* **284**, 3662–3683 (2017).
43. de la Fuente-Núñez, C. *et al.* Inhibition of Bacterial Biofilm Formation and Swarming Motility by a Small Synthetic Cationic Peptide. *Antimicrob Agents Chemother* **56**, 2696–2704 (2012).
44. Liu, W. *et al.* Antimicrobial Peptide Cec4 Eradicates the Bacteria of Clinical Carbapenem-Resistant Acinetobacter baumannii Biofilm. *Front Microbiol* **11**, (2020).
45. Hancock, R. E. W., Alford, M. A. & Haney, E. F. Antibiofilm activity of host defence peptides: complexity provides opportunities. *Nature Reviews Microbiology* vol. 19 786–797 (2021).
46. STEPANOVIĆ, S. *et al.* Quantification of biofilm in microtiter plates: overview of testing conditions and practical recommendations for assessment of biofilm production by staphylococci. *APMIS* **115**, 891–899 (2007).
47. Trentin, D. da S. *et al.* Potential of medicinal plants from the Brazilian semi-arid region (Caatinga) against Staphylococcus epidermidis planktonic and biofilm lifestyles. *J Ethnopharmacol* **137**, 327–335 (2011).
48. Pelay-Gimeno, M., Glas, A., Koch, O. & Grossmann, T. N. Structure-Based Design of Inhibitors of Protein-Protein Interactions: Mimicking Peptide Binding Epitopes. *Angewandte Chemie International Edition* **54**, 8896–8927 (2015).
49. Papini, A. M. From morphine to endogenous opioid peptides, e.g., endorphins: the endless quest for the perfect painkiller. *An International Journal of the History of Chemistry* **2**, 81–91 (2018).
50. Farmer, P. S. & Ariëns, E. J. Speculations on the design of nonpeptidic peptidomimetics. *Trends Pharmacol Sci* **3**, 362–365 (1982).
51. Ripka, A. S. & Rich, D. H. *Peptidomimetic design Abbreviations ACE angiotensin-converting enzyme ECE endothelin-converting enzyme GPIIb/IIIa glycoprotein IIb/IIIa ICE interleukin-1 P-converting enzyme NEP neutral endopeptidase PRP platelet-rich plasma SAR structure/activity relationship*. *Current Opinion in Chemical Biology* vol. 2 (1998).
52. Adessi, C. & Soto, C. *Converting a Peptide into a Drug: Strategies to Improve Stability and Bioavailability*. *Current Medicinal Chemistry* vol. 9 (2002).
53. Gante, J. Peptidomimetics—Tailored Enzyme Inhibitors. *Angewandte Chemie International Edition in English* **33**, 1699–1720 (1994).
54. Choudhary, A. & Raines, R. T. An Evaluation of Peptide-Bond Isosteres. *ChemBioChem* **12**, 1801–1807 (2011).
55. Nielsen, L., Lindsay, K. B., Faber, J., Nielsen, N. C. & Skrydstrup, T. Stereocontrolled Synthesis of Methyl Silanediol Peptide Mimics. *J Org Chem* **72**, 10035–10044 (2007).
56. Kim, J. & Sieburth, S. McN. Silanediol peptidomimetics. Evaluation of four diastereomeric ACE inhibitors. *Bioorg Med Chem Lett* **14**, 2853–2856 (2004).

57. Rodriguez, M., Dubreuil, P., Bali, J. P. & Martinez, J. Synthesis and biological activity of partially modified retro-inverso pseudopeptide derivatives of the C-terminal tetrapeptide of gastrin. *J Med Chem* **30**, 758–763 (1987).
58. *Peptidomimetics in Organic and Medicinal Chemistry*.
59. White, C. J. & Yudin, A. K. Contemporary strategies for peptide macrocyclization. *Nat Chem* **3**, 509–524 (2011).
60. Li, P., Roller, P. & Xu, J. Current Synthetic Approaches to Peptide and Peptidomimetic Cyclization. *Curr Org Chem* **6**, 411–440 (2002).
61. Ursu, A., Vézina-Dawod, S. & Disney, M. D. Methods to identify and optimize small molecules interacting with RNA (SMIRNAs). *Drug Discov Today* **24**, 2002–2016 (2019).
62. Huang, L. *et al.* Structure of an E6AP-UbcH7 Complex: Insights into Ubiquitination by the E2-E3 Enzyme Cascade. *Science (1979)* **286**, 1321–1326 (1999).
63. Huang, B. *et al.* Activation of E6AP/UBE3A-Mediated Protein Ubiquitination and Degradation Pathways by a Cyclic γ-AA Peptide. *J Med Chem* **65**, 2497–2506 (2022).
64. Wtorek, K. *et al.* Synthesis, pharmacological evaluation, and computational studies of cyclic opioid peptidomimetics containing β3-lysine. *Molecules* **27**, (2022).
65. Lenci, E. & Trabocchi, A. Peptidomimetic toolbox for drug discovery. *Chem Soc Rev* **49**, 3262–3277 (2020).
66. Weber, I. T., Wang, Y. F. & Harrison, R. W. Hiv protease: Historical perspective and current research. *Viruses* vol. 13 (2021).
67. Patrick, G. *An Introduction to Medicinal Chemistry* . (Oxford University Press, 2017).
68. Owen, D. R. *et al. An oral SARS-CoV-2 M pro inhibitor clinical candidate for the treatment of COVID-19*. https://www.science.org.
69. Ahmad, B., Batool, M., Ain, Q. ul, Kim, M. S. & Choi, S. Exploring the Binding Mechanism of PF-07321332 SARS-CoV-2 Protease Inhibitor through Molecular Dynamics and Binding Free Energy Simulations. *Int J Mol Sci* **22**, 9124 (2021).
70. Bolarinwa, O., Nimmagadda, A., Su, M. & Cai, J. Structure and Function of AApeptides. *Biochemistry* **56**, 445–457 (2017).
71. Hu, Y., Li, X., Sebti, S. M., Chen, J. & Cai, J. Design and synthesis of AApeptides: A new class of peptide mimics. *Bioorg Med Chem Lett* **21**, 1469–1471 (2011).
72. Niu, Y., Hu, Y., Li, X., Chen, J. & Cai, J. γ-AApeptides: design, synthesis and evaluation. *New Journal of Chemistry* **35**, 542 (2011).
73. *Peptides*. (Elsevier, 1995).
74. Gu, L. & Guo, Z. Alzheimer's Aβ42 and Aβ40 peptides form interlaced amyloid fibrils. *J Neurochem* **126**, 305–311 (2013).
75. Debaene, F., da Silva, J. A., Pianowski, Z., Duran, F. J. & Winssinger, N. Expanding the scope of PNA-encoded libraries: divergent synthesis of libraries targeting cysteine, serine and metallo-proteases as well as tyrosine phosphatases. *Tetrahedron* **63**, 6577–6586 (2007).
76. Sang, P. *et al.* Antimicrobial AApeptides. *Curr Top Med Chem* **17**, 1266–1279 (2017).
77. Padhee, S. *et al.* Non-hemolytic α-AApeptides as antimicrobial peptidomimetics. *Chemical Communications* **47**, 9729 (2011).

78. Poissonnier, A. *et al.* Disrupting the CD95–PLCγ1 interaction prevents Th17-driven inflammation. *Nat Chem Biol* **14**, 1079–1089 (2018).
79. Nguyen, H. T. *et al.* Synthesis of peptidomimetics and chemo-biological tools for CD95/PLCγ1 interaction analysis. *Bioorg Med Chem Lett* **29**, 2094–2099 (2019).
80. Wu, H., Teng, P. & Cai, J. Rapid Access to Multiple Classes of Peptidomimetics from Common γ-AApeptide Building Blocks. *European J Org Chem* **2014**, 1760–1765 (2014).
81. Friedrich-Bochnitschek, S., Waldmann, H. & Kunz, H. Allyl esters as carboxy protecting groups in the synthesis of O-glycopeptides. *J Org Chem* **54**, 751–756 (1989).
82. Fields, G. B. Methods for Removing the Finoc Group. in *Peptide Synthesis Protocols* 17–28 (Humana Press). doi:10.1385/0-89603-273-6:17.
83. Eto, K., Yoshino, M., Takahashi, K., Ishihara, J. & Hatakeyama, S. Total Synthesis of Oxazolomycin A. *Org Lett* **13**, 5398–5401 (2011).
84. Maegawa, T. *et al.* Novel deprotection method of Fmoc group under neutral hydrogenation conditions. *Amino Acids* **36**, 493–499 (2009).
85. Porcheddu, A., Giacomelli, G., Piredda, I., Carta, M. & Nieddu, G. A Practical and Efficient Approach to PNA Monomers Compatible with Fmoc-Mediated Solid-Phase Synthesis Protocols. *European J Org Chem* **2008**, 5786–5797 (2008).
86. Abid, O. H. & Ramadan, A. khames. Preparation and Identification of Novel 1, 3-Oxazepine Derivatives by Cycloaddition Reactions [2+5] of Selected Carboxylic Acid Anhydrides with Imines Derived from 4-methyl aniline. *Al-Mustansiriyah Journal of Science* **29**, 93–100 (2018).
87. Murugesan, K. *et al.* Catalytic reductive aminations using molecular hydrogen for synthesis of different kinds of amines. *Chem Soc Rev* **49**, 6273–6328 (2020).
88. Gribble, G. W. & Nutaitis, C. F. SODIUM BOROHYDRIDE IN CARBOXYLIC ACID MEDIA. A REVIEW OF THE SYNTHETIC UTILITY OF ACYLOXYBOROHYDRIDES. *Org Prep Proced Int* **17**, 317–384 (1985).
89. Abdel-Magid, A. F. & Mehrman, S. J. A Review on the Use of Sodium Triacetoxyborohydride in the Reductive Amination of Ketones and Aldehydes. *Org Process Res Dev* **10**, 971–1031 (2006).
90. Abdel-Magid, A. F., Carson, K. G., Harris, B. D., Maryanoff, C. A. & Shah, R. D. Reductive Amination of Aldehydes and Ketones with Sodium Triacetoxyborohydride. Studies on Direct and Indirect Reductive Amination Procedures [1]. *J Org Chem* **61**, 3849–3862 (1996).
91. McGonagle, F. I. *et al.* Development of a solvent selection guide for aldehyde-based direct reductive amination processes. *Green Chemistry* **15**, 1159 (2013).
92. El-Faham, A. & Albericio, F. Peptide Coupling Reagents, More than a Letter Soup. *Chem Rev* **111**, 6557–6602 (2011).
93. Tsukamoto, H., Suzuki, T. & Kondo, Y. Remarkable Solvent Effect on Pd(0)-Catalyzed Deprotection of Allyl Ethers Using Barbituric Acid Derivatives: Application to Selective and Successive Removal of Allyl, Methallyl, and Prenyl Ethers. *Synlett* **2007**, 3131–3136 (2007).
94. Gomez-Martinez, P., Dessolin, M., Guibé, F. & Albericio, F. Nα-Alloc temporary protection in solid-phase peptide synthesis. The use of amine–borane complexes as allyl group scavengers. *J Chem Soc Perkin 1* 2871–2874 (1999)
95. Bajwa, J. S. Chemoselective deprotection of benzyl esters in the presence of benzyl ethers, benzyloxymethyl ethers and n-benzyl groups by catalytic transfer hydrogenation. *Tetrahedron Lett* **33**, 2299–2302 (1992).

96. Andersson, L. *et al.* Large-scale synthesis of peptides. *Biopolymers* **55**, 227–250 (2000).
97. Mollica, A., Pinnen, F., Azzurra, S. & Costante, R. The Evolution of Peptide Synthesis: From Early Days to Small Molecular Machines. *Curr Bioact Compd* **9**, 184–202 (2014).
98. Takahashi, D., Yano, T. & Fukui, T. Novel diphenylmethyl-Derived Amide Protecting Group for Efficient Liquid-Phase Peptide Synthesis: AJIPHASE. *Org Lett* **14**, 4514–4517 (2012).
99. Isidro-Llobet, A., Álvarez, M. & Albericio, F. Amino Acid-Protecting Groups. *Chem Rev* **109**, 2455–2504 (2009).
100. CHRISTENSEN, K., RAUNKER, M., SEVERINSEN, R. & NORRILD, J. C. DIPEPTIDE CONTAINING NON-PROTEIN AMINO ACID. (2012).
101. Amblard, M., Fehrentz, J.-A., Martinez, J. & Subra, G. Fundamentals of Modern Peptide Synthesis. in *Peptide Synthesis and Applications* 3–24 (Humana Press, 2005). doi:10.1385/1-59259-877-3:003.
102. Al-Warhi, T. I., Al-Hazimi, H. M. A. & El-Faham, A. Recent development in peptide coupling reagents. *Journal of Saudi Chemical Society* **16**, 97–116 (2012).
103. Goodman, M. & McGahren, W. J. Mechanistic studies of peptide oxazolone racemization. *Tetrahedron* **23**, 2031–2050 (1967).
104. JONES, J. H., RAMAGE, W. I. & WITTY, M. J. MECHANISM OF RACEMISATION OF HISTIDINE DERIVATIVES IN PEPTIDE SYNTHESIS. *Int J Pept Protein Res* **15**, 301–303 (2009).
105. Li, H. *et al.* 3-(Diethoxyphosphoryloxy)-1,2,3- benzotriazin-4(3 *H*)-one (DEPBT): A New Coupling Reagent with Remarkable Resistance to Racemization. *Org Lett* **1**, 91–94 (1999).
106. Carpino, L. A. 1-Hydroxy-7-azabenzotriazole. An efficient peptide coupling additive. *J Am Chem Soc* **115**, 4397–4398 (1993).
107. Albericio, F. *et al.* On the use of PyAOP, a phosphonium salt derived from HOAt, in solid-phase peptide synthesis. *Tetrahedron Lett* **38**, 4853–4856 (1997).
108. Abdelmoty, I., Albericio, F., Carpino, L. A., Foxman, B. M. & Kates, S. A. Structural studies of reagents for peptide bond formation: Crystal and molecular structures of HBTU and HATU. *Letters in Peptide Science* **1**, 57–67 (1994).
109. Poulain, R. F., Tartar, A. L. & Déprez, B. P. Parallel synthesis of 1,2,4-oxadiazoles from carboxylic acids using an improved, uronium-based, activation. *Tetrahedron Lett* **42**, 1495–1498 (2001).
110. Chen, F. M. F. & Benoiton, N. L. The preparation and reactions of mixed anhydrides of *N* -alkoxycarbonylamino acids. *Can J Chem* **65**, 619–625 (1987).
111. Cremin, D. J., Hegarty, A. F. & Begley, M. J. Mechanism of reaction of 2-ethoxy-1-ethoxycarbonyl-1,2-dihydroquinoline (EEDQ) with nucleophiles and its crystal structure. *Journal of the Chemical Society, Perkin Transactions 2* 412 (1980).
112. Magano, J. Large-Scale Amidations in Process Chemistry: Practical Considerations for Reagent Selection and Reaction Execution. *Org Process Res Dev* **26**, 1562–1689 (2022).
113. Augustine, J. K., Vairaperumal, V., Narasimhan, S., Alagarsamy, P. & Radhakrishnan, A. Propylphosphonic anhydride (T3P®): an efficient reagent for the one-pot synthesis of 1,2,4-oxadiazoles, 1,3,4-oxadiazoles, and 1,3,4-thiadiazoles. *Tetrahedron* **65**, 9989–9996 (2009).

114. Li, B.-F. *et al.* Efficient Synthesis of (2 *S* ,3 *S*)-2-Ethyl-3-methylvaleramide Using (1 *S* ,2 *S*)-Pseudoephedrine as a Chiral Auxiliary. *Org Process Res Dev* **13**, 463–467 (2009).
115. Marstokk, K.-M. *et al.* The Synthesis of Pure threo-1-Oxiranylethanol, and its Structure, Conformational Composition and Intramolecular Hydrogen Bonding as Studied by Microwave, Infrared and NMR Spectroscopy and Ab Initio Computations. *Acta Chem Scand* **46**, 325–337 (1992).
116. Kugelman, M., Gala, D., Jaret, R. S., Nyce, P. L. & McPhail, A. T. Synthesis of Azetidinones from L-Threonine: Formation of Unusually Stable Bicyclic Hemiketals and *cis* -Azetidinones. *Synlett* **1990**, 431–432 (1990).
117. Sánta, Z., Párkányi, L., Németh, I., Nagy, J. & Nyitrai, J. Synthesis of pure methyl [(2S,3R,αR)-1-(3-bromo-4-methoxyphenyl)-3-(α-acetoxy)ethyl-4-oxoazetidin-2-carboxylate] and its enantiomer. *Tetrahedron Asymmetry* **12**, 89–94 (2001).
118. Madarász, Z., Németh, I., Toscano, P., Welch, J. & Nyitrai, J. Stereocontrolled Synthesis of Methyl αR,2S,3R-3-(l-Acetoxyethyl)-1- (4-methoxyphenyl)-4-oxoazetidine-2-carboxylate. *Tetrahedron Lett* **36**, 8303–8306 (1995).
119. Bartoli, G. *et al.* Unusual and Unexpected Reactivity of *t*- Butyl Dicarbonate (Boc $_2$ O) with Alcohols in the Presence of Magnesium Perchlorate. A New and General Route to *t*- Butyl Ethers. *Org Lett* **7**, 427–430 (2005).
120. Shahsavari, S. *et al.* Tritylation of alcohols under mild conditions without using silver salts. *Tetrahedron Lett* **57**, 3877–3880 (2016).
121. Kurzer, F. & Douraghi-Zadeh, K. Advances in the Chemistry of Carbodiimides. *Chem Rev* **67**, 107–152 (1967).
122. Williams, A. & Ibrahim, I. T. Carbodiimide chemistry: recent advances. *Chem Rev* **81**, 589–636 (1981).
123. Bofill, J. M. & Albericio, F. Understanding the structure/reactivity of aminium/uronium salts as coupling reagents in peptide synthesis. *Tetrahedron Lett* **40**, 2641–2644 (1999).
124. Carpino, L. A. *et al.* The Uronium/Guanidinium Peptide Coupling Reagents: Finally the True Uronium Salts. *Angewandte Chemie International Edition* **41**, 441–445 (2002).
125. Albericio, F., Bofill, J. M., El-Faham, A. & Kates, S. A. Use of Onium Salt-Based Coupling Reagents in Peptide Synthesis [1]. *J Org Chem* **63**, 9678–9683 (1998).
126. Mehta, A., Jaouhari, R., Benson, T. J. & Douglas, K. T. Improved efficiency and selectivity in peptide synthesis: Use of triethylsilane as a carbocation scavenger in deprotection of t-butyl esters and t-butoxycarbonyl-protected sites. *Tetrahedron Lett* **33**, 5441–5444 (1992).

Table of figures

Table of schemes

Table of tables

UNIVERSITÉ DE RENNES 1

Titre : Synthèse d'un α-AApeptide dérivé d'un peptide RNase antibiofilm

Mots clés : AApeptide, Peptide antibiofilm, RNase peptide

Contexte : Le biofilm microbien est un problème de santé publique selon l'Organisation mondiale de la santé, lié à 75 % des infections humaines. Les biofilms sont des associations microbiennes bien organisées dans une matrice extracellulaire complexe. Les biofilms jouent le rôle de pool de bactéries et de barrière contre les antibiotiques ou pour héberger les cellules immunitaires. Les peptides ont été étudiés au cours des dernières décennies et ont montré une activité antibiofilm considérable même sur des micro-organismes résistants. Bien que très prometteuses, ces biomolécules présentent certaines limites *in vivo*, telles qu'une sensibilité protéolytique et une faible stabilité. Les peptidomimétiques, comme les AApeptides, sont une alternative viable pour résoudre ces limitations avec une plus grande résistance à la dégradation protéolytique.

Objectif : Synthèse d'un α-AApeptide à partir d'un peptide 11-mer naturel hautement actif conçu à partir de plusieurs séquences génétiques du système de défense humain, montrant 50 % d'activité d'inhibition du biofilm à 15 µM vis-à-vis de *Staphylococcus epidermidis*. **Méthode :** La synthèse chimique est du type peptidique et a reposé sur la préparation d'unités AAdipeptidiques puis à la conjugaison de celles-ci selon un processus convergent. **Résultats :** Le 11-mer α-AApeptide a été synthétisé avec succès. La molécule peptidomimétique n'a en revanche pas démontré d'activité vis-à-vis des souches bactériennes étudiées em comparaison avec le peptide naturel **Conclusions :** Des études supplémentaires devront être menées sur le peptide et son peptidomimétique afin de justifier de cette différence d'effet. Une attention particulière sera portée à la structuration tridimensionnelle de ceux-ci.

Title: Synthesis of an α-AApeptide derived from an antibiofilm RNase peptide

Keywords: AApeptides, Antibiofilm peptides, RNase peptide

Background: Microbial biofilm is a public health concern according to the World Health Organization, linked to 75% of human infections. Biofilms are well-organized microbial association in a complex extracellular matrix. Biofilms play as a pool of bacteria and as a barrier to antibiotics or to host immune cells. Peptides have been studied in recent decades and have shown considerable antibiofilm activity even on resistant microorganisms. Although quite promising, these biomolecules have some limitations *in vivo*, such as proteolytic susceptibility and low stability. Peptidomimetics, like AApeptide, are a viable alternative for solving these limitations with higher resistance to proteolytic degradation.

Objective: Synthesize an α-AApeptide from a highly active natural 11-mer peptide designed from several genetical sequences of the human host defense system, showing 50% of biofilm inhibition activity at 15 µM for Staphylococcus epidermidis stains. **Methods:** All the chemical synthesis has been performed in solution. A convergent synthetical approach was designed to reach the targeted peptidomimetic. **Results:** The 11-mer α-AApeptide was successfully synthesized. However, it did not show any antibiofilm activity compared to the original peptide. **Conclusions:** Despite the achievement of the targeted compound, it did not present the expected activity compared to its natural counterpart on the strains assessed. Some studies have to be envisioned in order to understand this result.

Résumé

Les bactéries produisent naturellement des composés à activité antibiotique et les sécrètent dans l'environnement pour leur développement et survie, raison pour laquelle la plupart des antibiotiques actuels provenaient de micro-organismes. Ces bactéries productrices d'antibiotiques ont également des gènes de résistance pour éviter l'autotoxicité. Dans ce scénario, un schéma apparaît, où les bactéries productrices d'antimicrobiens exercent une pression évolutive sur d'autres espèces bactériennes, conduisant à une endurance mutuelle. Des bactéries multirésistantes ont été découvertes à partir d'échantillons archéologiques, montrant que la résistance est aussi ancienne que les antibiotiques eux-mêmes.

La résistance aux antibiotiques ou aux antimicrobiens est la capacité d'un micro-organisme à survivre et à se développer à des concentrations d'un médicament habituellement utilisé pour son éradication. Cette résistance, due aux activités anthropiques, est accélérée, entraînant le développement de mutants résistants à un rythme plus rapide que celui de nouveaux médicaments.

Les biofilms sont omniprésents dans la vie organique mais peuvent générer plusieurs dangers dans le corps humain. Ils sont responsables de 80 % des infections microbiennes chroniques chez l'homme et entraînent une augmentation des taux de mortalité et de morbidité et, par conséquent, une augmentation des taux d'hospitalisation et des coûts des soins de santé. La formation d’un biofilm est considérée comme l'un des principaux facteurs de virulence dans les infections chroniques, provoquant des infections principalement liées aux implants de dispositifs médicaux, étant également présente dans des infections non liées à des processus chirurgicaux. Les cellules bactériennes dans un biofilm sont jusqu'à 1 000 fois plus résistantes à plusieurs antibiotiques et désinfectants par rapport à leurs homologues planctoniques, ce qui crée d'énormes défis dans la stérilisation de surface et dans la prévention ou la gestion des infections associées au biofilm.

Au cours de la dernière décennie, environ 700 000 décès par an sont imputés mondialement à des infections résistantes aux médicaments et, si aucune mesure n'est prise, ces infections pourraient causées 10 millions de victimes par an d'ici 2050. Ces infections sont l'une des principales causes de rejet dans les dispositifs biomédicaux.

Bien que les maladies liées aux infections bactériennes soient de plus en plus préoccupantes et qu'elles ne soient pas sélectives en fonction des groupes ethniques ou des régions, il y a encore peu d'intérêt et d'investissement des gouvernement et de l'industrie pharmaceutique dans la recherche.

Les peptides ont été étudiés comme un médicament possible pour éviter la formation de biofilm ou pour éradiquer le biofilm déjà formé. Ils sont connus en clinique depuis plusieurs décennies et ont été utilisés avec succès pour traiter des maladies.

A partir de 128 séquences connues de peptides antibactériens, 23 nouveaux peptides ont été proposés en utilisant la séquence conservée des peptides originaux contenant de 6 à 13 résidus d'acides aminés. Au sein de ces peptides, une ARNase contenant 11 résidus d'acides aminés (Ase3), inhibant respectivement plus de 50 % et environ 30 % de la formation de biofilms de *S. epidermidis* et *P. aeruginosa*, a été découverte. Une étude de simplification moléculaire a été réalisée dans le but de réduire le nombre d'acides aminés et, par conséquent, l'effort de synthèse pour synthétiser son mimétique. Non seulement la taille du peptide s'est avérée importante, mais le rôle de la partie N-terminale s'est également avérée essentielle lors des essais de sondage.

En raison de leurs caractéristiques particulières, les peptides antibiofilms étaient considérés comme des candidats valables pour lutter contre les biofilms, mais des problèmes tels que la mauvaise absorption, la biodistribution, le métabolisme et les propriétés d'excrétion peuvent expliquer leur échec en tant qu'agent antibiofilm. Une stratégie émergente repose sur le développement de peptidomimétiques pour surmonter les principaux problèmes liés aux peptides naturels. Les peptidomimétiques sont des molécules dont les pharmacophores miment un peptide ou une protéine naturelle dans un espace tridimensionnel et qui conservent la capacité d'interagir avec des cibles biologiques, présentant des effets pharmacologiques. Ces composés ont été conçus non seulement pour imiter les peptides naturels, mais aussi pour surmonter leurs inconvénients.

Dans les années 1970, le concept selon lequel une molécule non peptidique peut exercer le même effet biologique qu'un peptide ou une protéine a été postulé, mais il a fallu quelques décennies pour que l'intérêt pour le sujet atteigne les chimistes médicinaux. Le concept peptidomimétique a été une énorme percée dans plusieurs domaines scientifiques, plus profondément dans la biologie structurale, où les interactions protéine-protéine sont fondamentales pour la compréhension des processus cellulaires. Comme les peptides naturels, les peptidomimétiques ont une structure primaire et une structure

secondaire, parfois ils peuvent aussi avoir une structure tertiaire et quaternaire. Ces suprastructures sont fondamentales pour les interactions avec les protéines, les récepteurs et les enzymes.

Parmi les différents types de peptidomimétiques, le concept d'AApeptides a été introduit dans les années 2010. Ces pseudopeptides reposent sur des unités constituées d'acide aminé N-acylé-N-aminoéthyle et 2 sous-types, α et γ, décrits en fonction de la position de la chaîne latérale (soit le α-C ou le γ-C par rapport au groupe carboxyle). Ils présentent le même nombre de groupements fonctionnels que les peptides classiques de même longueur et une meilleure résistance à la dégradation protéolytique grâce à la présence de groupements fonctionnels amide tertiaire.

La séquence d'études de simplification sur Ase3 étant infructueuse, un mime 11-mer-Ase3 a été prévu. Sur la base de sa séquence, FTWAQWFETQH, le α-AApeptidomimétique correspondant, à savoir mimAse3, a été conçu pour améliorer les propriétés biologiques et pharmacodynamiques (schéma 1).

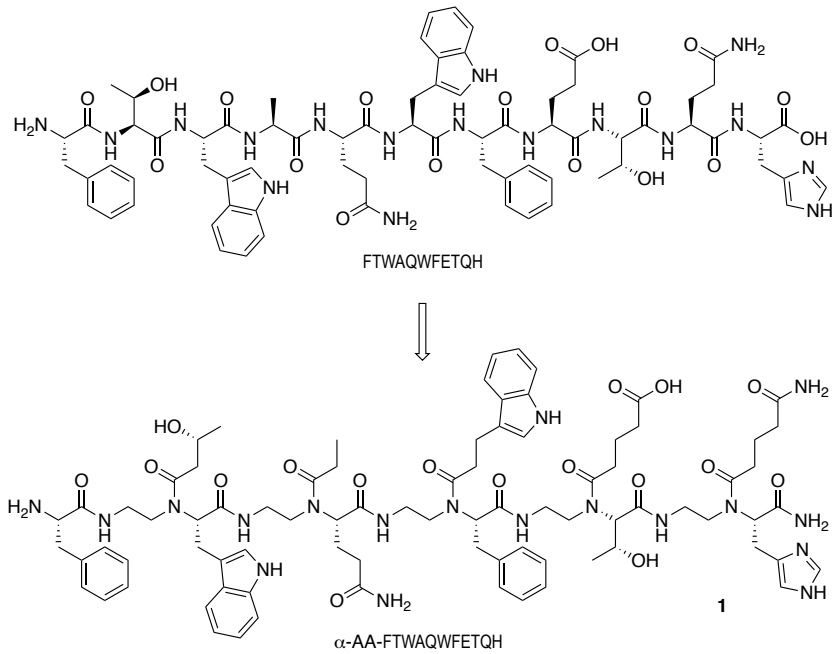

Schéma 1 : Transformation d'un peptide naturel en un a-AApeptide.

A partir d'un résidu naturel N-Fmoc-protégé, la synthèse d'un α-AApeptide consiste en une estérification en C-term ou un couplage trityl amine, suivi de la déprotection de l'amine primaire. Ensuite, une extension de chaîne est réalisée par une amination réductrice à l'aide de Fmoc-glycinaldéhyde et d'un agent réducteur pour fournir une amine secondaire qui est ensuite acylée avec un composé carboxyle. Enfin, l'acide

carboxylique ou le groupe fonctionnel amine est déprotégé, ce qui conduit au bloc de construction α-AApeptide attendu. Notez que le Fmoc-glycinaldéhyde est préparé en 2 étapes comprenant une oxydation Malaprade–Lemieux–Johnson de Fmoc-allylamine. Les blocs de construction sont ensuite couplés ensemble en phase liquide ou solide et, comme étape finale, une réaction de déprotection globale génère le pseudopeptide attendu, comme le montre le schéma 2. Ainsi, pour atteindre l'objectif, des groupes protecteurs orthogonaux ont été utilisés pour produire les blocs de construction nécessaires et le pseudopeptide attendu.

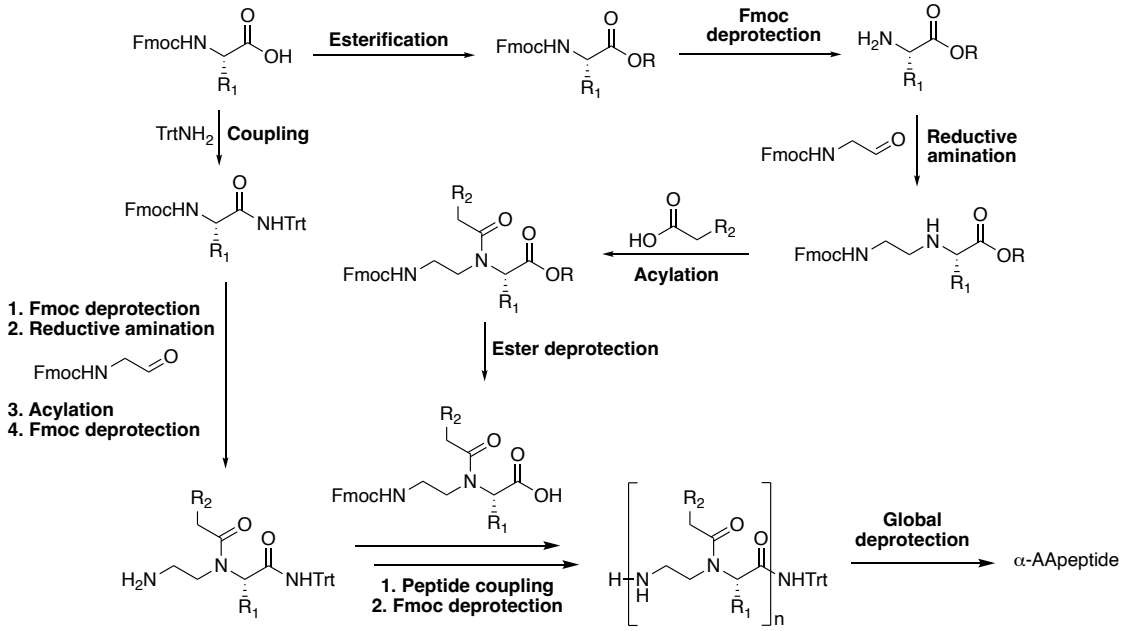

Schéma 2 : Synthèse générale des α-AApeptides

Bien que la synthèse peptidique en phase solide soit une méthode bien établie pour les α-peptides, cette technique produit des mélanges complexes de produits obtenus lors des étapes incomplètes de couplage et de déprotection en raison de l'impossibilité d'effectuer des purifications aux étapes intermédiaires. Pour pouvoir avoir plus de contrôle sur les processus et aussi pour pouvoir travailler à l'échelle du multigramme, ce travail a été réalisé en solution plutôt qu'en phase solide. La synthèse peptidique en phase liquide nécessite la mise en place de procédures de traitement pour chaque intermédiaire, cependant, elle fournit des peptides de haute pureté.

Basé sur le peptide de onze résidus d'acides aminés, un peptidomimétique original a été conçu et synthétisé. Après 47 étapes de synthèse, 20 mg d'un α-AApeptidomimétique pur à 95 % ont été synthétisés avec un rendement global de 2,1 %.

Le peptidomimétique, mimAse3, a été testé à trois concentrations différentes en même temps que le peptide Ase3 contre deux souches dont il avait déjà démontré l'activité, *S. epidermidis* et *P. aeruginosa*. Contrairement à ce qui était attendu, qui était une augmentation de l'activité de mimAse3 par rapport à Ase3, le peptidomimétique n'a pas inhibé la formation de biofilm de toutes les souches testées, même aux concentrations les plus élevées.

Le manque d'activité peut reposer sur la dégradation du peptidomimétique par les cellules bactériennes ou peut-être que le repliement de mimAse3 n'était pas ce qui était attendu et que sa conformation active n'a pas été atteinte. Les peptides A peuvent être étroitement liés à leur peptide parent, mais de petits changements dans la conformation finale peuvent entraîner une perte d'activité. La taille de ce peptide est importante, comme indiqué au début de ce travail, et pour une raison quelconque, si le peptide ne peut pas acquérir la conformation tridimensionnelle parfaite, il perdra son activité. Des études de RMN liquide à haut champ ou de dichroïsme circulaire peuvent être réalisées pour pouvoir vérifier si la structure secondaire du peptidomimétique garde le même repliement que le peptide naturel. Des études *in silico* pourraient également aider à comprendre sa conformation. Plus d'études pour essayer de déchiffrer le mécanisme d'action précis pourraint également aider à comprendre les résultats des tests biologiques.